Dolomites as Promising Natural CaO-based Sorbents for Ca-Looping Cycle CO_2 Capture

Magdalena Iwona Trzcionka

Thesis to obtain the Master of Science Degree in

Energy Engineering and Management

Supervisors: Prof. Carla I. C. Pinheiro
Dr. Paula Alexandra Lourenço Teixeira
Dr. Adam Klimanek

Examination Committee

Chairperson: Prof. Francisco Manuel da Silva Lemos
Supervisor: Dr. Paula Alexandra Lourenço Teixeira
Member of the Committee: Dr. Auguste Fernandes

September 2017

Education is the most powerful weapon which you can use to change the world.

Nelson Mandela

Acknowledgments

First of all, I would like to express my sincere gratitude to my supervisors from Instituto Superior Técnico, Prof. Carla Pinheiro and Dr. Paula Teixeira and to my supervisor from Silesian University of Technology, Dr. Adam Klimanek for their continuous support in the development of my dissertation research activity. I would like to sincerely thank for dedicated time, valuable advice related to this work and for the professional support and understanding.

I would like to thank CaReCi project team which I collaborated with for the last six months working in the laboratory at IST, Lisbon. The meetings during my research and giving me suggestions for improvements during the following thesis allows for successful completion of my dissertation.

Moreover, I would like to thank my family for support me during my master degree which allowed me to accomplish my objectives.

A big thank you to all of you!

This thesis is based on work conducted within the InnoEnergy Master School, in the MSc programme called Clean Fossil and Alternative Fuels Energy. It is supported financially by the InnoEnergy.
The author of MsC thesis received financial support from InnoEnergy, which is gratefully acknowledged.
The MsC thesis was carried out in the Department of Chemical Engineering (DEQ) at Instituto Superior Técnico in Lisbon, Portugal.

InnoEnergy is a company supported by the European Institute of Innovation and Technology (EIT) and has the mission of delivering commercial products and services, new businesses, innovators and entrepreneurs in the field of sustainable energy through the integration of higher education, research, entrepreneurs and business companies. Shareholders in KIC InnoEnergy are leading industries, research centers, universities and business schools from across Europe.

Clean Fossil and Alternative Fuels Energy MSc programme is a collaboration of three Universities:
SUT Silesian University of Technology, Gliwice, Poland,
AGH University of Science and Technology, Kraków, Poland,
IST Instituto Superior Técnico, Lisbon, Portugal

Abstract

The work developed in this MSc thesis is in the scope of an ongoing research project “CaReCI - Carbon Footprint Reduction in Cement Industry” carried out at Instituto Superior Técnico in Lisbon, Portugal, in collaboration with CIMPOR (Cimentos de Portugal), which is the largest Portuguese Cement Industry.

Dolomites ($CaMg(CO_3)_2$) are commonly available in nature and it has been reported that calcined dolomite becomes a more efficient sorbent than calcined limestone for CO_2 capture by Ca-Looping. Therefore, natural dolomites could be used to produce promising cost-effective and eco-friendly improved CaO-based sorbents for industrial CO_2 capture applications. In this work, two dolomite samples were tested in an experimental unit lab scale fixed bed reactor and were characterized by the characterization techniques: X-ray diffraction (XRD), N_2 sorption, Thermogravimetric analysis (TGA) and Scanning Electron Microscope (SEM). The CO_2 capture capacity and stability along the cycles of carbonation-calcination of the dolomite samples were studied under different thermal pre-treatment atmospheres and with a carbonation gas feed composition of 15% and 25%.

The results showed that pre-calcination with CO_2 improves the sorbents carrying capacity and stability when compared with pure N_2 atmosphere. The best results were obtained with dolomite pre-calcined with 25% of CO_2.The gas feed CO_2 composition during carbonation was not so relevant.

The results are promising because they show that dolomites can be used as Ca-looping sorbents for CO_2 capture in power plants which flue gases CO_2 concentration is around 10-15% and in the cement industry where flue gases CO_2 concentration is around 25-30%.

Key words: calcium looping, carbon capture and storage, CO_2 capture, dolomite, natural sorbent

Resumo

Esta dissertação de mestrado foi desenvolvida no âmbito do projecto de investigação CaReCI (*Carbon Footprint Reduction in Cement Industry*) que está a decorrer no Instituto Superior Técnico da Universidade de Lisboa, Portugal, em colaboração com a CIMPOR (Cimentos de Portugal), a maior indústria de cimentos portuguesa.

As dolomites estão disponíveis na natureza, e a literatura refere, que quando calcinadas apresentam maior eficiência na adsorção de CO_2, pelo ciclo do cálcio, do que o calcário calcinado. Além disso, como a utilização de dolomites é economicamente e ambientalmente viável, a sua aplicação na indústria é promissora.

Neste trabalho, estudou-se a reatividade de duas dolomites num reactor de leito fixo laboratorial e utilizaram-se as seguintes técnicas de caracterização: difracção de raios-X (DRX), adsorção de N_2, análise termogravimétrica (TG) e microscopia electrónica de varrimento (MEV).

Avaliou-se a capacidade de captura de CO_2 e a estabilidade das dolomites ao longo dos ciclos de carbonatação-calcinação, utilizando pré-tratamentos térmicos com diferentes atmosferas e diferentes composições de CO_2 na carbonatação, nomeadamente, 15% e 25%.

Comparativamente com os adsorventes pré-calcinados com N_2, verificou-se que a pré-calcinação com CO_2 melhora a capacidade de captura e estabilidade. Os melhores resultados foram obtidos com a dolomite pré-calcinada com 25% de CO_2. A concentração de CO_2 durante a carbonatação não foi relevante.

Os resultados são promissores porque evidenciaram que as dolomites podem ser usadas para capturar CO_2 através ciclo do cálcio, em Centrais Termoeléctricas e na Industria Cimenteira, onde a concentração de CO_2 nos efluentes gasosos varia respectivamente entre 10-15 % e 25-30%.

Palavras-chave: ciclo do calcio, captura de carbono e armazenamento, captura de CO_2, dolomite, adsorventes naturais

Table of Contents

1 Introduction 1

1.1 Carbon capture and storage technologies 4

1.2 Overview of the CO_2 capture post-combustion technology 6

2 Chemical looping cycle for CO_2 capture 10

2.1 Overview of industrial application of post-combustion Calcium looping cycle 11

2.1.1 European CaOling Project 12

2.1.2 ITRI Calcium Looping Pilot Plant 13

2.2 Natural Sorbents and Synthetic sorbents for CO_2 capture 14

2.2.1 Comparison of limestone, waste marble powder and dolomite in terms of CO_2 carrying capacity 16

2.3 Sorbent performance and deactivation phenomena 17

2.4 Enhancement of sorbents carrying capacity 19

2.4.1 Sorbents thermal pre-calcination with different atmosphere 20

2.5 Thesis Objectives 24

3 Materials and Methods 25

3.1 Chemical composition of the sorbents 25

3.2 Nitrogen sorption technique 26

3.3 Nitrogen sorption equipment 27

3.4 X-ray powder diffraction 28

3.5 Scanning Electron Microscope (SEM) 29

3.6 Thermogravimetric analyser (TGA) 30

3.7 Fixed bed unit 30

3.7.1 Experimental Set up 30

3.7.2 Experimental procedure carried out in the Fixed Bed Unit Reactor 32

3.7.3 Assessment of CO_2 capture during carbonation–calcination cycle 33

3.8 Experimental planning 34

3.8.1 Calibration of mass flowmeters 36

4 Results and discussion 38

4.1 Characterization of natural dolomite sorbents 38

4.1.1 Chemical and mineralogical composition of dolomites 38

4.1.2 Textural and morphological properties of dolomites 39

4.2 Fixed Bed Unit tests 40

4.2.1 Comparison of CO_2 carrying capacity of two natural dolomites 40

4.2.2 Influence of pre-calcination and carbonation atmosphere on CO_2 carrying capacity 47
5 Conclusions 58
6 References 61

List of Tables

Table 1.1 List of chosen sorbents/solvents used for CO_2 capture in Power Plants [22] 9
Table 2.1 Some types of sorbents with the pore grain size and specific surface area (CSI report) [34] 12
Table 3.1 The specific product data for dolomite α and dolomite β (adapted from company specific product data: Omya Madencilik) 25
Table 3.2 Summary of the tests carried out in the fixed bed unit 35
Table 3.3 Summary of the tests performed to evaluate the CO_2 carrying capacity of the selected dolomite β 35
Table 3.4 Experimental data used in N_2 mass flowmeter calibration 36
Table 3.5 Experimental data used in CO_2 mass flowmeter calibration 36
Table 4.1 Chemical elemental analysis of dolomites 38
Table 4.2 Specific surface area and total pore volume of dolomite α and β 40
Table 4.3 BET specific surface area and total pore volume for dolomite α and β 42
Table 4.4 Comparison of dolomite α and dolomite β 46

List of Figures

Figure 1.1 Globally averaged (a) land and ocean surface temperature; (b) sea level change (c) GHG concentrations in the atmosphere; (d) anthropogenic CO_2 emissions [6] 2

Figure 1.2 Comparison of different technology shares in reduction of CO2 between 2012 and 2050 [5] 3

Figure 1.3 Greenhouse gas emissions, by source sector, EU-28, 1990 and 2014 [9] 3

Figure 1.4 Types of CCS technology (adapted from [11]) 4

Figure 1.5 Pre-Combustion Capture Process (as cited in [14]) 5

Figure 1.6 Oxy-Fuel Capture Process (as cited in [14]) 5

Figure 1.7 Post-Combustion Capture Process (as cited in in [14]) 6

Figure 1.8 Separation techniques [15] 6

Figure 1.9 Gas separation membrane (as cited in [14]) 7

Figure 1.10 CO_2 Separation by Adsorption Process (as cited in [14]) 8

Figure 1.11 Scheme of CO_2 post-combustion capture process (as cited in [14]) 8

Figure 2.1 Chemical Looping Diagram (adapted from [26]) 10

Figure 2.2 Equilibrium vapour pressure of CO_2 over CaO as a function of temperature (adapted from [28]) 11

Figure 2.3 The 1.7 MWth La Pereda pilot plant [33] 13

Figure 2.4 The 1.9 MWth pilot plant, HECLOT Installation [31] 14

Figure 2.5 Carbonation-Conversion of WMP and $CaCO_3$ sorbents-CO_2 capture capacity [44] 16

Figure 2.6 Carrying Capacity vs 20 cycles for three types of natural sorbents (adapted from CaReCi project) 17

Figure 2.7 Scheme of the textural transformation of the CaO sorbent over many cycles [50] 18

Figure 2.8 Pore Size Distribution after calcination- carbonation [52] 18

Figure 2.9 Carrying capacity of CaO sorbent through 50 cycles. CO_2 capture in terms of mass change vs. time (TGA data for Havelock limestone) [37] 19

Figure 2.10 Results of cyclic adsorptions for diverse types of limestone [43] 21

Figure 2.11 Summary of results of TGA and XRD of decomposition of dolomite in CO_2 (a): TGA and DTG; (b) XRD patterns [43] 21

Figure 2.12 Summary of results of TGA and XRD of decomposition of dolomite in pure N_2 (a): TGA and DTG; (b) XRD patterns [43] 22

Figure 2.13 Effect of calcination temperature on reactivity [64] 22

Figure 2.14 Carrying Capacity for different calcination atmospheres [68] 23

Figure 3.1 Prepared sorbent ready to be placed in the fixed bed reactor 25

Figure 3.2 Types of adsorption isotherms for nitrogen adsorption [71] 26

Figure 3.3 Micrometrics ASAP 2010 equipment available at Instituto Superior Técnico 28

Figure 3.4 X-ray diffractometer - Bruker D8 Advance 29

Figure 3.5 SEM: Analytical JEOL 7001F FEG-SEM available at MicroLab Electron Microscopy Laboratory (adapted from IST website) 29
Figure 3.6 TGA-DSC Setsys Evo 16 device (Setaram) equipment available at Instituto Superior Técnico 30
Figure 3.7 Fixed Absorption Unit (a) and Fixed bed quartz reactor (b) 31
Figure 3.8 Alicat (a) and Brook (b) mass flowmeters 31
Figure 3.9 Guardian Plus® CO_2 gas analyser 31
Figure 3.10 Variation of CO_2 concentration in the exiting gas during one cycle of carbonation and calcination (a) CO_2 evolution along the carbonation-calcination cycle and (b) criterion for splitting carbonation and calcination areas in the overlapping S zone [44] 33
Figure 3.11 Experimental data used in N_2 mass flowmeter calibration 36
Figure 3.12 Experimental data used in CO_2 mass flowmeter calibration 36
Figure 4.1 XRD patterns of dolomite α and dolomite β 39
Figure 4.2 N_2 sorption isotherms of fresh dolomite α and β 39
Figure 4.3 SEM images of dolomite α (a) and dolomite β (b) 40
Figure 4.4 Comparison of CO_2 carrying capacity for dolomite α and dolomite β 41
Figure 4.5 N_2 sorption isotherms for the used dolomite α and dolomite β samples along the cycles 42
Figure 4.6 Relation between CO_2 capture deactivation (%) and the specific surface area 43
Figure 4.7 Pores size distribution (PSD from BJH desorption branch) for used dolomites 44
Figure 4.8 Comparison of X-ray patterns of dolomite α and dolomite β 44
Figure 4.9 Crystallite Size for dolomite α and dolomite β along the cycles 45
Figure 4.10 SEM images of the dolomite α (a) and dolomite β (b) after 20 cycles (70000x) 46
Figure 4.11 SEM images of the dolomite β: (a) 0 cycle; (b) after 20 cycles (40000x) 46
Figure 4.12 Influence of different pre-calcination and carbonation atmospheres in CO_2 carrying capacity of dolomite β for 20 cycles 47
Figure 4.13 XRD patterns of dolomite β pre-calcined under different atmospheres 48
Figure 4.14 Carrying Capacity of dolomite β using different experimental conditions (10 and 20 cycle's tests) 49
Figure 4.15 Carrying Capacity of $CaCO_3$, WMP and dolomite β pre-calcined with 100% of N_2 49
Figure 4.16 Comparison of S_{BET} and V_p of dolomites tested using different experimental conditions 51
Figure 4.17 Pores size distribution (PSD from BJH desorption branch) for used dolomites 52
Figure 4.18 Comparison of X-ray patterns of dolomite β tested under different experimental conditions 53
Figure 4.19 Crystallite Grain Size for different pre-calcination of dolomite β 54
Figure 4.20 Comparison of 1st carbonation profile of different sorbents 55

Figure 4.21 SEM images of dolomite β (a) Precal: 100% N_2, Carb: 15%; (b) Precal: 100% N_2, Carb: 25%CO_2; (c) Precal: 25%CO_2, Carb: 15%CO_2; (d) Precal: 25%CO_2 with Carb 25%CO_2 (magnification 40000x) 56

Figure 4.22 Carrying Capacity of the dolomite β through 50 cycles 56

Figure 4.23 Graphical representation of carbonation conversion of dolomite β during 50 cycles presented for chosen cycle-number 57

1 Introduction

Nowadays due to the climate change, engineers, scientists and policy makers are looking for the solution to reduce the greenhouses gases emissions (GHG), which has been priority for developed countries. The main reason of fast growth of global CO_2 emission in atmosphere is the combustion of fossil fuels and chemical processes in cement manufacture [1]. Moreover, steel production is also a significant contributor of GHG emission and climate change. It is observed that climate is changing due to fluctuated concentrations of GHG which are the main reason of average increase of temperature of Earth. Therefore, the concern about the climate change led to sign the Kyoto Protocol under the United Nations Framework Convention on Climate Change (UNFCCC) in 1997. It is an international agreement, which main objective is to reduce the emission of six main GHG compounds such as carbon dioxide (CO_2), methane (CH_4), nitrous oxide (N_2O), hydrofluorocarbons (HFCs), perfluorocarbons (PFCs) and sulphur hexafluoride (SF_6) [2]. The main aim of UNFCCC agreement is the *"stabilization of GHG concentration in atmosphere at the level which will prevent anthropogenic emission to interfere with the climate and will allow ecosystems in natural way to adjust to the climate change"* [3].

The Paris climate agreement was signed in 2016 by 195 countries and European Union. The agreement contains the plan to reduce the emission of GHG by all the countries who signed the document. The main objective is to maintain an increase in global warming below 2 °C. It also establishes that there should be an equilibrium between emission and absorption of CO_2 by forests. All the countries which signed the protocol up to 2030 should present their action aimed at reduction of GHG such as introduction of clean coal technologies such as Carbon Capture and Storage (CCS) or increase the implementation of renewable energies [4].

CO_2 is mostly emitted during industrial processes such as cement manufacture, coal and biomass combustion [5]. Landfilling is another reason of increase of concentrations of CO_2 and CH_4 in the atmosphere. These gases appear through decomposition of solid wastes. To avoid this, it is significant to implement proper waste management in the country, which aims to ban landfilling and promotes recycling among society. Moreover, factors such as population development, economic activity influence on release of GHG into atmosphere. The consequences of emission can be observed in Figure 1.1 which presents the data related with the impact of changes on Earth caused by the increase of GHG emissions. The temperature of atmosphere and ocean level has been increased, so the amount of ice on Arctic sea has been declined [6]. Some of the gases enter into the oceans and some of them are used in photosynthesis process. The rest of gases take part in the geochemical carbon cycle. The anthropogenic emission disturbs the equilibrium of natural carbon cycle. Moreover, the weather changes too and results in drought or flood seasons. The land usage for agriculture changes local environment, increases degradation of soil and fosters deforestation process due to increasing demand for new agriculture land. Society is warned about increased concentration of CO_2 in the atmosphere. There is a wide research going on that aims to reduce accelerated emissions emitted mainly as outcome of human activity.

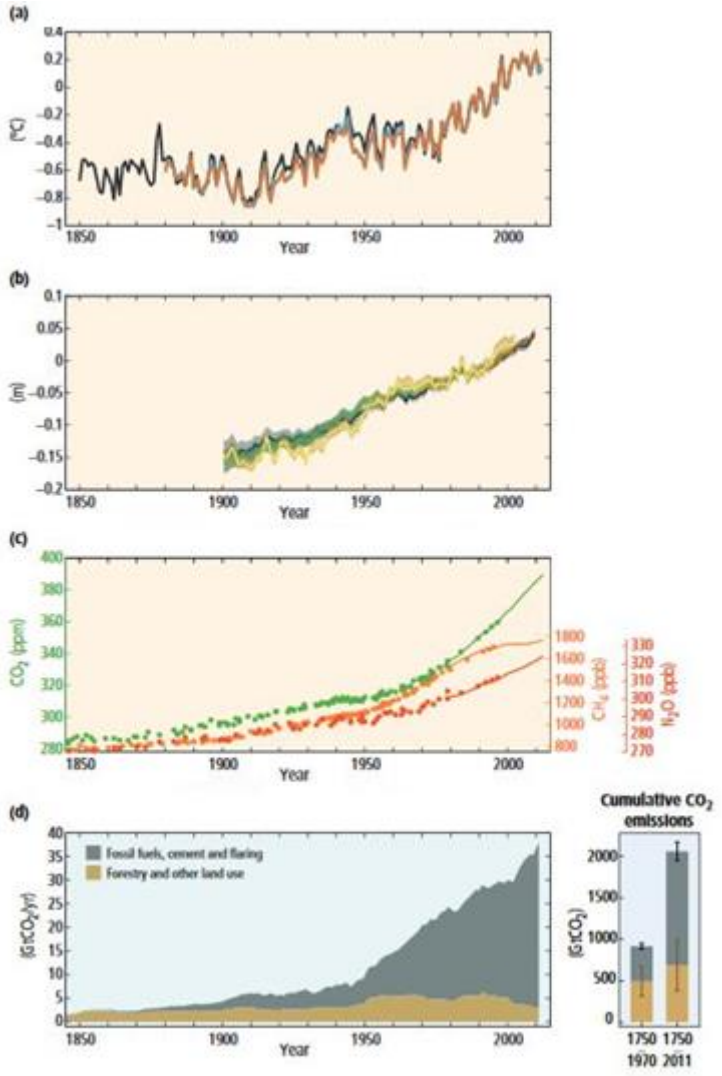

Figure 1.1 Globally averaged (a) land and ocean surface temperature; (b) sea level change (c) GHG concentrations in the atmosphere; (d) anthropogenic CO_2 emissions [6]

Figure 1.2 presents the share of CO_2 reduction by different clean energy technologies. The idea is to switch into sustainability by decarbonization of energy sectors. There are many strategies like: reduction in the demand by increasing energy efficiency, switching into fuels which are less carbon based (from coal to natural gas), make investments in renewable energy sources (wind and solar power), increase the use of nuclear power energy and make development in CCS (carbon capture and storage) technologies in the industry [6]. The main concern about the CCS installation is that it is very costly and requires a lot of energy. The costs depend on the facility scale and storage process in the geological form where it can be stored in an amount evaluated by the CCS storage operator.

The formation of Earth, where it can be stored should be known to estimate a risk which is related with safety storage underground. The Carbon Capture Utilisation (CCU) is a promising approach which allows to utilise captured CO_2. Due to the availability of fossil fuels, the utilization can be made by conversion of CO_2 coming from GHG to carbon (C). It is environmentally friendly conversion which allow to transform CO_2 into renewable carbon source. The utilization of the biofuel (alternative fuel) with the

connection of CCS installation is more sustainable than carrying out utilization of fuel from crop fermentation. The emission of GHG is increased due to the usage of equipment for crop production. From CO_2, two main products can be obtained such as: methanol (CH_3OH) and dimethyl ether (CH_3OCH_3). Oil prices are increasing, fossil fuels will soon deplete, so it is important to use biofuels in a transport sector which not only will significantly decrease the emissions but will be cheaper and an environmentally friendly fuel [7]. In the opinion of the Commission of the European Communities, implementation of CCS will allow to reduce emissions by 30% by 2020 and by 60-80% by the end of 2050 [8].

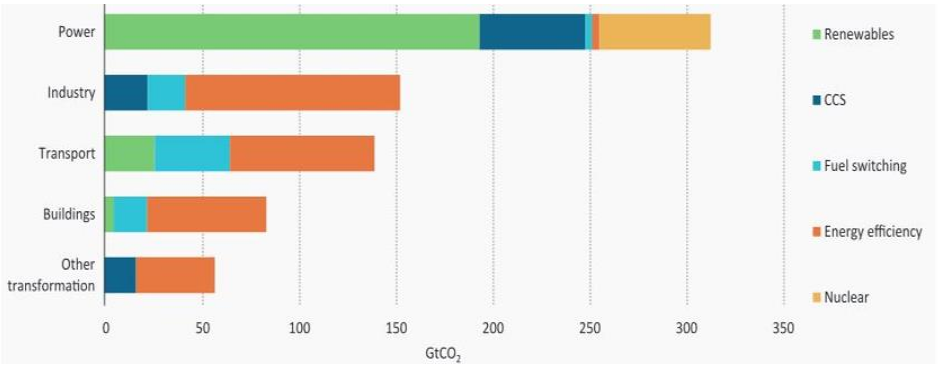

Figure 1.2 Comparison of different technology shares in reduction of CO2 between 2012 and 2050 [5]

Figure 1.3 presents two pie charts which show the comparison of emissions by different sectors. It can be noticed that there is a significant reduction of CO_2 due to technological improvement of the industrial processes. However, not in all sectors, there is a decrease of the emission. Comparing 1990 and 2014 there is an increase of GHG in transport by 8.3% and in agriculture around 0.3%. These changes are the effect of increased combustion of fossil fuels in cars, which leads to air pollution in cities. Decrease of the emissions is possible by the implementation of technological innovations such as CCS technologies, improvements of the efficiency of vehicle (use the engines with the higher fuel efficiency and lower emissivity), use of the renewable energy and improve the issues related with better planning of the road network. Cement Industry is one of the biggest emitter of CO_2. One approach for decreasing the level of CO_2 emissions is the implementation of CCS technologies, mainly in cement manufacturers.

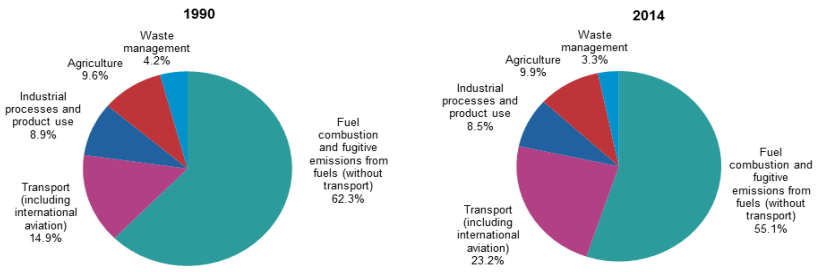

Figure 1.3 Greenhouse gas emissions, by source sector, EU-28, 1990 and 2014 [9]

There are many types of CCS technologies as shown in Figure 1.4. One of the most interesting is Calcium Looping Cycle which uses calcium based sorbents in the post-combustion technology. There are natural and synthetic sorbents which can be implemented in large stationary sources such as power plant or cement industry. Technology of CO_2 capture can significantly contribute to reduce greenhouse gases effect. However, there is a lot of concern about the long-term behavior of natural sorbents in large systems which are related to the sorbent activity loss with increasing number of carbonation/calcination cycles. In a large application, cost is considered before implementation any of the CCS technologies. Post-combustion is an expensive technology but the implementation of the natural sorbents can significantly reduce its costs. However, main drawbacks are related with the fast deactivation of the sorbent to capture more CO_2 and sintering phenomena. To overcome this challenge, scientists are working on improvements of the sorbent ability to uptake more CO_2 [10].

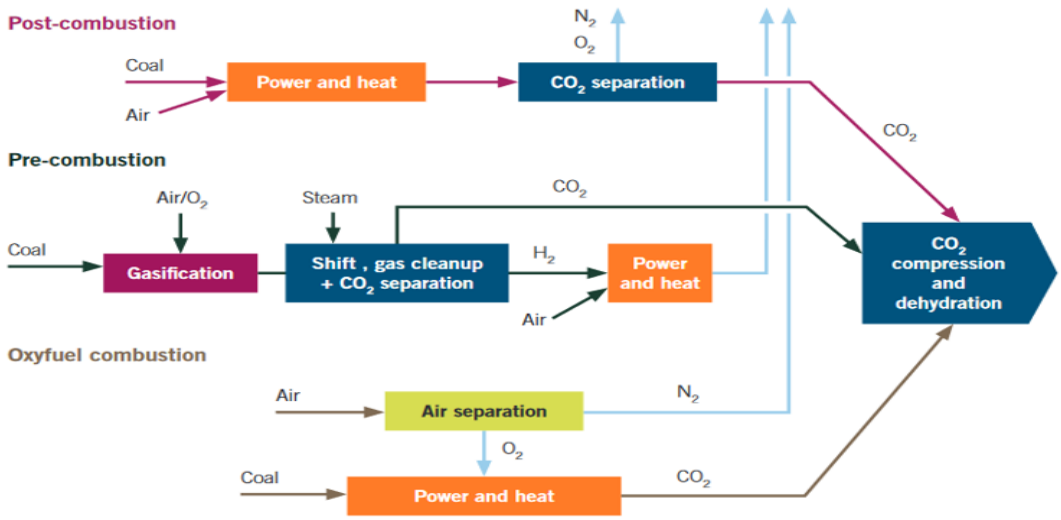

Figure 1.4 Types of CCS technology (adapted from [11])

1.1 Carbon capture and storage technologies

There are many methods to reduce and capture CO_2 from fossil fuels power plants, which generate relevant amounts of emissions into the atmosphere. Among all these possibilities, CCS-related with future utilisation is considered as one of the promising tools to deal with climate change.

European Commission presented the strategy which introduced that there will be significant impact of implementation of low carbon technologies. The main goal is to reduce the amount of CO_2 in the flue gases. It is estimated that the share of CCS will increase around 60% in 2020, 80% in 2030 and 100% in 2050. In Europe variety range of renewable technologies will be distributed and it will be cheaper and more available. The CCS technologies will improve the idea of transition to low carbon-based economy [12].

Regarding the implementation of CCS, there are three different approaches which are presented in the Figure 1.4. The technology consists of three important steps: separation, transportation, and storage. Separation process of CO_2 from flue gases is expensive and it can be classified into main

categories as: pre-combustion capture technology, oxy-fuel combustion technology and post-combustion capture process [13]. In this chapter, all three methods for carbon capture are explained.

Pre-combustion capture technology is illustrated in Figure 1.5. The main idea of the technology is partial oxidation process which occurs in a gasifier where solid fuel is converted to gaseous product called syngas (synthesis gas). It is a mixture of hydrogen (H_2) and carbon monoxide (CO). CO_2 is captured, separated and compressed and sent to storage. In IGCC (Integrated Gasification Combined Cycle) system, after CO_2 removal, the remaining synthesis gas which is rich in H_2 can be used to move gas turbine to produce electricity or used in fuel cells. The rest of the mixture of H_2 and N_2 is combusted and used as a steam to move the turbine to produce electricity [14].

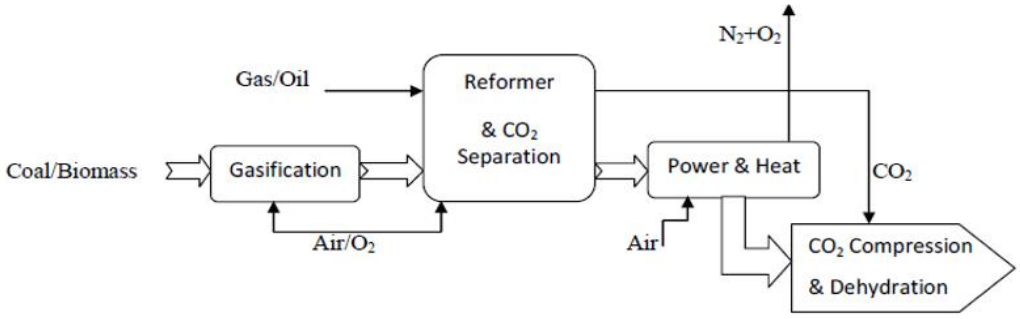

Figure 1.5 Pre-Combustion Capture Process (as cited in [14])

In oxy-fuel combustion, the main goal is to reduce the amount of N_2 in the flue gases, that is why air separation unit (ASU) is used to separate oxygen from air. Next, pure oxygen is used to burn the fuel which influences on the formation of the flue gases composition like CO_2, water vapor (H_2O), particulate matter (PM) and (sulphur dioxide) SO_2. CO_2 is compressed, transported and stored. SO_2 is removed during the desulphurization process and particulate matter (PM) can be extracted by electrostatic precipitators. H_2O is recovered in cooling towers. Oxy-fuel is one of the cheapest options among CCS. It has high efficiency and flexible technology which can be implemented in new and old power plants systems [16]. Oxy-fuel combustion is illustrated in Figure 1.6

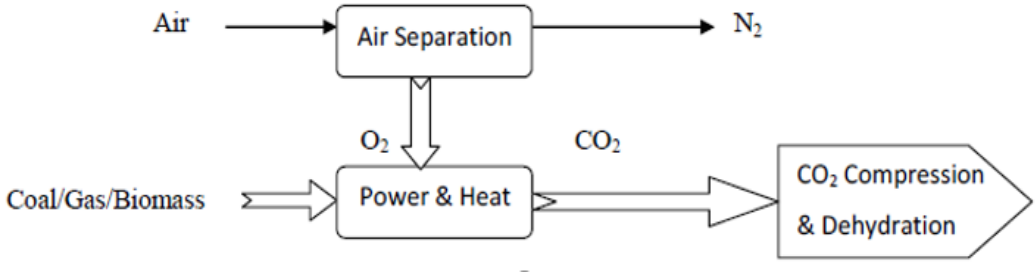

Figure 1.6 Oxy-Fuel Capture Process (as cited in [14])

Post-combustion is shown in Figure 1.7. The main idea is to remove CO_2 from flue gases after combustion process. The post-combustion technologies have the biggest chance to cut CO_2 emissions in future in the cement and fossil fuel power plants. The methods of that technology will be described more detailed in the next sub-section [14].

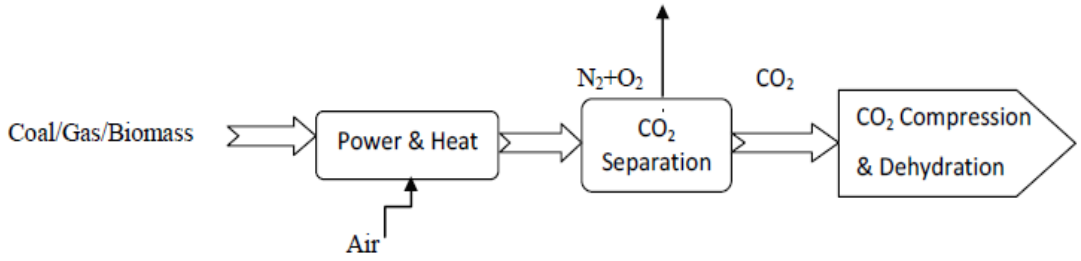

Figure 1.7 Post-Combustion Capture Process (as cited in in [14])

1.2 Overview of the CO_2 capture post-combustion technology

This section presents detailed classification of several post-combustion gas separation and carbon capture technologies. The scheme presented in Figure 1.8 illustrates the division of CO_2 separation into physical and chemical techniques. Physical methods are: PSA (pressure swing adsorption), TSA (temperature swing adsorption), membrane separation and adsorption using activated carbon. Chemical techniques can be divided into absorption in selective solvents or absorption in solid-state sorbents. The first group contains: ammonia scrubbing, amine scrubbing, NaOH solvents, K_2CO_3 solvents and Na_2CO_3 solvents. The second group includes sorbents based on Na, Ca and other metals oxides.

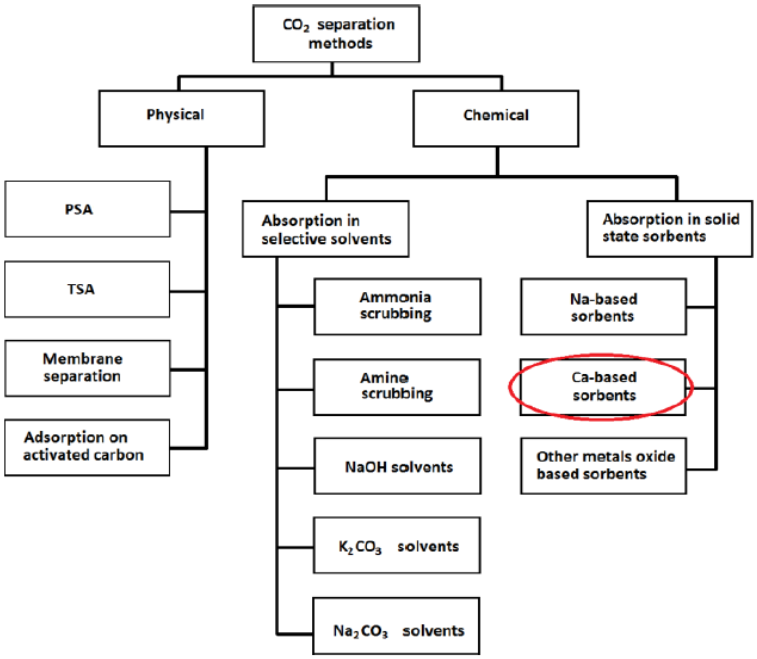

Figure 1.8 Separation techniques [15]

PSA is a technology which is used to remove and recover CO_2 from flue gases. It can be easily implemented in the power plant system. Adsorption and desorption process is carried out based on higher and lower pressure. There is a strong need to find out a sorbent which can be used in PSA and will separate CO_2 efficiently [16].

TSA is another option to remove CO_2 from flue gases. However, before the implementation to technology system, the knowledge about thermodynamic properties of adsorbent should be known [17].

Membrane separation obeys two types of membranes: polymeric and organic one. It is schematically shown in Figure 1.9. In that process; low concentration of CO_2 is separated from flue gases with the use of membrane's material. The principle is based on the differences in pressure on both sides of the membrane. They are high selectivity materials and in the end of the process, they allow to obtain purified gas [7]. Membranes haven't been tested yet in power plants because of need to improve properties of the material [18].

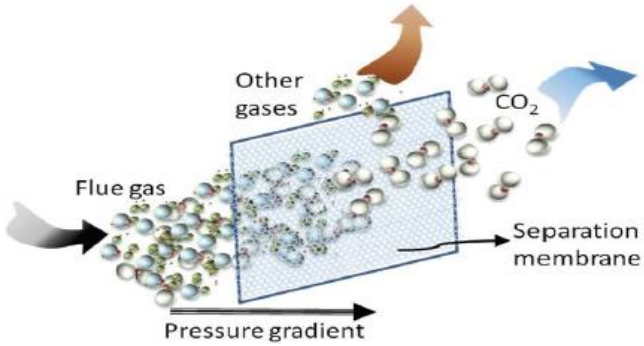

Figure 1.9 Gas separation membrane (as cited in [14])

Physical adsorption method in which the liquid or gas is absorbed by a solid surface of sorbent is illustrated in Figure 1.10. Different solid sorbents can be used for reversible process of CO_2 capture from flue gases. This ability depends on adsorption capacity and kinetics of chemical substances. Sorbents which can be used are divided into two groups: carbonaceous and noncarbonaceous. Carbonaceous sorbents are the most used for CO_2 separation. These materials are cheap, have high surface area and ability to regenerate quickly. Examples of carbonaceous materials are: activated carbon, graphene, calcium and magnesium. Activated carbon (AC) is the most common physical sorbent which is used to capture CO_2. It has good thermal stability properties, high porosity, high surface area and high surface reactivity. It is widely available and cheap sorbent [7]. Calcium and magnesium sorbents will be described separately in another chapter called the Natural Sorbents and Synthetic sorbents for CO_2 capture.

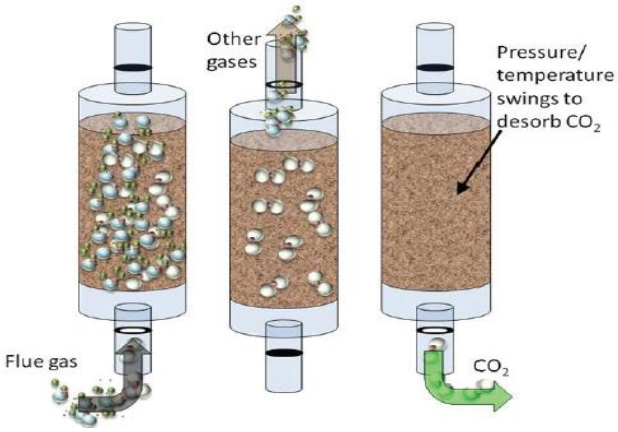

Figure 1.10 CO_2 Separation by Adsorption Process (as cited in [14])

In the chemical absorption process, alkanolamines are the most widely used absorbents for CO_2 capture. Among amines, there is MEA (monoethanolamine), diethanolamine (DEA) and N-methyldiethanolamine (MDEA) [19]. The absorption with amines is very well known commercialized technology. The mechanism is shown in Figure 1.11. Presented technology uses liquid solvents like monoethanolamine (MEA) to capture CO_2 from flue gases during the combustion process. The installation contains following devices such as: absorber, desorber (stripper) and heat exchanger. The flue gases enter at the bottom of the absorber and contact with the counter-current liquid solvent which flows from the top. Next, MEA becomes rich in CO_2 loading and is pumped to desorber. Amine is cycled in both columns to capture CO_2. In the outlet of desorber, a pure stream of CO_2 is obtained [19].

The noncarbonaceous group can be classified: zeolites, metal organic frameworks, porous polymers, and silica materials. Zeolites are the most popular; they are microporous crystalline synthetic or natural silicate materials. The adsorption of these materials depends on their structure and composition [20].

Another type is microporous polymer (MOPs). It is a new type of polymer which can be implemented in CO_2 separation from flue gases in CCS technology [21].

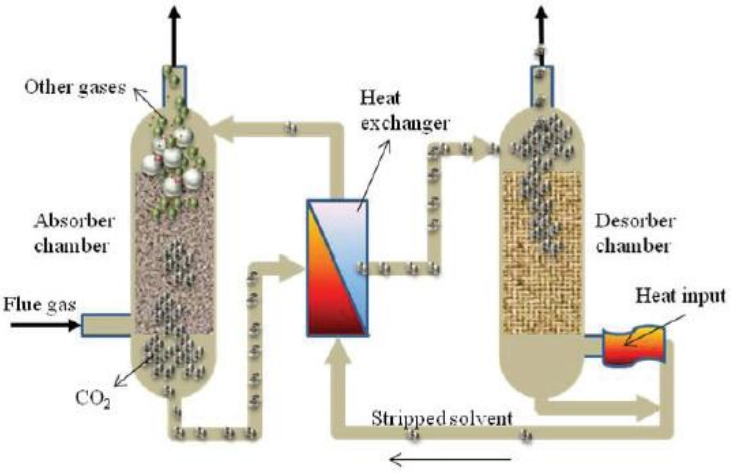

Figure 1.11 Scheme of CO_2 post-combustion capture process (as cited in [14])

To sum up this chapter, CCS technology is one of the main options used to reduce the emission of CO_2 which is released in industrial processes. Then CO_2 is transported to storage or utilization, which aims to control and protect against CO_2 leakage into atmosphere. Post-combustion technologies are investigated to be better used in the future and significantly reduce the CO_2 emission which is one of the main problem of climate change.

The next chapter presents chemical looping cycle for CO_2 capture, where solid sorbents like metal oxides, can be implemented. In the reaction with CO_2, metal oxides are converted to the carbonated form when the regeneration occurs by heating beyond the decomposition temperature point which allow to release stream of CO_2. Using sorbents in the post-combustion carbon capture technology has many advantages such as: [20]

- low costs of natural solid sorbents, allow to use them in high quantities in the system,
- they can be a possible viable solution to limit CO_2 emissions;
- solid sorbents require less energy in the regeneration process compared to aqueous amines;
- they can be easily transported and send to the power plant;
- high capacity to capture CO_2, (this property is different and depends on type of the sorbent).

Table 1.1 presents the comparison between chosen sorbents used for CO_2 separation processes.

Table 1.1 List of chosen sorbents/solvents used for CO_2 capture in Power Plants [22]

Sorbent/solvent material	**Carrying capacity (gCO_2/kgsorbent/solvent material)**
CaO oxides (assume 50% repeatable cycles)	393
Activated Carbon	88
Silica gel	13
MEA solvent	60

2 Chemical looping cycle for CO_2 capture

Chemical Looping is a promising CCS technology, due to its ability to capture CO_2 during coal gasification and large industrial scale post-combustion processes. It can be implemented in cement manufacture, steel and fossil-fired power plants. After the combustion of fuel, products such as CO_2 and H_2O are separated from flue gases. The method uses solid sorbents which contain metal oxides such as calcium (Ca) to capture CO_2 from flue gases [23]. It has many advantages; the most important ones are high capture capacity and possibility of sorbents' regeneration. The biggest challenge in Ca-Looping is the choice of metal oxide which should be resistant to long cycling and other conditions which are present during combustion of fuel, such as temperature [24].

Figure 2.1 illustrates the scheme of Ca-Looping in combustion process. Flue gases containing CO_2 enter a carbonator, where solid sorbent containing CaO is ready to capture CO_2 through carbonation reaction. During calcination, $CaCO_3$ decomposes into CaO and CO_2 at temperatures between 800 °C and 900 °C. CaO is sent to the carbonator where the cycle (calcination and carbonation) is repeated [25].

From the calciner, CO_2 is compressed and utilized or stored. CCU (Carbon dioxide utilisation) enables to convert CO_2 to valuable products. By direct utilisation, many products: as bio-oils, chemicals, and fuels can be obtained.

The most significant reaction in Ca-Looping is carbonation (*Eq. 2.1*), where CaO reacts with CO_2 to obtain calcium carbonate $CaCO_3$ as given by the following equation:

$$CaO_{(s)} + CO_{2_{(g)}} \leftrightarrow CaCO_{3(s)} \quad \Delta H_{700\,℃,1\,bar} = -170\ {}^{kJ}/_{mol^{-1}} \quad \textbf{(Eq. 2.1)}$$

Obtained $CaCO_3$ goes to calciner where it decomposes into CaO and CO_2. Then it is sent again to carbonator and finally, the chemical loop is completed. Calcination reaction is presented below (*Eq. 2.2*).

$$CaCO_{3(s)} \leftrightarrow CaO_{(s)} + CO_{2_{(g)}} \quad \Delta H_{900\,℃,1\,bar} = +165\ {}^{kJ}/_{mol^{-1}} \quad \textbf{(Eq. 2.2)}$$

The first reaction (*Eq.2.1*) which occurs between CaO and CO_2 is exothermic whereas the second reaction, regeneration of $CaCO_3$, is endothermic (*Eq. 2.2*).

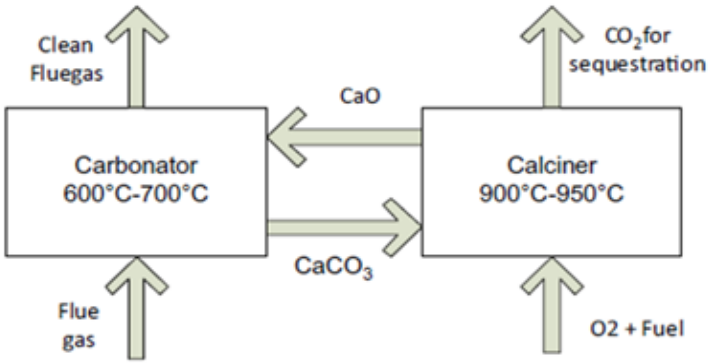

Figure 2.1 Chemical Looping Diagram (adapted from [26])

Two main reversible reactions, calcination and carbonation, are different and at this point, it is important to observe the graph depicting the relationship between vapor pressure and temperature, as shown in Figure 2.2. Carbonation depends on temperature and pressure of its vessel. The reaction is carried out at temperatures higher than 596.85 °C (870 K) under high CO_2 partial pressures which aim to produce pure stream. Unfortunately, degradation of the sorbent increases with the increase of temperature leading to a sintering process. Therefore, in the carbonator vessel, the temperature is lower and it enables to regenerate the sorbent capacity, in order to reuse the sorbent in the next cycle to capture CO_2. The calcination temperature depends on CO_2 pressures, given by the equation: [27]

$$log_{10}P_{eq}(atm) = 7.079 - \frac{8308}{T}(K) \quad \textbf{(Eq. 2.3)}$$

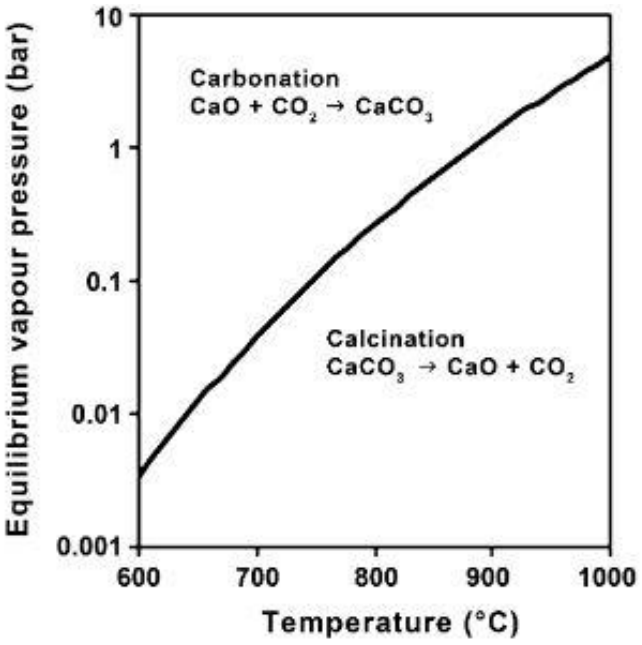

Figure 2.2 Equilibrium vapour pressure of CO_2 over CaO as a function of temperature (adapted from [28])

2.1 Overview of industrial application of post-combustion Calcium looping cycle

This section presents a brief overview of contemporary post-combustion technologies which use Ca-looping. So far, the main capture technologies, mentioned in the introduction, are being developed for power plants. Post-combustion, pre-combustion and oxy-fuel are the three renowned CCS technologies which are continuously improved. These technologies are rated using a parameter called Technology Readiness Level (TRL). It uses a nine-point scale indicating the status of development and technological maturity. The scale progresses from the initial formulation of research, through the testing of technology ultimate commercial demonstration by industrial implementation.

The capture of CO_2 by post-combustion Ca-looping has reached between 6th and 7th stages of development, meaning the technology has already been tested in pilot plants and will soon be switched

MW_{th} scale. Compared with other capture technologies, direct Ca-looping is the fastest progressing technology that is to reach the 7th stage of TRL by 2020 [29-30].

There are two known Calcium Looping pilot scale plants implemented in the industrial sector. The most known is the European project – CaOling which is integrated with a coal power plant.

The second largest installation is High-efficiency Calcium Looping Technology (HECLOT), in Taiwan, that collaborates with a cement industry [31]. It was estimated that *"Cement factories emit between 0.6-1 kg of CO_2 per tonne of cement"*, [32] justifying the implementation of CCS or CCU.

Many plants use activated carbon (from bituminous or lignite coal), other non-carbon materials, biomass, zeolite and lime sorbents. The main goal is to control the mercury emission, from combustion of fuel. Moreover, during the production of clinkers, CO_2 is produced which necessitates the use of sorbents in kiln system. The selection of sorbent is crucial as it depends on the prevailing conditions in the cement factory. Testing sorbents at high temperatures (in situ) enables to make a good decision before implementing a sorbent [33].

Table 2.1 Some types of sorbents with the pore grain size and specific surface area (CSI report) [34]

Sorbents	Zeolite	Lime products	Activated lignite	Activated carbon
Grain size	0-50 μm	0-2 mm	0-0.4 mm	0-0.2 mm
Specific surface area	400-600 m^2/g	1-50 m^2/g	300 m_2/g	50 -1600 m^2/g

The table 2.1 compares pore size and specific surface area of 4 sorbents. These physical properties need to be considered as they influence the capture capacity. The data included in the table were reported by CSI (Cement Sustainability Initiative). There are many sorbents which can be used and the choice depends on the intended application [34]. This MSc thesis focuses on implementation of dolomite in the Calcium Looping Cycle.

2.1.1 European CaOling Project

CaOling Project is so far the biggest European initiative which concerns chemical Ca- looping as one of the main methods to capture CO_2 from flue gases. The post-combustion 1.7 MWth installation is integrated with existing 50 MWe CFB (coal fluidized boiler). As part of the project, scientists use diverse types of sorbents and simulation tools to test the efficiency of that technology. The main goal of the project is to achieve zero emissions of CO_2 and to put special emphasis on rising carbon prices. Results show that post-combustion technologies can be retrofitted in coal power plants due to their reliable performance related to high CO_2 capture efficiency. Figure 2.3 illustrates the scheme of power plant installation with the two towers. Main reactions occur in calciner and carbonator. Limestone is placed together with coal in the calciner. During combustion, coal is burnt and $CaCO_3$ decomposes to CaO. Sorbent is purified with water in solid removal system. During this process occurring in the calciner, gas composition, temperature, and pressure are monitored. Limestone is analyzed in terms of reactivity to CO_2 and SO_2 capture with the use of thermogravimetric analyzers. At the inlet and outlet of carbonator tower, molar flow of CO_2 with flue gases is measured. In both towers, operation temperatures are

maintained. In the carbonator, the temperature range is 650 °C-700 °C and 900 °C-950 °C in the calciner. Implementation of Ca-looping installation in La Pereda Power Plant was carried out for 380 h. The capture efficiency of CO_2 was registered around 95%. Recently, during the International Conference on Greenhouse Gas Control Technologies held from 14th to 18th November 2016, there was strong emphasis on deployment of CCS technologies, with discussion about scaling up the aforementioned installation to 20 MWth [35].

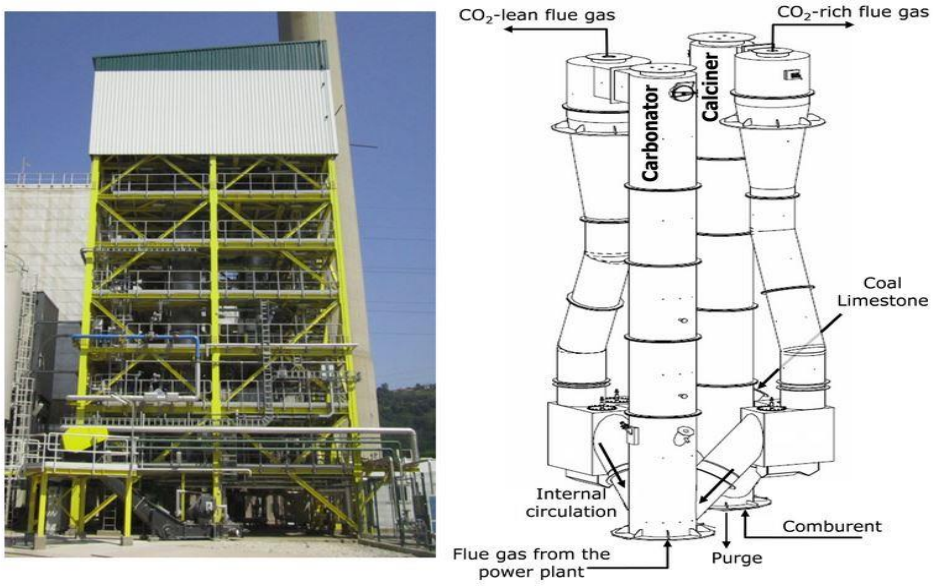

Figure 2.3 The 1.7 MWth La Pereda pilot plant [33]

2.1.2 ITRI Calcium Looping Pilot Plant

Industrial Technology Research Institute (ITRI) is the world's leading research center developing High-Efficiency Calcium Looping Technology (HECLOT). The primary goal is to reduce CO_2 emission from power plants and find a perfect solution to produce "clean electricity". The designed pilot installation is located in Heping, Cement Power Plant. This technology uses limestone sorbent ($CaCO_3$) to capture CO_2. The idea is the same as Calcium Looping cycle. The installation illustrated in Figure 2.4 captures around 1 t CO_2/h from 3 t/h flue gases. It comprises a bubbling fluidized bed carbonator and a moving bed calciner. The capture capacity is around 80-95%. In the carbonator, temperature is around 650 °C. So, cooling system is implemented to maintain the constant temperature (water tube towers.) For calcination, heat comes from oxy-combustion of diesel in rotary kiln calciner. This means that some part of cooled flue gases come back to the combustion chamber. There is around 10 t of CaO feedstock and the calcination time is around 9 minutes. The used solid sorbent is taken to cement power plant as a feedstock for cement production. The implementation of the Ca-looping technology with cement plant is a big advantage as it reduces the costs of the sorbent and energy needed for endothermic calcination reaction.

ITRI signed an agreement with Taiwan Cement Company (TCC) to build the world's largest installation (1.9 MWth) which will reduce CO_2 released during cement production. The initial commercial installation is expected to be built in 2025-2030 [36].

Figure 2.4 The 1.9 MWth pilot plant, HECLOT Installation [31]

2.2 Natural Sorbents and Synthetic sorbents for CO_2 capture

Before sorbents can be implemented in large scale units to capture CO_2, the following properties should be checked. First, one of the most important factors is to estimate the capacity to adsorb CO_2, which defines the quantity of sorbent which can be used in a system. Second most important feature is selectivity, which enables to sequestrate pure CO_2 for transportation purposes. Another property is kinetics of the sorbent which controls the cycles because it maintains repeatable reaction of carbonation and calcination in fixed bed unit reactor. Also, the sorbent should be mechanically strong and resistant to operating conditions of the installation such as temperature or flow of flue gases. That should be related with CO_2 capture process which should be effective and enable fast adsorption and desorption processes, so that the least possible quantity of sorbent can be used to capture emission from flue gas every time [20].

Sorbent should regenerate in each cycle, so it can be effectively used until it reaches point when it will not be able to capture more CO_2; and its regenerability will decrease significantly. Regeneration will reduce the costs of capture process and it should be maintained carefully without any changes in the adsorptive properties. Flue gases contain impurities such as SOx, NOx, and metals that can influence CO_2 conversion and stability during the cycles. Moreover, such contaminants should be effectively removed because they decrease the CO_2 carrying capacity of the sorbent. The cost of production of sorbents are considered and should be as low as possible [20]. In Ca-looping, sorbent reactivity decreases due to pore blockage and sintering process [37]. These factors are described in section 2.3. There are natural and synthetic sorbents. They both can be used to capture CO_2 in the cement industry process [38].

Natural carbonate rocks used in the chemical looping technology are waste marble powder (WMP), limestone, and dolomite. Less common are egg shells and sea shells [39]. These materials can be crushed to powder and then used as sorbents in many industrial processes.

Limestone (known as lime) is a rock composed of $CaCO_3$. It is a well-known sorbent which can be used in Calcium Looping. There are many advantages of using sorbents derived from limestone.

First of all, price of the sorbent is low, it is natural, non-toxic for environment, has high reactivity in the initial cycles, can be used in FBR (fluidized bed reactor) and can be reused for cement production.

It is important to mention that different limestones present different behaviors to capture CO_2 [36,38].

Experimental tests on several types of limestones by Grasa and Abanades [40] show that decrease in reactivity is fast [40].

Other important and available sorbent in natural environment is dolomite with the chemical formula $CaMg(CO_3)_2$. The percentage of calcium and magnesium oxides depends on the composition of the dolomite. Recently, scientists conducted more research on dolomite. Due to the chemical composition and availability of magnesium in its structure, the conditions of carbonation and calcination are different [41]. It was verified that capture capacity of dolomite is lower than that of limestone, which is justified by the CaO lower content. Besides the MgO is almost inert. However, its reactivity among the cycles lasts longer, the main reason is less sintering compared to limestone [42].

The ratio of CaO/MgO has major influence on CO_2 capture behavior of the sorbent. During calcination process, $MgCO_3$ decomposes contributing to improvement of CO_2 compound to enter into particles by an increase in surface area and pore volume [43]. In a pure CO_2 atmosphere, dolomite decomposes as given by *(Eq.2.4)* [43]:

$$CaMg(CO_3)_2 \rightarrow Mg_xCa_{1-x}CO_3 + MgO + CO_2 \rightarrow CaCO_3 + MgO \rightarrow CaO + MgO + CO_2 \quad \textbf{(Eq.2.4)}$$

As shown in the above equation, the intermediate, unstable compound, $Mg_xCa_{1-x}CO_3$ appears as dolomite is composed of $MgCO_3$. Generally, decomposition depends on the percentage of oxides which can be formed based on the chemical compound. The calcination of $MgCO_3$ occurs at lower temperature so it decomposes before $CaCO_3$ [43]. It is given by the *(Eq. 2.5):*

$$MgCa(CO_3)_2 \rightarrow MgO + CaCO_3 + CO_2 \quad \textbf{(Eq. 2.5)}$$

The obtained product is partially calcined, and when temperature increases, complete calcination of the dolomite occurs. The complete calcination reaction is given by the *(Eq. 2.6)* [43]:

$$MgO + CaCO_3 \rightarrow MgO + CaO + CO_2 \quad \textbf{(Eq.2.6)}$$

Dolomite is a complex compound compared to limestone. It is examined that dolomite has greater performance than limestone due to higher thermal stability and slower loss of CaO carbonation reactivity, owing to the Mg in its structure [42]. Previous studies have shown that dolomite could be used in the industry to capture high concentration of CO_2 in flue gases [42].

Waste Marble Powder (WMP) is the third natural sorbent which is currently being investigated and it was presented for the first time by Pinheiro *et al.* [44]. Marble is a natural resource of calcium as limestone. Marbles are widely available in the Alentejo region of Portugal. Marble is called metamorphic rock because it was created through chemical modification of limestone structure found in the environment. It exhibits good capture capacity, and low sorbent deactivation when compared with

$CaCO_3$. The biggest advantage of using WMP is the reduction in pollution resulting from marble production. However, the main drawback is the price. Marbles are more expensive than limestone; so, only WMP from cutting the marble can be used, from economical point of view, as sorbents for the capture of CO_2 [44].

Other types of natural sorbent wastes, which can be used in the chemical looping technology, are eggshells and mussels. Eggshell contains around 95% of $CaCO_3$ and can be used to produce sorbents for CO_2 capture [45].

Synthetic sorbents have the highest CO_2 capture among cycle of carbonation/calcination. The main reasons are high surface area and the presence of inert material (magnesium) which prevent the sintering process. Compared to natural CaO sorbents, synthetic ones have rougher surface, more pores and smaller grains. That leads to better capture capacity. However, natural sorbents like dolomite and limestone are more commonly investigated due to low costs and availability in the environment [46,47].

2.2.1 Comparison of limestone, waste marble powder and dolomite in terms of CO_2 carrying capacity

Portuguese waste marble powder (WMP) was tested to be implemented in Ca-Looping. Figure 2.5a presents results obtained by Pinheiro *et al.* [44] for several types of WMP and compares them to a reference sorbent, $CaCO_3$. CO_2 capture profile is shown for 10 cycles. In the beginning of the first cycle reactivity is high (89.7% to 93.3%), but along the cycles, it decreases and this phenomenon is observed for every sorbent which was tested. Moreover, WMP carbonation conversion is higher compared to limestone, and deactivation rate is slower. As observed, WMP reactivity stabilises after 10 cycles [45].

WMPα is presented separately (Figure 2.5b) because it was chosen as one which has the highest capture capacity and was tested among 20 cycles to observe its stability; the carbonation conversion reached constant level at 43.3%. Based on previous work found in the literature, it is concluded that differences between WMPα and WMP$_\beta$ occurs because of the differences in structural and textural properties which are responsible for CO_2 capture ability during the cycles.

WMP is an interesting sorbent which can be used in the post-combustion CO_2 capture because it is inexpensive, natural and widely available [44].

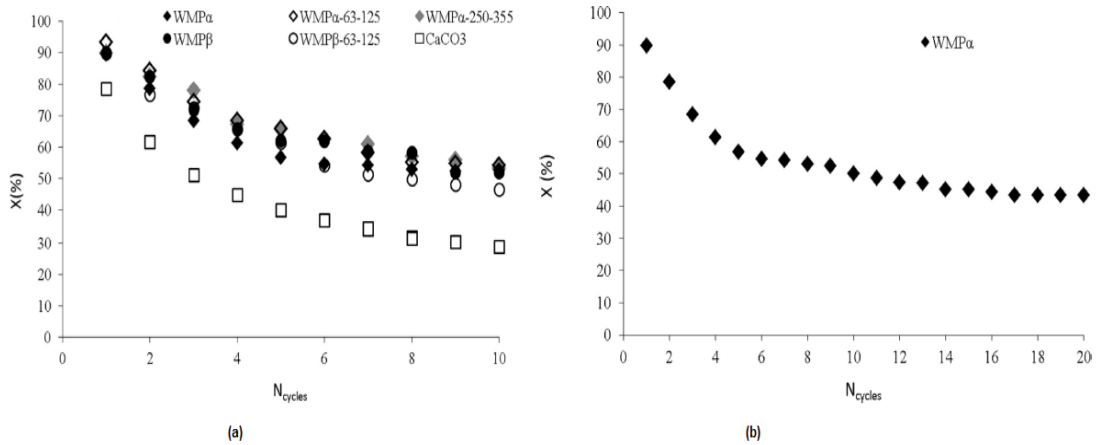

Figure 2.5 Carbonation-Conversion of WMP and $CaCO_3$ sorbents-CO_2 capture capacity [44]

Based on previous studies where WMP was compared with limestone, it was decided by CaReCI project team to carry out the study of the CO_2 carrying capacity with another natural sorbent, dolomite. The comparison between the three sorbents is illustrated in Figure 2.6. In the beginning of the cycles, the WMP and $CaCO_3$ have higher CO_2 capture activity, but after 5 cycles dolomite presents higher carrying capacity than the other two sorbents. In the end of 20 cycles, dolomite CO_2 uptake is twice the $CaCO_3$ carrying capacity. That is the reason why dolomite was chosen to be tested and evaluation of its potential CO_2 carrying capacity will be presented in the experimental work.

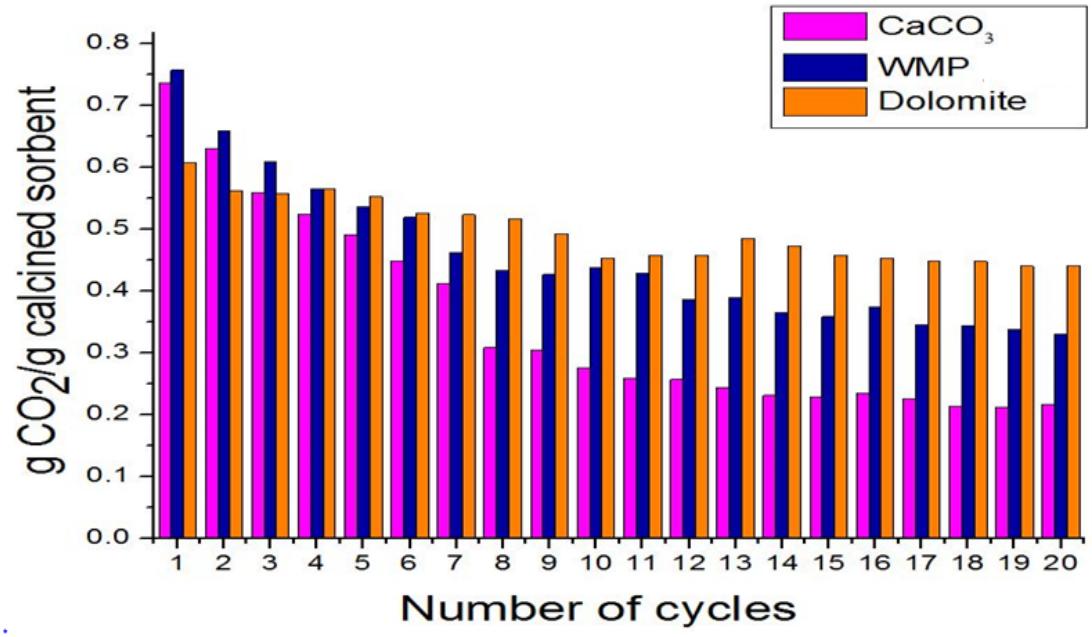

Figure 2.6 Carrying Capacity vs 20 cycles for three types of natural sorbents (adapted from CaReCi project)

The results obtained by Wang *et al*. [43] who tested diverse dolomites, show that dolomites have different carbon conversions. Yang studied different MgO content on the sorbents and verified that the natural CaO–MgO sorbent with MgO content of 31.5%–38.7% should be good to improve the cyclic capture activity of CaO [47].

2.3 Sorbent performance and deactivation phenomena

Sintering and attrition mechanisms are responsible for losses in reactivity of the sorbent. Sintering rate is related to temperature and atmosphere composition. Impurities of the steam, and partial pressure also play a vital impact [48]. Attrition of the sorbents, especially relevant in case of fluidized bed reactors, occurs since the first injection of the particles into hot atmosphere of the reactor. Due to that, there can be a loss of Ca which is equal to the loss of sorbent activation [49].

Figure 2.7 presents the scheme of sintering of particles of Ca-based sorbents in which decomposition undergoes under specified pre-treatment conditions. With the increase of number of cycles, the surface area of sorbent and reactivity to capture CO_2 decrease simultaneously. The scheme

was proposed by Lysikov *et al.* [50] and it enables to observe changes in surface area which has impact on reactivity of the sorbent.

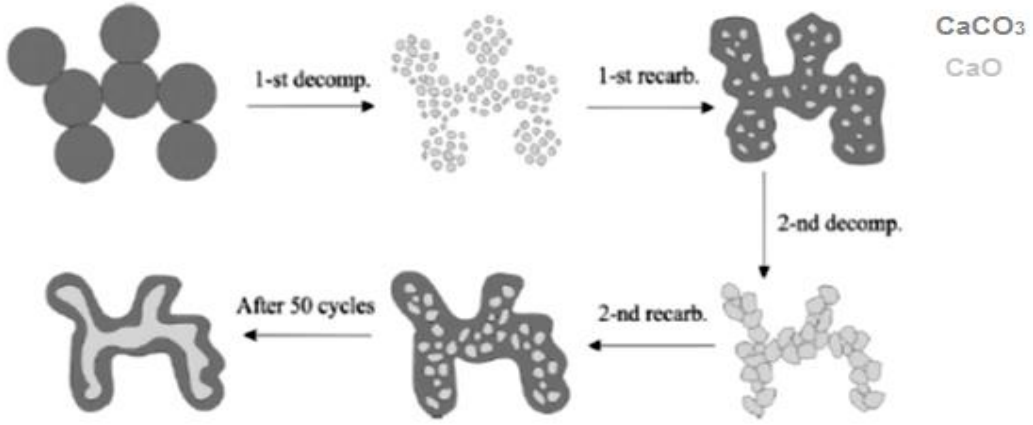

Figure 2.7 Scheme of the textural transformation of the CaO sorbent over many cycles [50]

The first stage of re-carbonation is not completed due to the shrinkage phenomenon which appears after the first decomposition of the solid sorbent. After many cycles of carbonation/calcination which occurs in time, CaO grains increase and they interconnect with each other in form of particle agglomerations leading to the sintering process [52]. The sorbent CaO uptake depends on the outer surface area and it changes with the increasing number of cycles. Sintering process is stopped after some time when a proper agglomeration of CaO is formed. In Figure 2.7, $CaCO_3$ has a dark grey color and CaO particle is depicted in a light grey [49].

Pore blockage phenomenon also appears with the increasing number of cycles along the carbonation reaction. It occurs due to formation of carbonate ($CaCO_3$) layer which closes the pore and inhibits the entry of CO_2 into the particle. Additionally, due to presence of sulphur in flue gases, sulfanation process occurs which also causes blockage of pore [37,50].

The Figure 2.8 illustrates the change in pore size distribution (PSD) of a limestone sorbent along the calcination-carbonation cycles. It was observed that along the cycles the small pores decrease in volume while big pores increase its volume [52], which could be related to the sintering process.

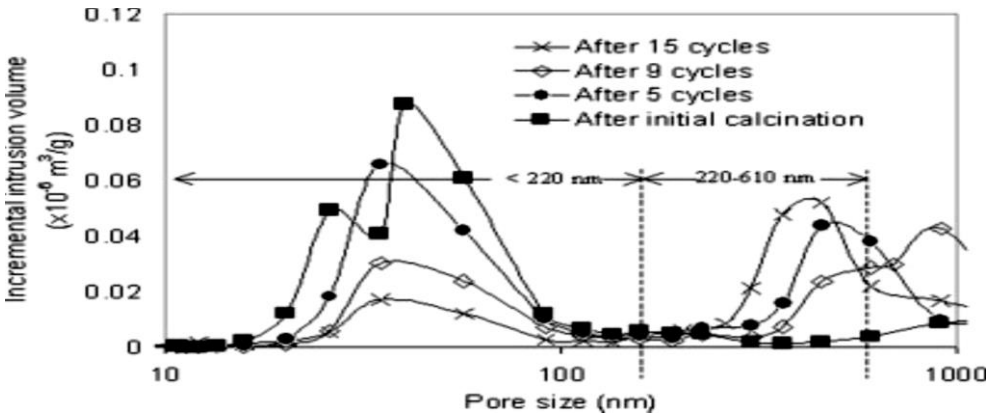

Figure 2.8 Pore Size Distribution after calcination- carbonation [52]

Figure 2.9 shows the relation between time and carbonation rate expressed in %. Carbonation reaction has two significant phases: first stage is fast and chemically controlled and the second is a slow, diffusion controlled phase. As the solid sorbent is exposed more in the second stage, the particles become more reactive during the next calcination reaction. It happens because the porous volume of particle is higher. Porosity is an advantage because it influences the surface area which is responsible for CO_2 capture [53].

It was justified by Chen *et al.* [54] that increasing the carbonation time enables to increase the capture uptake of the sorbent. However, with the increasing amount of cycles, the solid sorbents for which the carbonation reaction lasts longer present better performance. The kinetics of adsorption is described when CaO bonds with CO_2 and it is dependent on carbonation cycle profile.

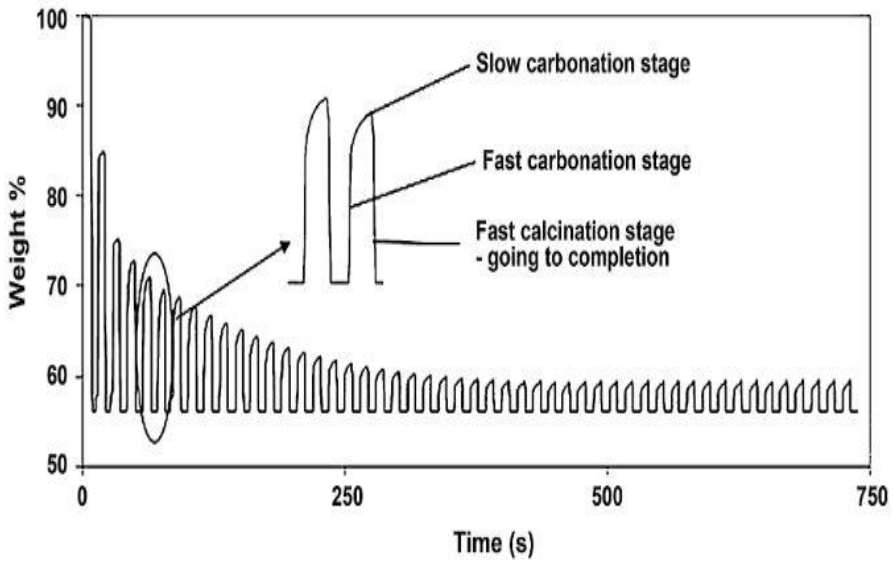

Figure 2.9 Carrying capacity of CaO sorbent through 50 cycles. CO_2 capture in terms of mass change vs. time (TGA data for Havelock limestone) [37]

2.4 Enhancement of sorbents carrying capacity

Scientists are working on additional materials which can improve the stability and carrying capacity performance of the sorbents. They are looking for solutions and apply modifications to improve the surface area, porosity of the material and try to overcome the problem of decrease in capture capacity. There are many techniques which are being developed known as "*rigid supports, additives, nanoparticles, synthetic materials, steam/thermal-treatment, doping methods, changing grain size of the sorbent"*. The most challenging factors are related with recyclability and improvement in decline in carrying capacity of the sorbent [55].

Rigid supports like alumina can protect calcium oxide. The study carried out by Feng [56] shows that alumina enables to maintain a high sorbent conversion around 90% after 9 cycles. However, the main drawback is implementation of the support in the CaO matrix. The additives are types of alkali metals which cover CaO. Research done by Aihara *et al.* [57] emphasizes that advantage of that process that reversibility between reactions lasts longer.

Nano technique presented by Wu *et al.* [58] show that nano $CaCO_3$ increases the adsorption of CO_2 among the cycles. Currently, this method is being developed. The nano particles covered with Al_2O_3 presents similar capacity after 50 cycles. The biggest advantage is that nano materials possess better carrying capacity, good kinetics, stability along the cycles and attrition process occurs slower. However, a significant low density forces to implement nano materials in large volume of the reactor. The problem can cause particle agglomeration during combustion process if the low stream of gas velocity is implemented. The costs of production of nanomaterial are high, so that is why there is a strong attempt to implement materials which are less expensive and widely common in the environment [51].

Another common technique for enhancing the sorbents CO_2 carrying capacity is the use of synthetic sorbents in the Ca-Looping process. Chemical precursors of CaO have better microporosity, higher carbonate conversion and surface area compared to natural sorbents. Some examples are: PCC (precipitated calcium carbonate), calcium hydroxide $Ca(OH)_2$, calcium acetate $Ca(C_2H_3O_2)_2$. MgO can be used in improving the reactivity on surface area [50].

The known method called sol-gel helps preparing CaO-based sorbents with high surface area and pore size, which will be resistant to sintering process, so that the high reactivity can be maintained along the carbonation-calcination cycles. However, main drawbacks of this method are high costs and difficulties to implement in large industrial scale [58].

Another method which is being investigated is steam or water hydration. It can be used after the calcination reaction and before carbonation. Carrying capacity of lime is improved and hydrated lime can capture CO_2 effectively. It is a promising method which enables the regeneration of CaO in which sintering process occurred. By hydration and calcination, porosity of the material (limestone) is improved [61].

2.4.1 Sorbents thermal pre-calcination with different atmosphere

Thermal pre-treatment under different atmospheres can influence the regeneration of the surface area of the sorbent. Figure 2.10 presents different sorbents and their ability to capture CO_2 along increasing number of cycles. The graph shows that with increasing number of cycles there is a decline in CO_2 uptake by two different sorbents: dolomite (D) and limestone (L). In case of dolomite, after 30 cycles the CO_2 conversion is much higher than limestone (except for D-C9.5). The symbol L-N8 and D-N8 denote that the sorbent was treated under 100% of N_2 at 800 °C for 3 hours. This is an intriguing concern, which is related to the chemical composition of these sorbents. Dolomite which contains Mg is more stable in terms of CO_2 capture performance, because Mg blocks/reduces the appearance of sintering phenomena as described in the chapter 2.3 [43]. The symbol D-C7N8 denotes that calcination was carried out for 3 hours at 700 °C under 100% of CO_2 flow and in the second step for 3 hours under 100% of N_2 flow at 800 °C. Compared with D-N8, dolomite D-C7N8 shows better carrying capacity, as it was treated upon two-stage calcination, thus improving the sorbent performance (86.5% vs. 90.6%, respectively). Calcination performed at 950ºC with 100% of CO_2 considerably decreases the carrying capacity [43].

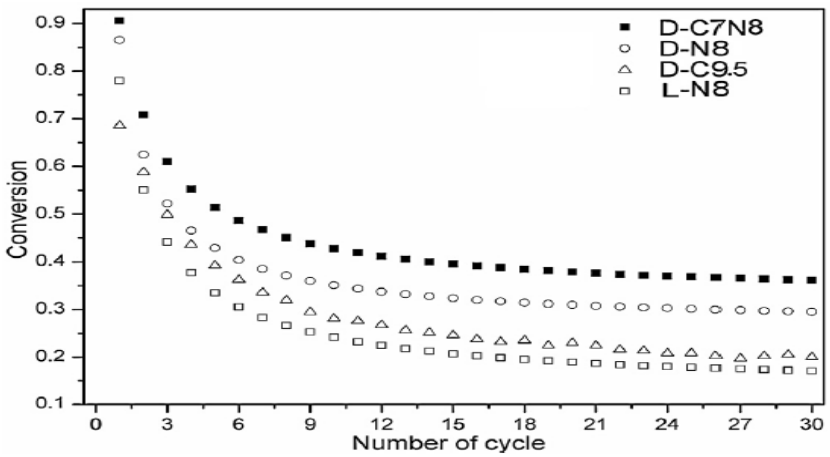

Figure 2.10 Results of cyclic adsorptions for diverse types of limestone [43]

The information about the compounds released during decomposition is picked up from TGA and XRD results as illustrated in Figure 2.11. These results are presented for dolomites calcined in a pure CO_2 atmosphere because the aim of this work is to analyse dolomite as a sorbent to be implemented in Ca-Looping. It can be seen that two peaks were registered at 729 °C and 908 °C. The first peak indicates the decomposition of $MgCO_3$ whereas the second peak suggests the decomposition of $CaCO_3$. The third peak appears at 595 °C due to grinding of the sorbent and similar appearance was observed by Samtani *et al*. [61] The result showed that CO_2 atmosphere conditions favor the two stages decomposition [43].

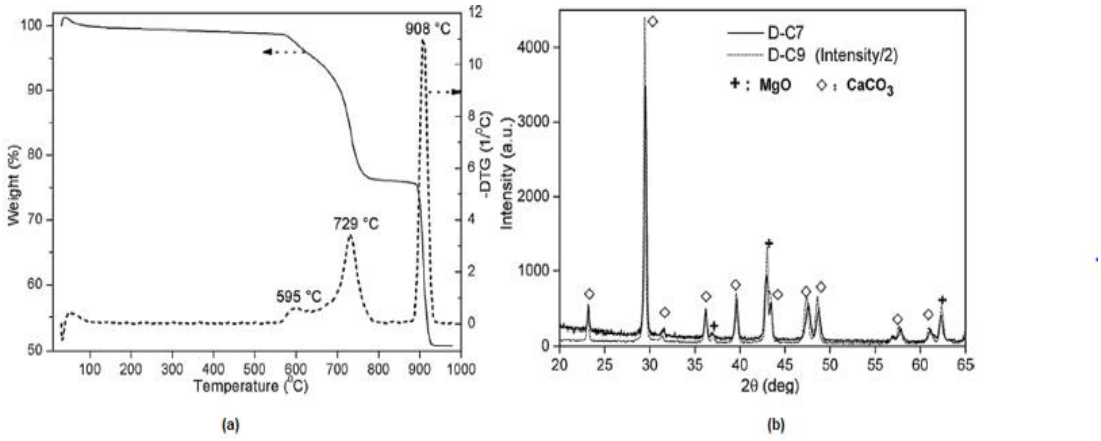

Figure 2.11 Summary of results of TGA and XRD of decomposition of dolomite in CO_2 (a): TGA and DTG; (b) XRD patterns [43]

The test carried out in pure N_2 atmosphere gives the results shown in Figure 2.12. It can be inferred that both investigated atmosphere calcinations allow to obtain Mg-calcite ($Mg_{0.06}Ca_{0.94}CO_3$) phase. This intermediate compound appears due to the decomposition of $MgCO_3$ in the sorbent. However, Wang *et al.* [62] obtained another intermediate compound with the formula $Mg_{0.129}Ca_{0.871}CO_3$ containing more Mg than in this presented study. This transient, intermediate compound of Mg-calcite shows different mechanisms which is dependent on the atmosphere in which decomposition of dolomite

is controlled [43]. Moreover, the presence of MgO and CaO means that both dolomites were fully calcined at temperature more than 800 °C [43,63].

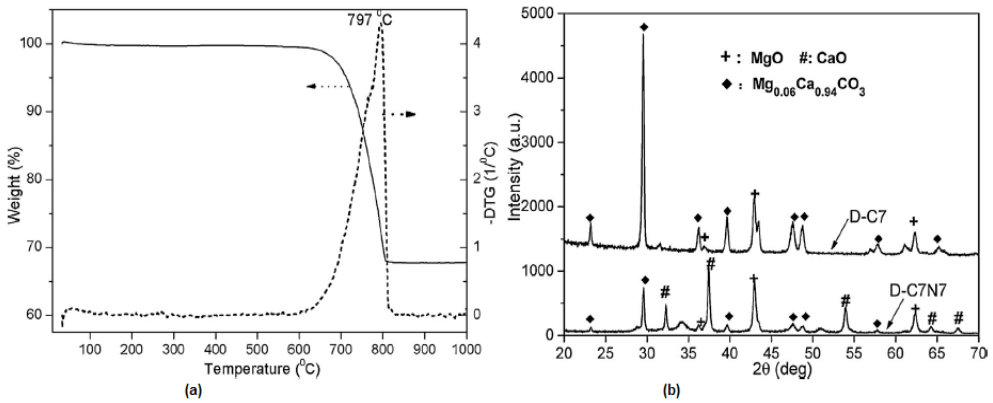

Figure 2.12 Summary of results of TGA and XRD of decomposition of dolomite in pure N_2 (a): TGA and DTG; (b) XRD patterns [43]

Thermal pre-calcination carried out at high temperatures and it was already verified in the experiments that thermal pre-treatment does not always improve the activity of the sorbent along the cycles.

Lysikov *et al.* [50] were the first to present some results related to effect of thermal pre-treatment of the limestone on carrying capacity. Figure 2.13 depicts how the increase of calcination temperature influences reactivity of the sorbent. Very high calcination temperature (above 1100 °C) under N_2 atmosphere, will reduce the surface area and porosity of the implemented sorbent. Calcination temperatures above the set equilibrium point (Figure 2.2) will enhance sintering process, which should be avoided [64]. Moreover, the carrying capacity will decrease. So, calcination should be carried out at the lowest temperature in the reactor.

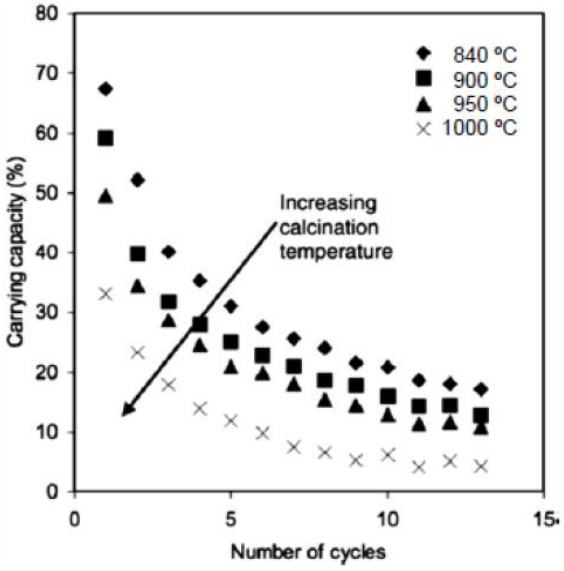

Figure 2.13 Effect of calcination temperature on reactivity [64]

In the experiment carried out an experiment with pre-calcination temperature around 1100 °C for limestone and dolomite with 1000 repeatable cycles, it was observed that after 20 cycles, both sorbents exhibited higher CO_2 carrying capacity than those which weren't pre-calcinated. [65]. However, Ozcan *et al.* [66] reported that in case of implementation of small particle size of CaO-based sorbents, there was no impact of the temperature during the pre-calcination.

Manovic and Anthony [67] focused on analysis of the sorbent which was pre-treated under different temperatures in the N_2 atmosphere. Comparing any pre-treated sorbent with untreated one, the former usually presents better carrying capacity.

The study of triggered calcination, called half calcination in CO_2 and N_2 of the dolomite sample, allows verifying the effect of pre-treatment on the carrying capacity. The studied calcination atmospheres were following: 100% N_2, 50% CO_2/50% N_2 and 50% CO_2/50% N_2 + 100%N_2. The carrying capacity studied for different conditions are illustrated in the Figure 2.14 [68].

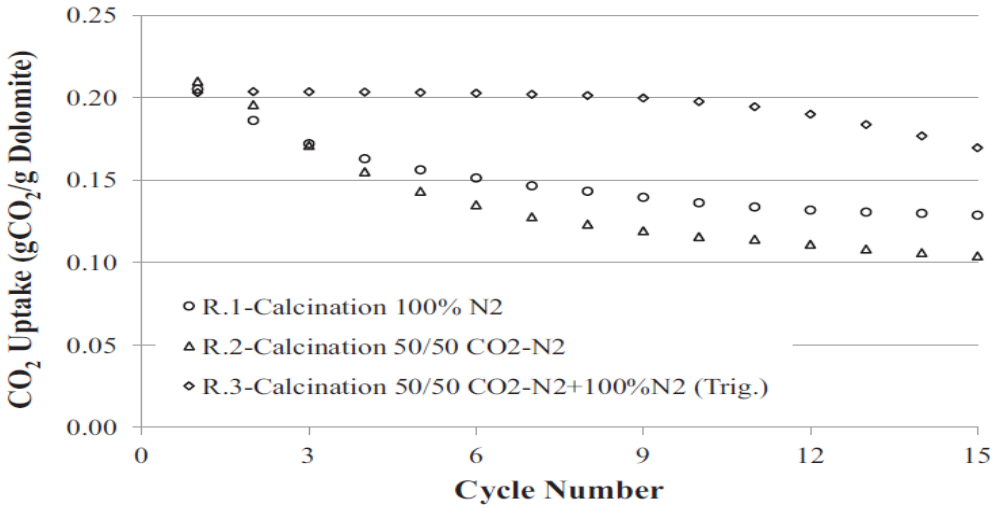

Figure 2.14 Carrying Capacity for different calcination atmospheres [68]

To sum up, the aim of working on the thermal pre-treatment is to improve the sorbent reactivity and slow down the deactivation rate, but some sorbents have higher carrying capacity and some of them have lower. The reason can be that sorbents are different and have different impurities in the structure.

2.5 Thesis Objectives

Dolomite ($CaMg(CO_3)_2$) is an important and abundant carbonate natural material, after limestone. It has been reported in literature that calcined dolomite can become a more efficient and stable sorbent than calcined limestone (CaO) to be used as CaO-based sorbent in the Ca-Looping (CaL) process for post-combustion CO_2 capture. Like limestone, dolomite can be used to capture CO_2 and could be applied in industrial scale. Previous studies developed within the scope of CaReCI project showed that comparatively with the WMP (waste marble powder) and $CaCO_3$, the initial reactivity of dolomite is lower, but after 20 cycles, dolomite presents a higher CO_2 carrying capacity than the other two sorbents. These results showed that natural dolomites could be used as promising carbonate based sorbents to be tested and studied in CaL CO_2 capture process.

The aim of this thesis is to test dolomites, which are natural sorbents widely available, for CO_2 capture by CaL.

The main objectives of this work are the following:

- To study the behavior of two dolomite samples during calcination and carbonation cycles in a fixed bed unit reactor;

- To evaluate the carrying capacity of both dolomites and correlate with the textural and morphological properties;

- To analyse the influence of pre-calcination atmospheres in the carrying capacity and in the stability along the cycles;

- To analyse the dolomites performance for two CO_2 gas mixture compositions of 15% and 25% in the carbonation step during repeated cycles.

3 Materials and Methods

In this section, the characterization of the sorbents and techniques, which were used during the experiments, will be described. The sorbents were characterized by the following techniques: N_2 sorption, X-ray powder diffraction (XRD), scanning electron microscopy (SEM) and thermogravimetric analysis (TGA). The CO_2 carrying capacity was tested in a fixed bed reactor.

The dolomites studied in this thesis are from a production plant in Turkey and have the commercial names: Omyadol 5-GZ and Omyadol SF-GZ. For simplicity, in this thesis these dolomite samples will be called as dolomite α and dolomite β, respectively.

Both types are obtained from high purity of white dolomite and contain calcium magnesium carbonate. Table 3.1 presents the data regarding the particle sizes for both dolomites. Dolomite β is more finely powdered compared with dolomite α. Commercial MgO sample from Merck was also tested (99.9% of purity). To guarantee that all the sorbent samples don't have any moisture, the samples were dried and maintained at 120°C in the oven before the experimental tests. The sorbent sample prepared to be used in the fixed bed reactor is illustrated in Figure 3.1

Table 3.1 The specific product data for dolomite α and dolomite β (adapted from company specific product data: Omya Madencilik)

Fineness Parameters (particle size distribution, % by weight)	**Dolomite α**	**Dolomite β**
Top cut (d98%)	28 μm	9 μm
Mean particle size (d50%)	6 μm	2.5 μm
Particles <2μm	23%	40%

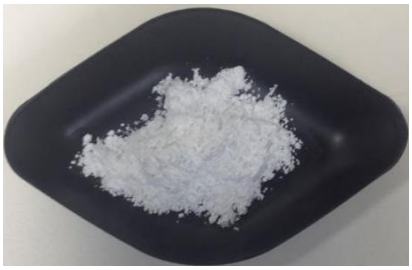

Figure 3.1 Prepared sorbent ready to be placed in the fixed bed reactor

3.1 Chemical composition of the sorbents

Both dolomite samples were experimentally tested for assessing their CO_2 carrying capacity. The elemental composition was carried out in the Laboratory of Analysis in IST (LAIST). The elements like: Ca, Mg, Al, Si and Fe were analysed by ISO 11885:2007 and the C was analysed by an internal method that is accredited by IPAC (Portuguese Institute of Accreditation). The elemental composition is

important to calculate the capacity of sorbents to capture CO_2 among the cycles. The general chemical formula for dolomite is $CaMg(CO_3)_2$.

3.2 Nitrogen sorption technique

Porous materials can be classified into three categories that differ in internal width of pore: micropore (< 2nm), mesopore (between 2-50 nm) and macropore (> 50nm). The absorption process between fluid and pore is different for each type of pore [69].

In N_2 sorption technique, the amount of absorbed gas is determined at the temperature of liquid nitrogen (-196 °C≈77 K). The results are plotted in the form of curve, which is called an isotherm. On x-axis, there is a relative pressure, which is a ratio of actual vapour pressure to a saturation vapour pressure (p/p°) at constant temperature (isothermal process). On y-axis, there is plotted adsorbed volume [70]. According IUPAC (International Union of Pure and Applied Chemistry, classification) there are six types of adsorption isotherms, which are indicators of the textural properties of the material.

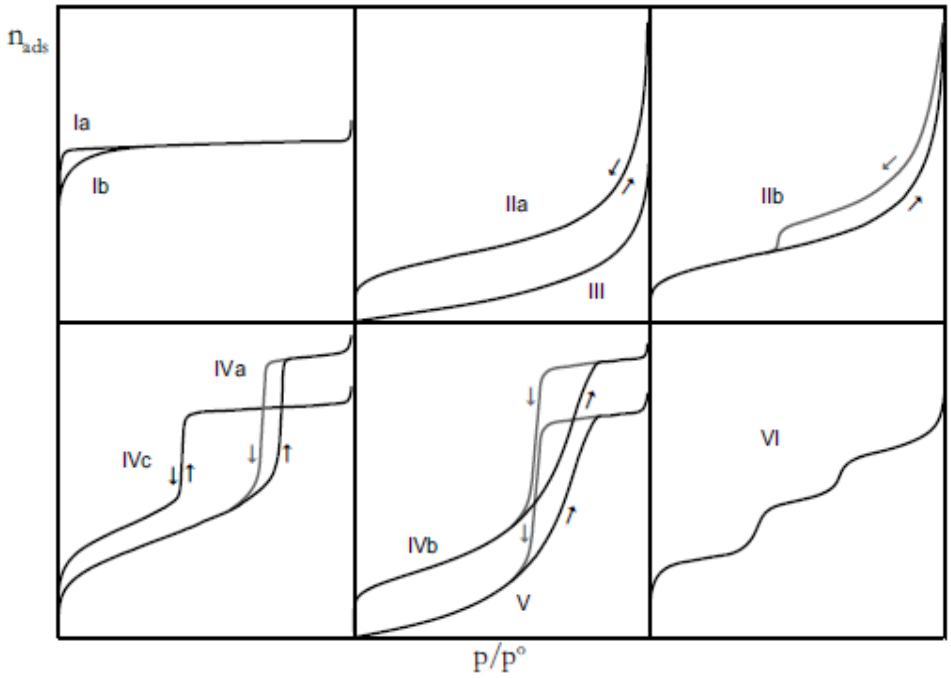

Figure 3.2 Types of adsorption isotherms for nitrogen adsorption [71]

The Figure 3.2 presents all the possible shapes of isothermal curves, which allow for further comparisons of results [71].

1. **Isotherm type I:** indicates the presence of microporous structure in the sorbent. There are two types a and b which differ in terms of micropore filling formation, which occurs at low relative pressure.
2. **Isotherm type II**: In that case, two formations of layers occurs: monolayer and multilayer. The gases are absorbed by a solid material, which can have mesoporous and non-porous solid. Monolayer is formed at low relative pressure filled with nitrogen while multilayer appears at high relative pressure. It is typical for non-porous and macroporous sorbent.

3. **Isotherm type III:** is not so common.
4. **Isotherm type IV**: indicated the mesoporous structure of solids (mesoporosity) formed at a low relative pressure. The multilayer formation appears at the higher relative pressure.
5. **Isotherm type VI:** is characterized by a staircase shape.

Brunauer – Emmett – Teller (BET) equation, determines the specific surface area. The BET model, which enables to calculate the surface of the solid sorbents, is given by the *(Eq.3.1)*:

$$\frac{1}{v\left[\left(\frac{p_0}{p}\right)-1\right]} = \frac{c-1}{v_m c}\left(\frac{p}{p_0}\right) + \frac{1}{v_m c} \qquad \textbf{(Eq.3.1)}$$

where p and p_o are equilibrium and saturation pressure at the temperature of sorption; v is the gas volume which is absorbed; v_m is the monolayer adsorbed gas quantity (nitrogen) and c is the BET constant which is defined by *(Eq.3.2):*

$$c = exp\left(\frac{E_1 - E_L}{RT}\right) \qquad \textbf{(Eq.3.2)}$$

where E_1 is the adsorption heat for the first layer; E_L is the adsorption heat for the second and next layers. The equations for v_m and c are given in *(Eq.3.3)* and *(Eg.3.4*):

$$v_m = \frac{1}{m+b} \qquad \textbf{(Eq.3.3)}$$

$$c = 1 + \frac{m}{b} \qquad \textbf{(Eq.3.4)}$$

The total surface area can be calculated with the *(Eq.3.5)*:

$$S_{total} = \frac{v_m N s}{V} \qquad \textbf{(Eq.3.5)}$$

where N is the constant Avogardo's number (6.022 x 10^{-23}), s is the adsorption cross section of the adsorbing species and V is the molar volume of the adsorbate gas. The specific surface area (S_{BET}) is presented by the *(Eq.3.6),* where S_{total} is the total surface area and m is the mass sample:

$$S_{BET} = \frac{S_{total}}{m} \qquad \textbf{(Eq.3.6)}$$

3.3 Nitrogen sorption equipment

The N_2 sorption analysis were performed in the Micrometrics ASAP 2010 apparatus presented in the Figure 3.3 which is available in the laboratory at Instituto Superior Técnico in Lisbon. The equipment was used to determine the specific surface area, pore size distribution (PSD) and total pore volume carried out the physical adsorption process. Before the measurements, it was necessary to remove the gas or any other impurities, which could be already adsorbed by the sorbent, under vacuum conditions. The outgassed pre-treatment was performed at 90 °C for 1 hour, and 5 hours at 350 °C

(used sorbents) or 120°C (fresh sorbents). The measurements of nitrogen adsorption were carried out at -196 °C≈77 K.

Figure 3.3 Micrometrics ASAP 2010 equipment available at Instituto Superior Técnico

The BET equation was applied to estimate the specific surface area and the pore size distribution (PSD) was achieved by using BJH desorption model. The pore volume (V_p) was calculated from the adsorbed volume of nitrogen for a relative pressure *(p/p_0 of 0.97)*.

3.4 X-ray powder diffraction

XRD equipment was used to identify the crystalline phases of fresh and used sorbents. An official definition of X-ray diffraction is: *"a technique based on constructive interference of monochromatic X-rays and a crystalline sample. A cathode ray tube, filtered to produce monochromatic radiation, concentrate and directed toward the sample, generates these X-rays. The interaction of the incident rays with the sample produces constructive interference (and a diffracted ray) when conditions satisfy Bragg's Law" (Eq.3.7)*: [72]

$$n\lambda = 2d \sin\theta \qquad \textbf{(Eq.3.7)}$$

where λ is the wavelength of electromagnetic radiation, n that is any integer number (usually 1), (θ) is the diffraction angle, lattice spacing (d) in a crystalline sample [73].

The device used for measurements was Bruker D8 Advance, X-ray diffractometer which is available in the laboratory at Instituto Superior Técnico in Lisbon. It is shown in Figure 3.4. Diffractometer used Cu Kα radiation (λ=1.5405 $\dot{A}$), operated at 40 kV and 40 mA. It collected data between 15 and 70° (2θ) with a step size of 0.03 ° and a step time of 3 s. The Crystallography Open Database (COD) was used to identify the crystalline phases.

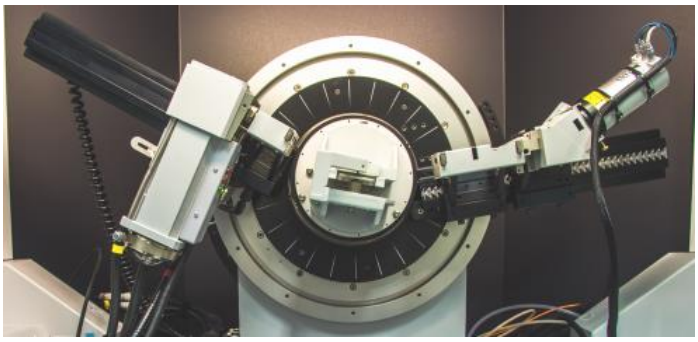

Figure 3.4 X-ray diffractometer - Bruker D8 Advance

The crystallite size of sorbents was estimated using Scherrer's equation *(Eq.3.8)* based on the XRD data.

$$D = \frac{k\lambda}{\beta cos\theta} \qquad \textbf{(Eq.3.8)}$$

where D is the crystallite size (nm), β is full width at half maximum in XRD diffractogram, λ is X-ray wavelength (0.15406 nm), θ is Bragg angle (degree) and *k* is Scherrer constant.

3.5 Scanning Electron Microscope (SEM)

SEM technique magnifies sorbent samples and enables to describe in detail the morphology of the fresh and used sorbents. The device, which was used to carry out the analysis is shown in Figure 3.5. It is called Field Emission Gun Scanning Electron Microscope. The samples were dispersed on a conductive adhesive and prior to analysis; they were sputter-coated with a thin film of Au-Pt to improve image quality.

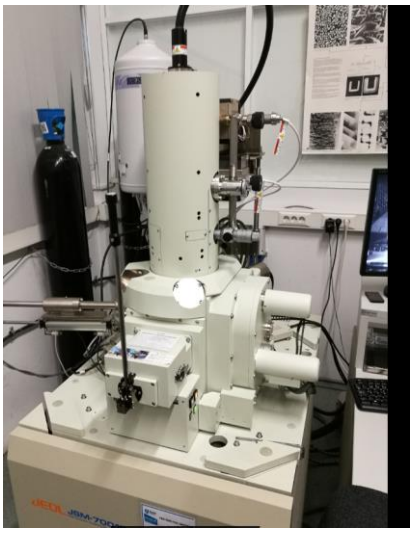

Figure 3.5 SEM: Analytical JEOL 7001F FEG-SEM available at MicroLab Electron Microscopy Laboratory (adapted from IST website)

3.6 Thermogravimetric analyser (TGA)

The ICTAC (International Confederation for Thermal Analysis and Calorimetry) has given the official definition of TGA is *"a technique in which the mass of a substance is measured as a function of temperature whilst the substance is subjected to a controlled temperature program"* [71].

In this MSc thesis, the experiments were carried out in TG-DSC Setsys Evo 16 (Figure 3.6) analyzer. About 15-20 mg of sample used in each test was heated from room temperature to 800 °C under nitrogen flow at a heating rate of 10 °C/min. The mass of sample was placed in the TGA's basket holder. All the sorbent samples were analyzed before the experimental tests were performed in the fixed bed reactor. The main objective was to estimate the mass of calcined sorbent sample and use this value to calculate the CO_2 carrying capacity of each calcined sorbent.

Figure 3.6 TGA-DSC Setsys Evo 16 device (Setaram) equipment available at Instituto Superior Técnico

3.7 Fixed bed unit

A lab-scale fixed bed reactor was used to test the CO_2 carrying capacity and stability of the sorbents in repeated cycles of carbonation and calcination.

3.7.1 Experimental Set up

The fixed bed unit, which was used, is shown in Figure 3.7a. It contains two elements: an oven and a fixed bed quartz reactor where main reaction occurs. The oven (diameter of 10 cm and 30 cm in height) has ceramic-coated elements, which conduct heat. The temperature was controlled by a Eurotherm® 2000 series controller. The quartz reactor (Figure 3.7b) is resistant to the high temperatures used in the experiment. The diameter of the reactor is 3 cm and the height is 10 cm. The sorbent was placed inside the reactor and tested under different conditions. The temperature was controlled manually during the experiment and it was changed accordingly for two different reactions, respectively, carbonation (700 °C) and calcination (800 °C). The temperature was monitored by the thermocouple of type K which was placed inside the quartz reactor. The stream of CO_2 and N_2 (in carbonation) or only N_2 (in calcination) was fed into the quartz reactor and the flow was controlled through mass flowmeters (around 1000 ml/min in total). Before the calcination-carbonation cycles experiments, the analytical

calibration of the mass flowmeters was performed, attending to the desired concentration of CO_2 during the carbonation (15% or 25%); an example is presented in chapter 4. Figure 3.8 shows the two mass flowmeters which were used to control the input of the N_2 (Alicat) and CO_2 (Brooks® 5800 series) in the quartz reactor.

Figure 3.7 Fixed Absorption Unit (a) and Fixed bed quartz reactor (b)

The concentration of CO_2 gas concentration in the outlet during the carbonation-calcination cycles was measured in a Guardian Plus® equipment and it is shown in Figure 3.9 The range of measurement is between 0-30% with ± 0.75% accuracy.

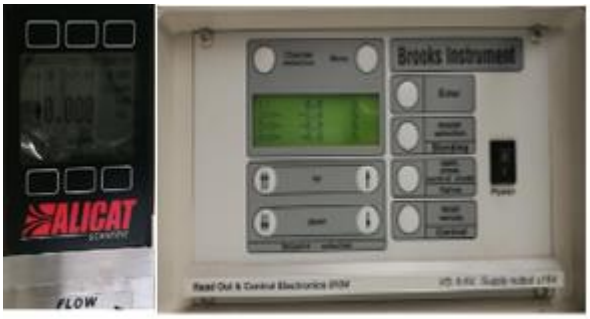

Figure 3.8 Alicat (a) and Brook (b) mass flowmeters

Figure 3.9 Guardian Plus® CO_2 gas analyser

A LABVIEW software interface was used for data acquisition by recording the time, the reactor temperature, the CO_2 concentration in the outlet gas stream and the N_2 input flow during the experiment. The recorded data were analysed in Microsoft Excel 2016.

3.7.2 Experimental procedure carried out in the Fixed Bed Unit Reactor

The reactivity experimental tests were carried out in the fixed bed unit. The sample was previously weighted (about 2 g) and uniformly distributed in the quartz reactor.

The following experimental procedure was implemented respectively, according to the following points:

1. Introduction of the quartz reactor with the sorbent in the fixed bed unit, turn on the oven (usually to 800 °C) and a nitrogen (the pressure gauge is set to 2 bars). The set-point of the flowmeters (Alicat and/or Brooks) depends on the pre-defined conditions defined in the calibration.
2. The valve responsible for the gas flow from the quartz reactor is turned on, as well as, the CO_2 detector that displays the values of the CO_2 gas in %.
3. The thermocouple is placed inside of the quartz reactor. After, it is verified if it touches the bottom of the reactor.
4. The clamps are placed in the top and the bottom of the quartz reactor to prevent the gas leakage. The gas flow should be verified using the bubbles flowmeter.
5. The top surface of the oven with the reactor is covered with the two ceramic plates. The thermal insulation tapes are placed on the bottom and top of the oven to avoid heat loss.
6. The CO_2 gas bottle is open and pressure gauge is set to 2 bars.
7. During the experiment, temperatures and flowmeter of N_2 and CO_2 are monitored.
8. The experiment is being continued for many cycles which are defined in the beginning of each test.
9. In the end of each experiment, CO_2 pressure gauge and the bottle are closed. The oven is turned off. The N_2 flow is reduced and the temperature of the reactor decreases until 300 °C - 400 °C.
10. Finally, when the target temperature is reached, the quartz reactor with the sorbent is carefully removed from the oven and analyzed immediately in N_2 sorption equipment and XRD to avoid H_2O and CO_2 sorption from atmosphere.
11. The data from the experiment are recorded in the LabView (the data treatment is described in 3.7.3).

3.7.3 Assessment of CO_2 capture during carbonation–calcination cycle

After the calcination-carbonation cycles, the data collected in the LabView Software was treated in a spreadsheet previously developed in Microsoft Excel 2016. The methodology used to estimate the amount of CO_2 captured was described in detail in a publication [44] and will be briefly presented here. The mass balance was calculated based on the *(Eq.3.9):*

$$\left(m_{CO_2}\right)_i = \left(m_{CO_2}\right)_{capt} + \left(m_{CO_2}\right)_{notcapt} \qquad \textbf{(Eq.3.9)}$$

where $\left(m_{CO_2}\right)_i$ corresponds to the mass of CO_2 fed to the reactor during the carbonation time;

$\left(m_{CO_2}\right)_{capt}$ is the mass of CO_2 captured;

$\left(m_{CO_2}\right)_{notcapt}$ is the mass of CO_2 not captured.

"On the left-hand side of (Eq. 3.9), the calculation of the amount of CO_2 in the inlet is done by multiplying the mass flow rate of CO_2 by the duration of the carbonation step. On the right-hand side of the equation, the parameters of (Eq. 3.9) are determined by calculating the area for carbonation and calcination stages" (Figure 3.10) [44].

Figure 3.10 is used to calculate the mass of CO_2 in carbonation and calcination steps. The area of S_1 determines the mass of CO_2 not captured during the carbonation and the S_4 the mass of CO_2 that was captured by the sorbent and is released during the calcination step. The area mentioned as S' is a transient situation between both processes and is marked as S_2 which represents CO_2 in the off-gas reaction and S_3 which represents the CO_2 released between 700 °C and 800 °C. The area of region S_2 is determined by integrating the CO_2 concentration (between the time of the splitting of the two curves, the real sorbent testing curve and the blank preliminary testing curve), whereas the area of region S_3 is determined by subtracting S_2 from the area of region S´ [44].

.

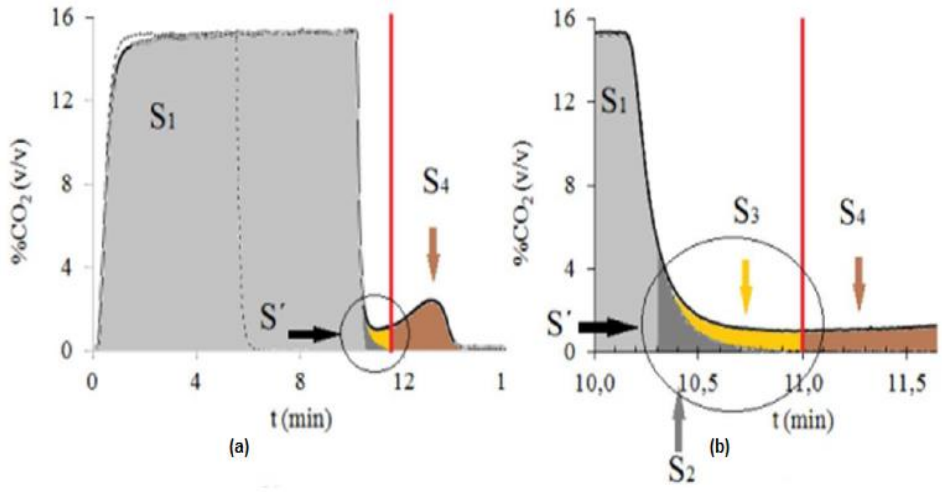

Figure 3.10 Variation of CO_2 concentration in the exiting gas during one cycle of carbonation and calcination (a) CO_2 evolution along the carbonation-calcination cycle and (b) criterion for splitting carbonation and calcination areas in the overlapping S zone [44]

The experiment calculations are considered as valid within an acceptable maximum mass balance error if the value of *(Eq.3.10)* is between 90% and 110%.

$$\frac{(m_{CO_2})_i}{(m_{CO_2})_{notcapt}+(m_{CO_2})_{capt}} \cdot 100 \qquad \textbf{(Eq.3.10)}$$

In the case of the dolomites, the CO_2 carrying capacity (CC) is determined by *(Eq. 3.11)*:

$$CC = \frac{(m_{CO_2})_{capt}}{m_{cal\_sorbent}} \quad \left[\frac{g CO_2}{g_{cal\_sorbent}}\right] \qquad \textbf{(Eq.3.11)}$$

where $m_{Cal\_Sorbent}$ is the mass of the calcined sorbent. Usually, the main component of the calcined sorbent is CaO from the $CaCO_3$, but in case of dolomites, the calcined sorbent has CaO and MgO. The calcined sorbent mass, $m_{cal\_sorbent}$ was determined in TGA analysis. Moreover, mass fraction of calcined sorbent, $w_{cal\_sorbent}$ (%) fed in the reactor after the pre-calcination can be estimated by the *(Eq. 3.12)*.

$$w_{cal\_sorbent} = \frac{m_{cal\_sorbent}}{m_{fresh\_sorbent}} \times 100 \ (\%) \qquad \textbf{(Eq.3.12)}$$

3.8 Experimental planning

The main aim of the experimental tests is to test dolomite samples for determining which could be successfully implemented in a pilot scale Calcium Looping technology. For this purpose, the experimental work was performed in two steps.

Step 1. Comparison of CO_2 carrying capacity of the two dolomites

Step 2. Effect of pre-calcination and carbonation atmospheres in CO_2 carrying capacity and stability of the selected dolomite sample.

In both steps, it was performed a systematic study of the textural (N_2 sorption), mineralogical (XRD) and morphological (SEM) properties of the fresh and used sorbents. These characterization techniques were already described in this chapter. To understand the deactivation of sorbents along the cycles, experimental calcination-carbonation tests with different number of cycles were performed. For comparison purposes, the same pre-calcination conditions (100% of N_2) were applied during the comparison of two dolomites. The dolomite with higher CO_2 carrying capacity was chosen to be studied in step 2. The table 3.2 summarizes the tests carried with both dolomites.

Table 3.2 Summary of the tests carried out in the fixed bed unit

Pre-calcination atmosphere	Carbonation atmosphere	Dolomite α	Dolomite β
100% N_2	15 % CO_2	0 Cycles 5 Cycles 10 Cycles 20 Cycles	

In the second step of the experimental planning, it was assessed the effect of different pre-calcinations (CO_2, N_2) and the effect of use different percentages of CO_2 during the carbonation. The goal in both cases is the same; enhance the capture carrying capacity of the sorbent and reduce the amount of CO_2 in the flue gases.

Taking into account the measurement range of the CO_2 detector (0-30%) installed in the fixed bed unit, it was decided to test the dolomites in two different pre-calcination atmospheres, namely, 25% of CO_2/ 75% of N_2 and 100% N_2. In the case of using 25% in the pre-calcination, the process included two steps: first, 10 minutes calcination at 800 °C with 25% of CO_2 and 75% of N_2, then the second, only with 100% of N_2 at 800 °C until the end of calcination. Two different conditions for CO_2 gas feed composition during the carbonation were chosen: 15% was used to reflect the amount of CO_2 in the flue gases which are usually released from coal power plants and 25% which is the amount of CO_2 which is released from cement production. The table 3.3 shows the tests performed to evaluate the performance of the CO_2 carrying capacity of the selected dolomite. Additional test using MgO as a sorbent was carried out to understand the role of this oxide on CO_2 capture and carrying capacity.

Table 3.3 Summary of the tests performed to evaluate the CO_2 carrying capacity of the selected dolomite β

Pre-calcination atmosphere	Carbonation atmosphere	Number of calcination-carbonation cycles
100% N_2	15% CO_2 (85% N_2)	0 10 20
	25% CO_2 (75% N_2)	0 10 20
25% CO_2 + 75% N_2	15% CO_2 (85% N_2)	0 10 20
	25% CO_2 (75% N_2)	0 10 20

3.8.1 Calibration of mass flowmeters

Before starting with the experimental tests, the calibrations of N_2 and CO_2 mass flowmeters were carried out. In this section, it will be presented only an example for each of the N_2 and CO_2 flowmeters. The calibration was always verified at the beginning and during the experimental tests, if a deviation higher than 5% was observed, an adjustment or new calibration was performed.

Table 3.4 and Figure 3.11 present the data used for the N_2 mass flowmeter calibration (Alicat device). A bubble flowmeter was used during the calibration and the volumetric flow (Q_v) was calculated based on the average of three measures in each Alicat position.

Table 3.4 Experimental data used in N_2 mass flowmeter calibration

Alicat Position	Q_v (ml/min)
0	0
0.1	110
0.2	203
0.4	398
0.6	607
0.7	705.8
0.8	812.8
0.9	921.9
1	1046.8

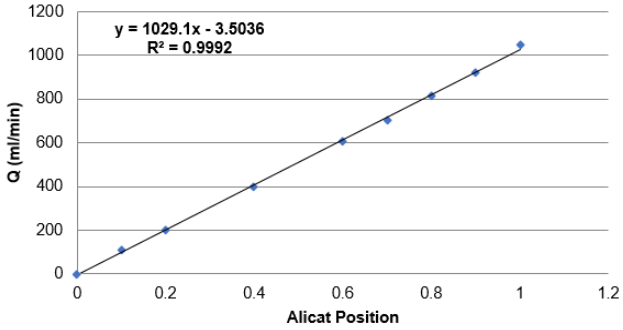

Figure 3.11 Experimental data used in N_2 mass flowmeter calibration

By interpolation it was possible to define the Alicat device position as a function of the volumetric flow desired (e.g. in this case, for 850ml/min the Alicat position should be 0.83).

The next step was to calibrate the CO_2 mass flowmeter. The procedure was the same but the N_2 flow was maintained constant. The calibration of Brooks mass flowmeter used the values displayed in Guardian CO_2 detector (% of CO_2), but the Labview software recorded the signal in volts. For practical purposes, only the values in % of CO_2 are presented here.

Table 3.5 and Figure 3.12 present the data used for the CO_2 mass flowmeter calibration (Brooks device).

Table 3.5 Experimental data used in CO_2 mass flowmeter calibration

Brooks Position	CO_2 (%)
0	0.00
10	4.40
30	12.25
40	15.75
50	18.95
60	21.85
70	24.65

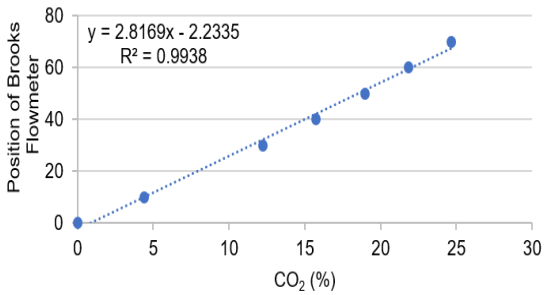

Figure 3.12 Experimental data used in CO_2 mass flowmeter calibration

By interpolation it was possible to define the Brooks device position in function of the % of CO_2 desired (e.g. in this case, for 15% of CO_2 the Brooks position should be 40.0). The same calibration is used to estimate the CO_2 amount released by the exhausted gases during the carbonation-calcination cycles. However, the values in volts are used (e.g. % of CO_2 *vs.* Instrumental Signal (v)).

4 Results and discussion

In the previous studies developed within CaReCI project, the CO_2 carrying capacity of WMP and commercial $CaCO_3$ were tested in a fixed bed unit reactor and compared (chapter 2.2.1). In this work, the dolomites are tested as also natural sorbents. The experiments were performed following the procedure described in section 3.7.2. In this chapter, the experimental results concerning characterization and reactivity of the dolomite sorbents in terms of carrying capacity are presented. This study allowed comparing the reactivity of the dolomites with other natural sorbents. First, the two previously mentioned dolomites were studied, then the dolomite sample with the best performance was selected to carry out complementary studies under different conditions in the fixed bed laboratory scale unit. The characterization of the used and fresh sorbent samples was performed by X-ray diffraction, SEM and N_2 sorption. The results will indicate future research directions that can be followed for the use of dolomites in the industrial CO_2 capture applications.

4.1 Characterization of natural dolomite sorbents

Before starting the experimental tests in the fixed bed unit, the elemental chemical composition, mineralogical, textural and morphologic properties were evaluated.

4.1.1 Chemical and mineralogical composition of dolomites

Table 4.1 includes the data of the chemical composition of dolomite α and dolomite β. Based on data in the table 4.1, it can be concluded that dolomite α has slightly less amount of calcium (Ca) than dolomite β, but a little more magnesium (Mg) in its composition. That small differences between them can influence the carrying capacity to capture CO_2 among the cycles. Besides the main elements which will be considered, the dolomite contains another elements which are treated as impurities like silicon (Si), aluminium (Al) and iron (Fe).

Table 4.1 Chemical elemental analysis of dolomites

Fresh Sorbent	**Element Content (weight %)**					
	Si	**Ca**	**Mg**	**Al**	**Fe**	**C**
Dolomite α	0.05	24.0	11.7	0.02	0.02	12.8
Dolomite β	0.04	24.9	10.2	0.01	0.01	12.6

Figure 4.1 presents the XRD patterns of both sorbents. Both dolomites exhibit the $Ca_{0.5}Mg_{0.5}CO_3$ peak and it is possible to confirm that some Ca is present as $CaCO_3$, however, $MgCO_3$ wasn't identify individually.

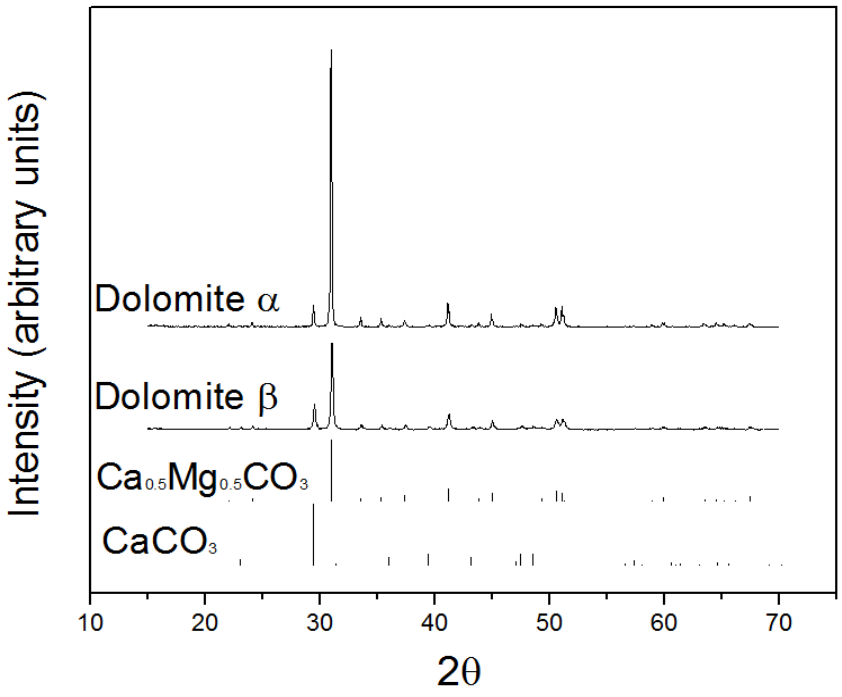

Figure 4.1 XRD patterns of dolomite α and dolomite β

4.1.2 Textural and morphological properties of dolomites

Figure 4.2 shows the N_2 sorption isotherms of fresh dolomite α and β. Table 4.2 presents the specific surface area, S_{BET} and the total pore volume of both dolomites, V_p (not including macroporous with pore width higher than 1000 $\dot{A}$).

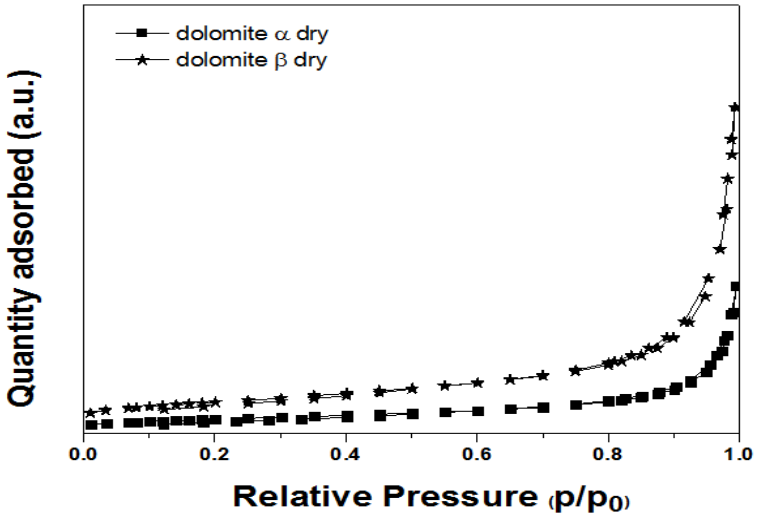

Figure 4.2 N_2 sorption isotherms of fresh dolomite α and β

Table 4.2 Specific surface area and total pore volume of dolomite α and β

Sorbents	S_{BET} (m^2/g)	V_p (cm^3/g)
Dolomite α	2.35	0.006
Dolomite β	5.13	0.013

The isotherms are type II which are typical for non-porous and macroporous sorbent. The specific surface area of fresh dolomite β is higher (about 2 times) than dolomite α but the total pore volume is the same. Figure 4.3 presents the morphological aspect of both dolomites when the sorbent samples were magnified in SEM 5000x.

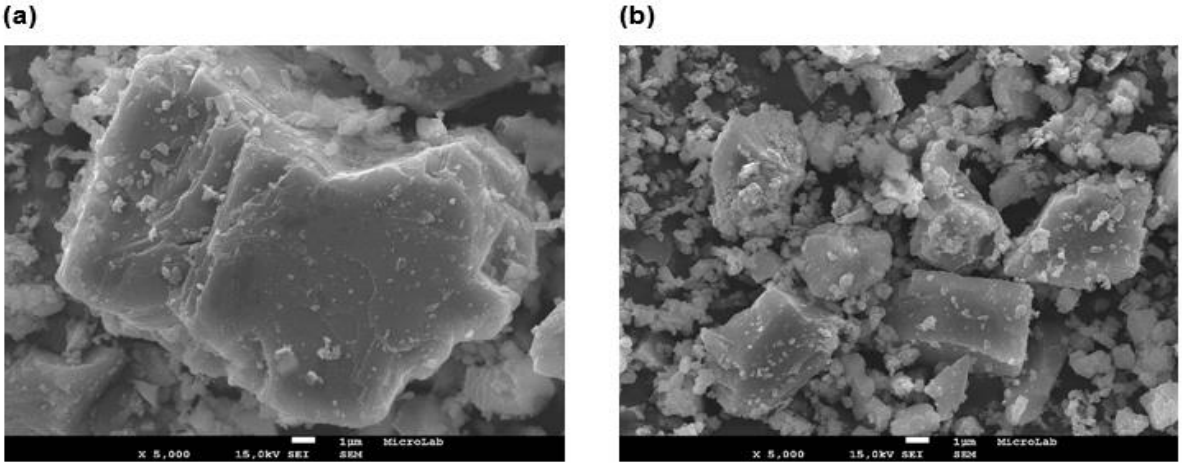

Figure 4.3 SEM images of dolomite α (a) and dolomite β (b)

Comparing SEM photos illustrated in Figure 4.3 of fresh dolomite α with dolomite β, dolomite α has less small particles than dolomite β. This is in the agreement with the data shown in table 3.1, which confirms that dolomite β sample has smaller particles.

4.2 Fixed Bed Unit tests

In this section, the dolomite α and dolomite β are tested in the fixed bed unit. First, the calibration of the mass flowmeters was performed. The CO_2 carrying capacity of dolomite α and dolomite β are presented, as well as the effect of using different pre-calcination atmospheres and CO_2 % during the carbonation.

4.2.1 Comparison of CO_2 carrying capacity of two natural dolomites

The dolomites were tested for determining their CO_2 capture performance ability during 5, 10 and 20 cycles to assess the textural, mineralogical and morphological changes of the sorbent, which enables the interpretation of sorbents modification along the cycles. For comparative reasons, it was performed a 0 cycles test, i.e., the sorbent was pre-calcined with 100% of N_2 in the fixed bed unit but no carbonation-calcination cycle was done. Figure 4.4 presents the carrying capacity of sorbents along the cycles for dolomite α and dolomite β. The data from the experimental tests were collected in the LabView and treated as described in section 3.7.3.

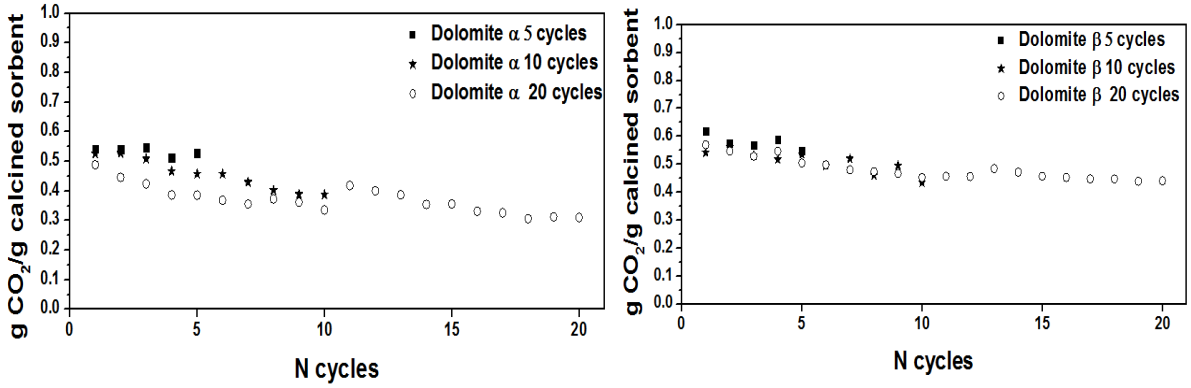

Figure 4.4 Comparison of CO_2 carrying capacity for dolomite α and dolomite β

It can be observed that dolomite β has a higher initial CO_2 capture capacity (10% higher). Probably, it can be partly justified by the slightly increase of calcium content in dolomite β comparatively with dolomite α (table 4.1) and to the different mean particle sizes of the two dolomites (2.5 μm vs. 6 μm, Table 3.1). The mean particle size might be a less significant reason attending to the results presented by Stendardo *et al*. [74] who studied the effect of dolomite particle size on CO_2 capture for average particles size of 98 μm, 780 μm, 1090 μm and 1550 μm. These authors did not found significant differences for dolomites of mean particle sizes between 98-1090 μm [74].

Due to the long time needed to perform 20 cycles, the experiment was performed in 2 days, i.e., after 10 cycles the fixed bed unit reactor which carried out the reactions was switched to pure N_2 at ambient temperature during the night. This can change the sorbent performance, because the sorbent could be exposed to some gas moisture, which can justify the slight increase of capture performance in the second day. The used sorbent hydration [60] is described in literature as a reactivation technique, which allows to improve the sorbent carrying capacity. It was evident in dolomite α but slightly less in dolomite β. In the end of the 20 cycles, the CO_2 capture capacity stabilized for both dolomites.

The theoretical maximum carrying capacity for dolomite α is 0.875 $g_{CO_2}/g_{(CaO+MgO)\ in\ dolomite\ \alpha\ calcined}$ and for dolomite β is equal to 0.864 $g_{CO_2}/g_{(CaO+MgO)\ in\ dolomite\ \beta\ calcined}$. The estimation was based on the theoretical CO_2 carrying capacity of CaO and MgO, respectively, 0.78 g CO_2/g CaO and 1.09 g CO_2/g MgO and attending to the chemical composition of dolomites (Table 4.1).

Theoretically, comparatively with dolomite β the carrying capacity of dolomite α should be slightly higher because of the higher MgO content. However, as mentioned in chapter 2, the MgO present should be almost inert, which means that only CaO should react along the carbonation-calcination cycles and lower carrying capacities are observed for dolomite α.

Textural properties were evaluated by N_2 sorption for both dolomites tested in the fixed bed reactor. Figure 4.5 compares the N_2 sorption isotherms, which are obtained for both dolomites for the different number of cycles (0, 5, 10 and 20 cycles). All the isotherms are type IV and present a hysteresis that is typical for mesoporous solid material. Hysteresis H1 is "*often associated with porous materials exhibiting a narrow distribution of relatively uniform (cylindrical-like) pores*" [75].

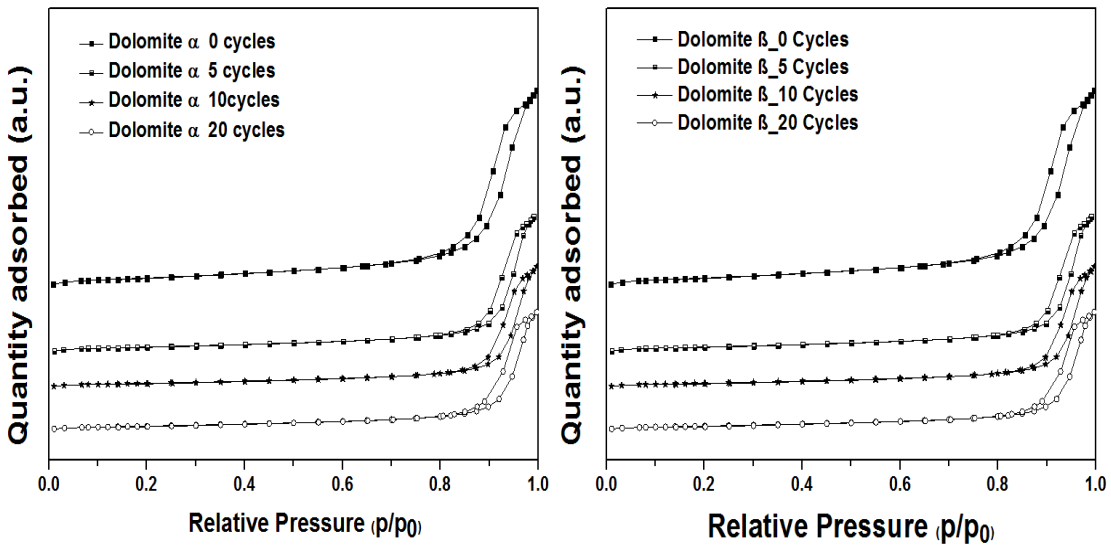

Figure 4.5 N_2 sorption isotherms for the used dolomite α and dolomite β samples along the cycles

Table 4.3 presents S_{BET} and V_p for both dolomites tested in the fixed bed reactor for the different number of cycles. The data provides insight into the carrying capacity differences between the two types of dolomites. In both cases, S_{BET} and V_p decrease along the cycles. Dolomite β, which has better carrying capacity, has higher S_{BET} in the end of the 20 cycles. These results could explain the improvement of CO_2 capture of dolomite β, comparatively with dolomite α, that has smaller S_{BET} and lower ability to capture CO_2.

It is known that sintering is one of the main reasons for the loss of sorbent reactivity, which is justified by the decrease of S_{BET} along the cycles. All the observations are in agreement with the results found in the literature [60].

Table 4.3 BET specific surface area and total pore volume for dolomite α and β

Sorbents	Number of cycles	S_{BET} (m^2/g)	V_p (cm^3/g)
Dolomite α	0	51	0.29
	5	27	0.17
	10	21	0.11
	20	19	0.11
Dolomite β	0	47	0.26
	5	28	0.16
	10	23	0.14
	20	23	0.13

Figure 4.6 presents the correlation between S_{BET} for the used samples and CO_2 capture deactivation (difference between the first and n^{th} cycle carrying capacity) for n=5, 10 and 20. For each dolomite, the carrying capacity observed in the 1st cycle was considered as reference value. Figure 4.6 shows a direct inverse proportional relation between S_{BET} and the deactivation of the sorbent, i.e., when the S_{BET} decreases the deactivation of sorbent increases. For 20 cycles, the deactivation was 36% and 23% for dolomite α and dolomite β, respectively. These results also indicate that for the same S_{BET}, dolomite β has a lower CO_2 capture deactivation, meaning that the decrease of S_{BET} along the cycles is not the only reason for the sorbents deactivation. This is also in agreement with the results presented by Pinheiro and *et al.* [44] for WMP sorbents.

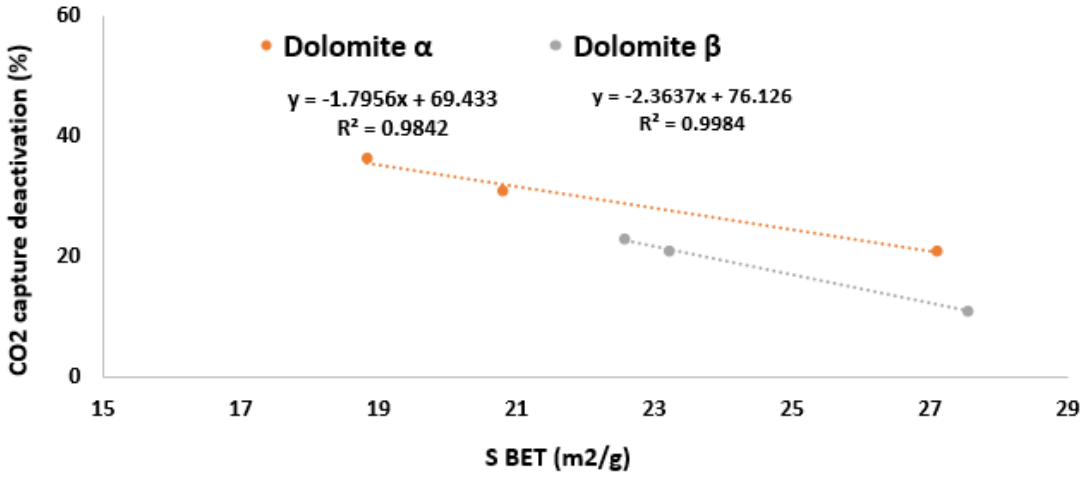

Figure 4.6 Relation between CO_2 capture deactivation (%) and the specific surface area

BJH model (desorption branch) was used to evaluate the pores size distribution (PSD) of used sorbent samples.

Figure 4.7 shows that the pore size is mainly within the range of mesopores (20-500 Å) which is in agreement with the N_2 sorption isotherms results presented in Figure 4.5. The pore volume is higher for dolomite α than dolomite β, especially for 0 cycles. It was observed an increase of mean pore size along the calcination-carbonation cycles for both dolomites, which could explain the decrease of S_{BET} along the cycles and CO_2 carrying capacity deactivation. Larger mesoporous may arise due to internal sintering of CaO particles causing small pores aggregation during the sintering process.

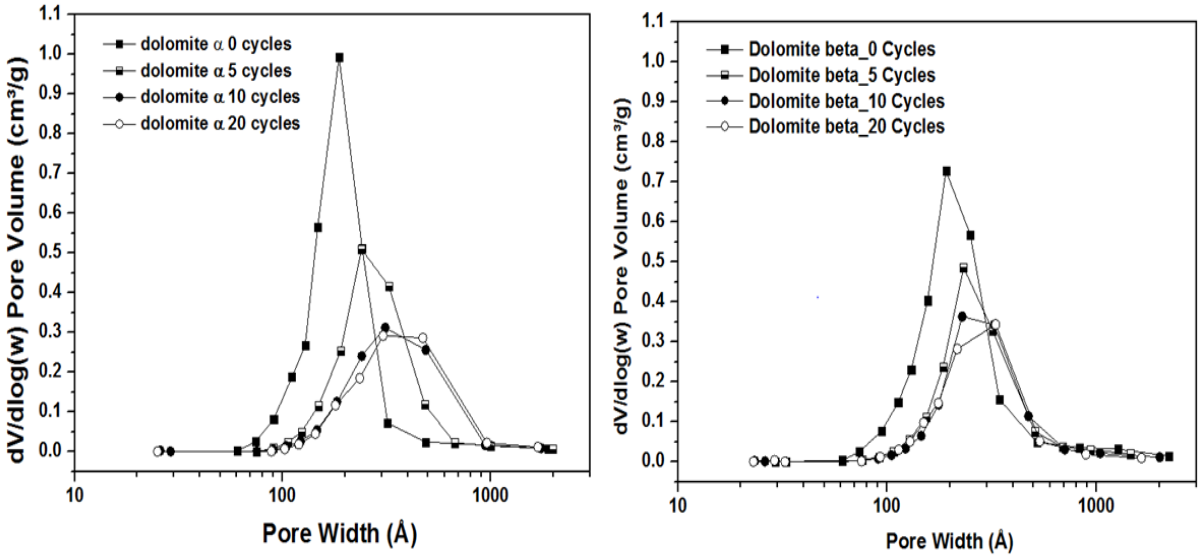

Figure 4.7 Pores size distribution (PSD from BJH desorption branch) for used dolomites

The mineralogical composition of used sorbents was evaluated in X-ray diffraction. X-ray patterns of the dolomite α and dolomite β revealed that the same phases were presented in both, i.e., CaO and MgO. The calcined sorbents are very hygroscopic. However, as the used sorbents were collected from the reactor and analysed immediately, there was no formation of $Ca(OH)_2$ and $Mg(OH)_2$ as can be observed in Figure 4.8.

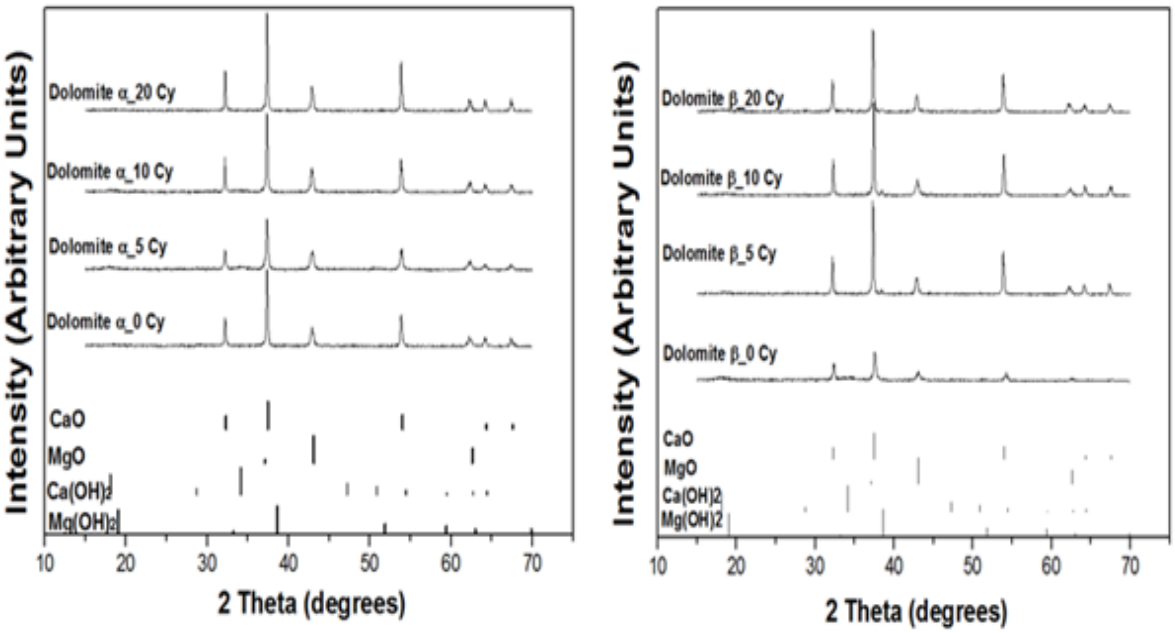

Figure 4.8 Comparison of X-ray patterns of dolomite α and dolomite β

The crystallite size was estimated by Scherrer's equation from XRD results (equation 3.8). It can be observed that CaO and MgO crystallite size increase along the number of cycles (Figure 4.9). These changes can be related to the sintering of the sorbent, which occurs in the calcination/carbonation reactions in the fixed bed reactor. In the case of dolomite α the CaO crystallite size is higher and after 20 cycles is around 47 nm. For dolomite β, after 20 cycles the CaO mean crystallite size is around

44 nm. In case of MgO, after 20 cycles the crystallite size is 28 nm and 24 nm for dolomite α and dolomite β, respectively. Zhu *et al*. [76], with the implementation of Scherrer's equation, found similar results for dolomites respectively, 38 nm and 22 nm for CaO and MgO. Wang *et al.* [43] evaluated the crystallite size when different experimental conditions were implemented and verified that it could change between 45-93 nm for CaO and 33-69 nm for MgO. The higher values were observed for calcinations performed at 950 ºC.

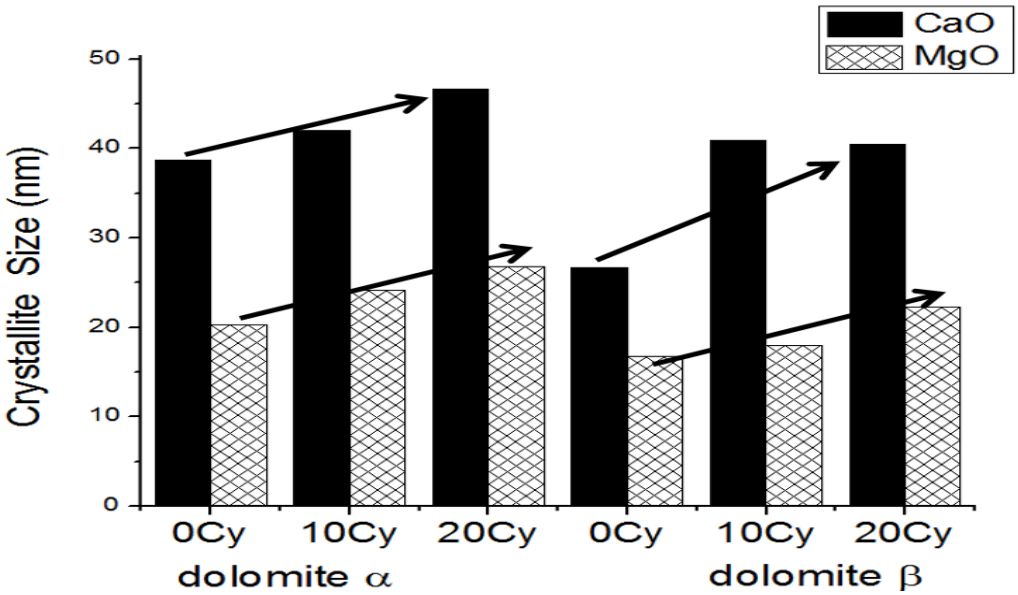

Figure 4.9 Crystallite Size for dolomite α and dolomite β along the cycles

The previous data are in agreement with the literature, i.e., the sorbent deactivation is correlated with the loss of mesoporosity due to the formation of macropores during sintering and with the increase of crystallite grain size (Figure 4.9), linked with the surface area and total pores volume reduction (Table 4.3), and to the pores size distribution profile (Figure 4.7) [77,78,79].

SEM images of dolomite α and dolomite β were magnified 70000x, after 20 cycles are illustrated in Figure 4.10. In both cases, it can be observed the presence of small grains (solid line circle) and more dense and compacted regions (dash circle). Due the limitations of SEM technique it is difficult to accurately identify a Ca and Mg presence in specific zones of the sorbent. Only High Resolution Transmission Electron Microscopy (HRTEM) technique allows to confirm accurately the CaO and MgO zones. Apparently, dolomite α presents more segregated and compacted particles, as it can be seen in dashed line circle and the dolomite β presents less segregation, less compaction and more voids between particles. This could justify the lower CO_2 carrying capacity of dolomite α, i.e., the diffusion of CO_2 molecule inside the pores is more difficult in dolomite α.

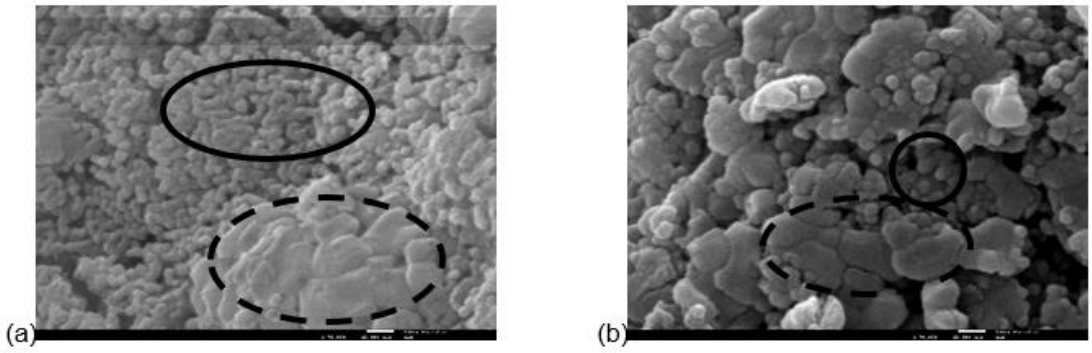

Figure 4.10 SEM images of the dolomite α (a) and dolomite β (b) after 20 cycles (70000x)

SEM images, presented in Figure 4.11, revealed that dolomite β after 20 cycles did not suffer a visible sintering process. However, there was a slight increase in the particles size. It can be observed that after a first pre-calcination (0 cycles) the sorbent has small grains with rough surface area which enables adsorption of CO_2. After 20 cycles, there is an increase of compacted and dense zones.

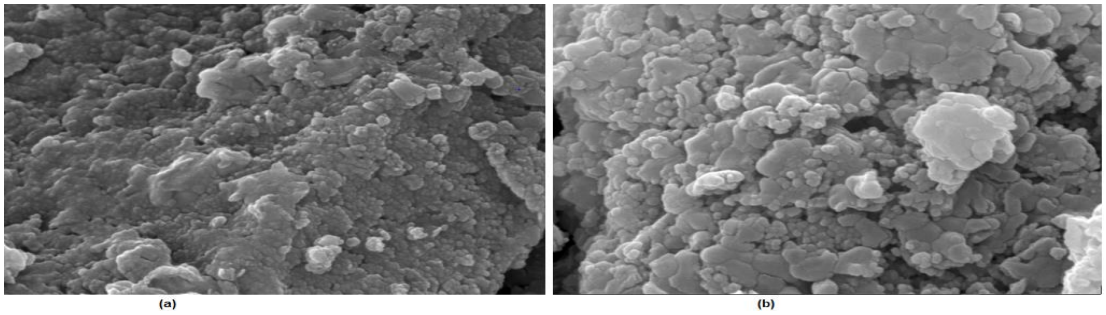

Figure 4.11 SEM images of the dolomite β: (a) 0 cycle; (b) after 20 cycles (40000x)

The comparison on both dolomites is shown in the Table 4.4. Based on the results included in the Table 4.4, dolomite β was selected due to its better performance for CO_2 capture, to be tested under different pre-treatment conditions and the results will be presented in section 4.2.2. This study is important due to the strong need to improve the sorbents performance that could be economically, technically and environmentally viable.

Table 4.4 Comparison of dolomite α and dolomite β

Dolomite α	**Dolomite β**
Lower initial CO_2 capture	Higher initial CO_2 capture
Higher Loss of CO_2 capacity (after 20 Cycles)	Lower Loss of CO_2 capacity (after 20 Cycles)
Smaller S_{BET} (after 20 Cycles)	Higher S_{BET} (after 20 Cycles)
Lower V_p	Higher V_p
Higher CaO and MgO crystallite size	Lower CaO and MgO crystallite size

4.2.2 Influence of pre-calcination and carbonation atmosphere on CO_2 carrying capacity

This section presents the study of the influence of different pre-calcination conditions (100% of N_2 or 25% of CO_2 in N_2) and different CO_2 gas feed composition (15% and 25%) during the carbonation step in dolomite β carrying capacity. There were performed tests with 10 and 20 cycles. For comparative reasons, it was performed a 0 cycles test for the different pre-calcinations conditions.

As in section 4.2.1., the data from the experimental tests were collected from the LabView software interface and treated as described in section 3.7.3. The performance of dolomite was compared in terms of the CO_2 capture efficiency and it is presented in Figure 4.12 as a function of the number of cycles and for different pre-calcination atmospheres and CO_2 % in the carbonation step.

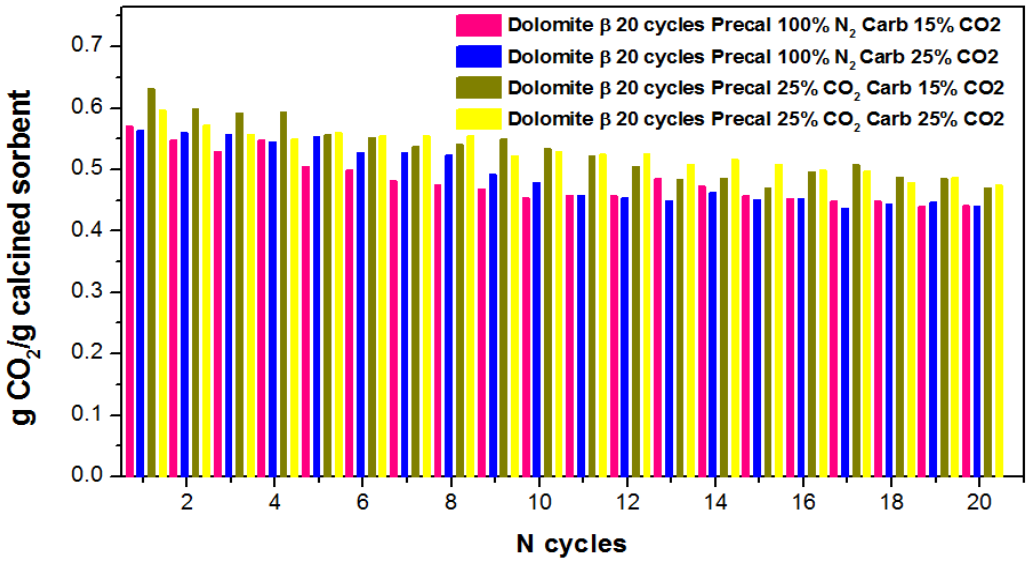

Figure 4.12 Influence of different pre-calcination and carbonation atmospheres in CO_2 carrying capacity of dolomite β for 20 cycles

The results showed that the initial carrying capacity is higher in the case of the dolomite pre-calcined with 25% of CO_2, which means that the pre-calcination atmosphere influences the carrying capacity. The influence of CO_2 % during the carbonation seems to be less relevant, especially when the number of cycles increase. The results confirmed that the use of 25% of CO_2 in the gas mixture during the carbonation step, did not influence significantly the dolomite performance as a sorbent, so it can be implemented in power plants or other industries which flue gases CO_2 concentration is around 10-15% and also in the cement industry, where the flue gases CO_2 concentration is around 25-30%.

As it is known from the literature, dolomite decomposes in a two-step process in the presence of CO_2 in the reactor [80,81].“*During the pre-calcination in a CO_2 atmosphere, an intermediate phase ($Mg_xCa_{1\_x}CO_3$) should be formed, which hindered the de-mixing of CaO and MgO in a secondary step of pre-calcination in a N_2 atmosphere*” [81]. This result in a higher and more stable uptake of CO_2 compared to the results from the pre-calcination only with N_2 [82] as it also can be observed in the results shown in Figure 4.12.

The XRD patterns of the sorbent samples half calcined were evaluated after the half pre-calcination step for both 100% of N_2 and 25% of CO_2 atmospheres, at 800 °C. In the first case, the sorbent was fed into the reactor and the temperature was increased until 800 °C, when this temperature was reached the calcination was stopped and the sample was collected. In the second case, the sample was heated until 800 °C with a 25% CO_2 atmosphere, and remained at this temperature for 10 minutes before the calcination was stopped. Both samples were analyzed by XRD (Figure 4.13).

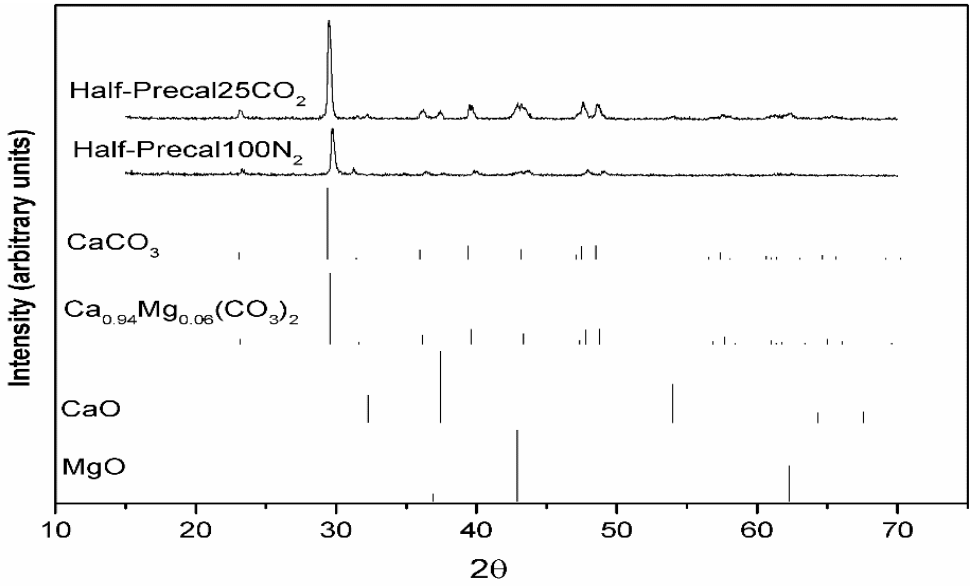

Figure 4.13 XRD patterns of dolomite β pre-calcined under different atmospheres

As can be observed in Figure 4.13 it is very difficult to distinguish between the $CaCO_3$ and $Ca_{0.94}Mg_{0.06}(CO_3)_2$ patterns. However, based on the database information (COD) and literature [81], it was accepted that during the half pre-calcination with 25% of CO_2, it was formed $CaCO_3$ and eventually some $Ca_{0.94}Mg_{0.06}(CO_3)_2$. In the case of half pre-calcination only with N_2, the presence of $CaCO_3$ appears to be less probable. MgO and CaO were identified in both XRD patterns.

The carrying capacity of the tested dolomites for 10 and 20 cycles are shown in Figure 4.14. It can be observed a good repeatability and agreement between the tests performed in the same experimental conditions.

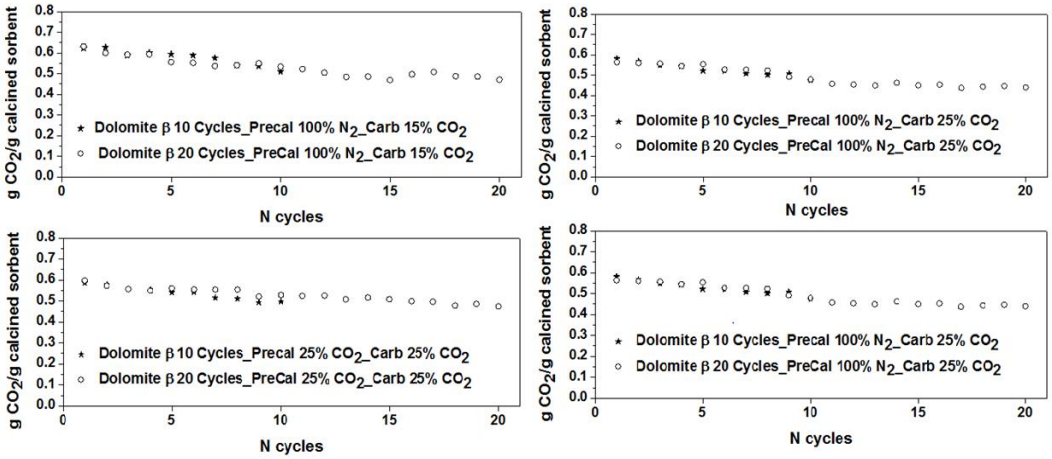

Figure 4.14 Carrying Capacity of dolomite β using different experimental conditions (10 and 20 cycle's tests)

The best results were selected from Figure 4.12 and compared with the results previously obtained within CaReCi project with other natural sorbents. From the analysis of Figure 4.15, one can conclude that:

- in the 1st cycle, the carrying capacity of $CaCO_3$ and WMP_β are similar, but lower for dolomite β probably due the lower Ca amount in this last sorbent,
- after 7 cycles, comparatively with $CaCO_3$ and WMP, dolomite presents a higher CO_2 carrying capacity,
- the best results are obtained for dolomite β pre-calcined in 25% of CO_2, where it is observed an improvement of the carrying capacity along the cycles and a lower sorbent deactivation in the end of the 20 cycles (Figure 4.12)
- the thermal pre-calcination atmosphere leads to the different sorbent performances (Figure 4.12)

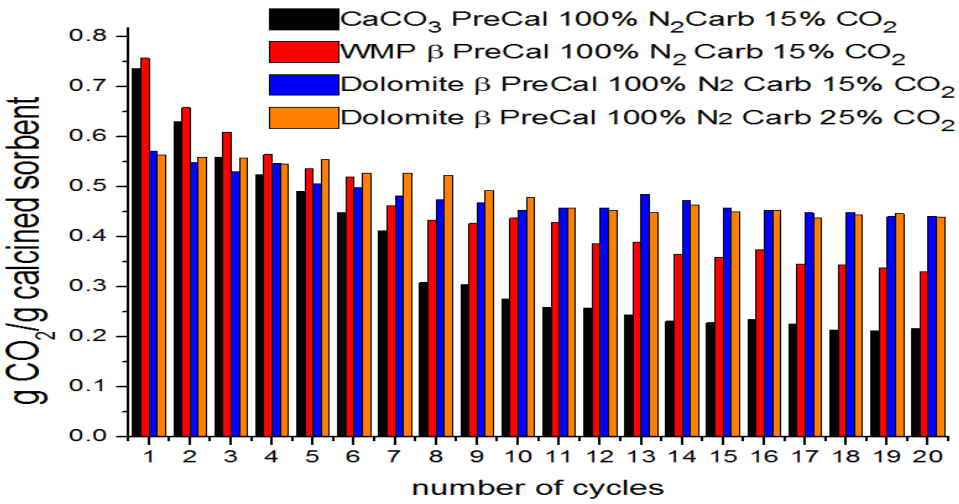

Figure 4.15 Carrying Capacity of $CaCO_3$, WMP and dolomite β pre-calcined with 100% of N_2

Textural properties were evaluated by N_2 sorption for dolomites tested under different pre-calcination and carbonation atmospheres in the fixed bed reactor. The N_2 sorption isotherms of used sorbents are type IV and present a hysteresis type H1 that is typical of mesoporous solid materials.
In order to confirm the importance of the pre-calcination and carbonation atmospheres on the sorbents textural properties, S_{BET} and V_p were compared for both experimental conditions (Figure 4.16).

Figure 4.16 shows that for all cases, there is an initial high decrease in S_{BET} and V_p between 0 and 10 cycles, but from 10 to 20 cycles those properties do not have significant changes. This result is in agreement with the dolomite CO_2 carrying capacity profiles along the 20 cycles previously presented in Figure 4.12. Concerning the effect of the pre-calcination atmosphere, it was observed that it influences the textural properties of the dolomite for 0 cycles. The S_{BET} was around 47-51 m^2/g and 37-38 m^2/g for 100% of N_2 and 25% of CO_2 pre-calcination atmospheres, respectively (Figure 4.16). Comparing these values, it can be concluded that pre-calcination under CO_2 reduces the initial surface area of the sorbent, however during the carbonation-calcination cycles the sorbent CO_2 carrying capacity is higher for the cases of pre-calcination with an atmosphere with CO_2 and a lower deactivation is observed (Figure 4.12). This means that the CO_2 carrying capacity does not only depend on the S_{BET}, and probably, the de-mixing of CaO and MgO during the CO_2 pre-calcination, contributes to a more stable sorbent structure/skeleton and a strong stabilisation of the sorbent is observed from the first cycles. In the dolomites, due to the MgO presence, the pre-calcination with CO_2 contributes to a faster stabilization of the sorbents that show a lower difference in the textural properties between 0 and 10 cycles. That leads to the conclusion that thermal pre-treatment of dolomites affected the textural properties in the firsts cycles but after some cycles, it stabilizes and after 20 cycles the S_{BET} is of the same order for all the other pre-treatments cases.

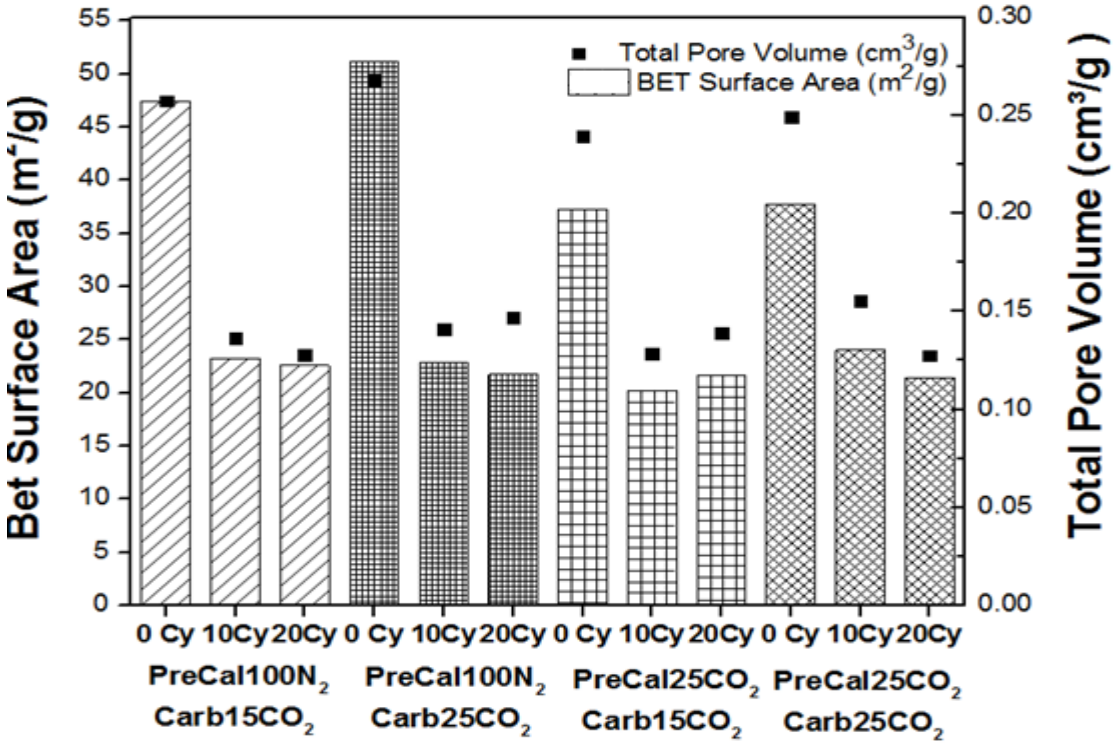

Figure 4.16 Comparison of S_{BET} and V_p of dolomites tested using different experimental conditions

Pore size distribution evaluated by BJH method (desorption branch) is illustrated in Figure 4.17. The results show that for the sorbents pre-calcined with CO_2 the average pore width stabilized, i.e., for 0, 10 and 20 cycles the average pore width was stabilized around 300 Å and did not increase. For the case of pre-calcination only with N_2, for 0 cycles the average pore width was around 200 Å, but for 10 and 20 cycles it increased to around 300 Å.

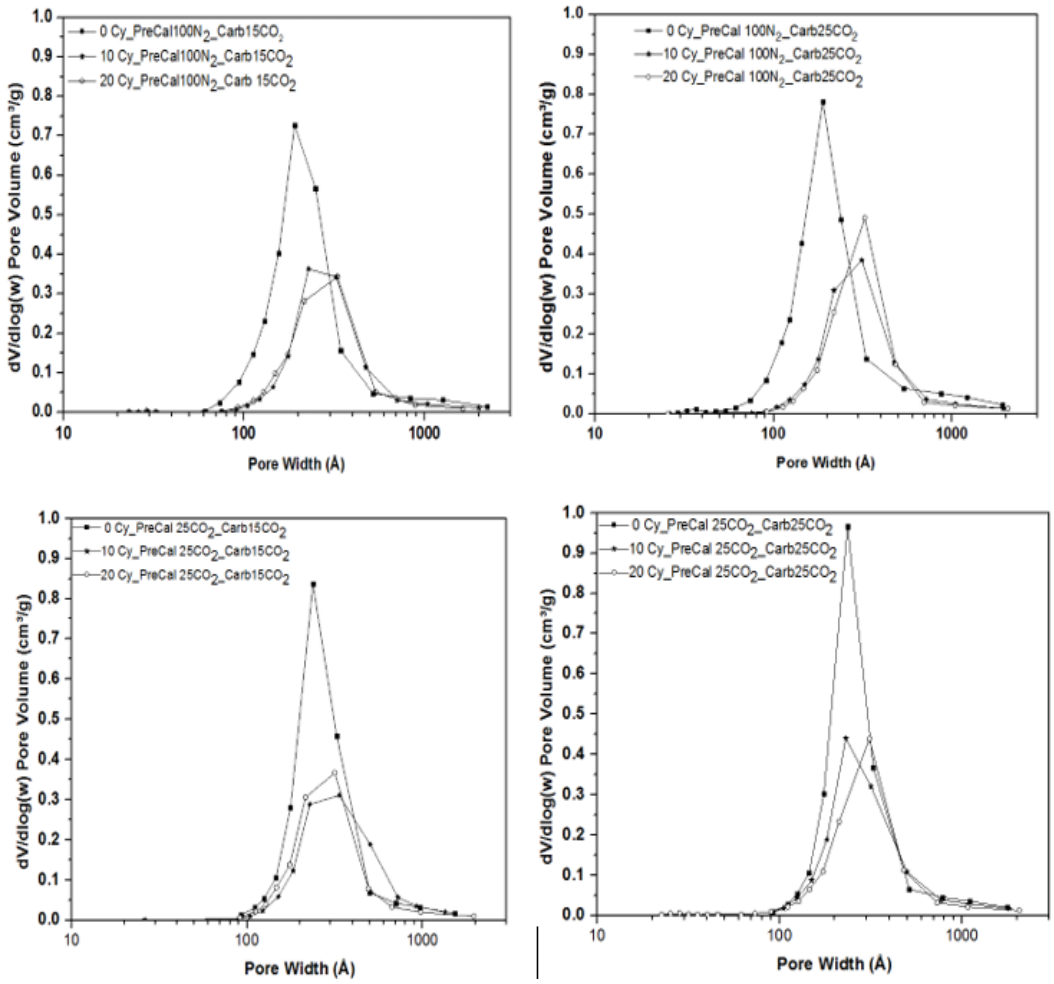

Figure 4.17 Pores size distribution (PSD from BJH desorption branch) for used dolomites

Figure 4.18 shows the results of XRD analysis for the four different conditions tested for the dolomite β. The presence of CaO and MgO was confirmed and no mixed phases were observed between CaO and MgO. It can be stated that in the end of the calcination steps, all the dolomite sorbents are mainly composed by CaO and MgO then they are ready for a new carbonation.

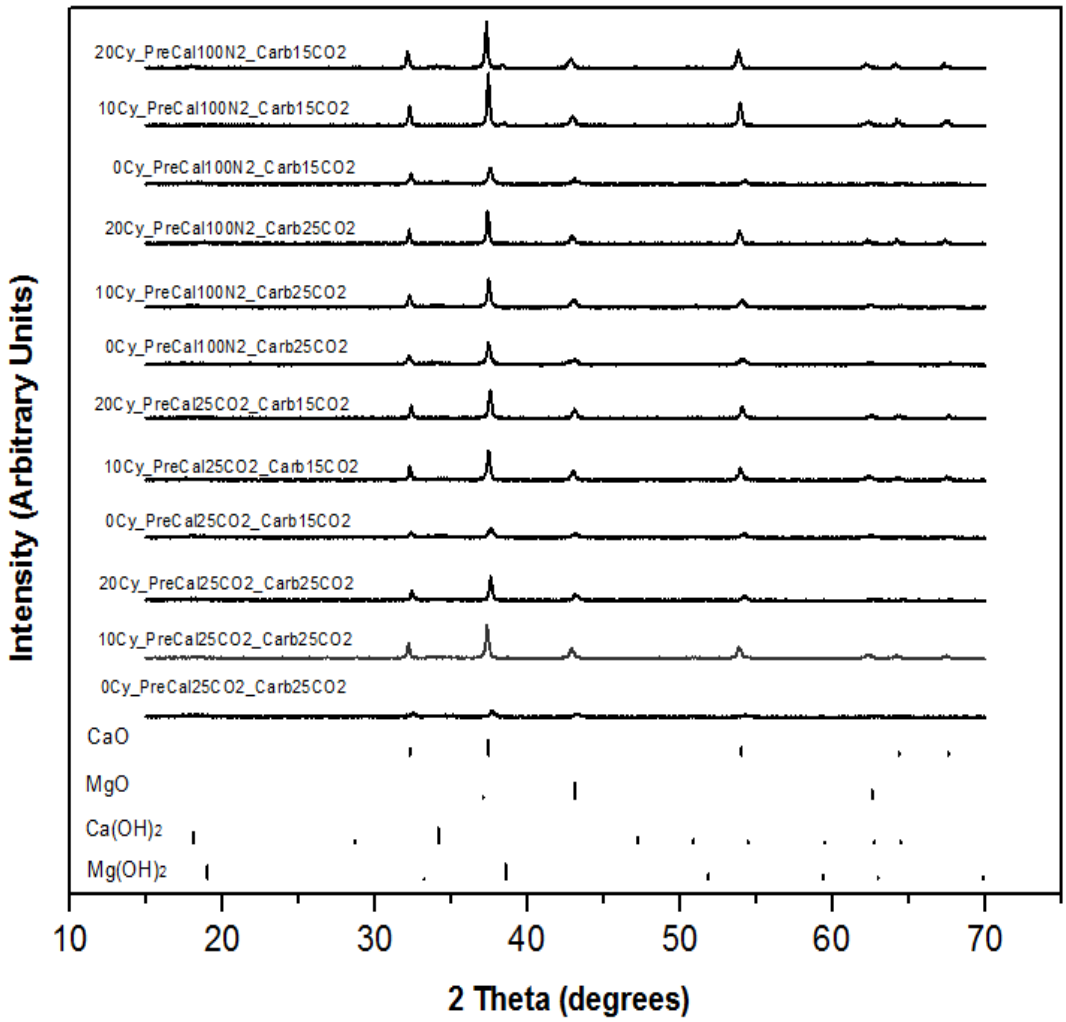

Figure 4.18 Comparison of X-ray patterns of dolomite β tested under different experimental conditions

The CaO and MgO crystallite size of sorbents was estimated by the Scherrer's equation from XRD results *(Eq.3.8).* Results for 0 and 20 cycles are presented for all the tested conditions (Figure 4.19). For all the conditions an increase of CaO and MgO crystallite size is observed between 0 and 20 cycles, as expected, according to the results presented in the section 4.2.2 and literature [59].

The relevant information from Figure 4.19 is related with the higher CaO crystallite size of sorbents pre-calcined with 100% of N_2, comparatively with the pre-calcined with 25% of CO_2. This was especially evident when 0 cycles experiments were compared. These results confirm that the pre-calcination with 25% of CO_2 delays the CaO sintering, especially in the first calcination-carbonation cycles. Wang *et al*. [43] performed 30 calcination-carbonation cycles using different pre-calcination atmospheres and observed a CaO crystallite size of 54 nm and 45 nm for a dolomite pre-calcined with 100% N_2 and 100% CO_2, respectively. These authors stated that *"the presence of the Mg-calcite phase hindered the demixing of Ca and Mg, which delayed the sintering of CaO particles over repeated carbonation/calcination cycles".* After 20 cycles, the difference between the crystallite sizes are smaller which evidence that the pre-calcination atmosphere loses relevance.

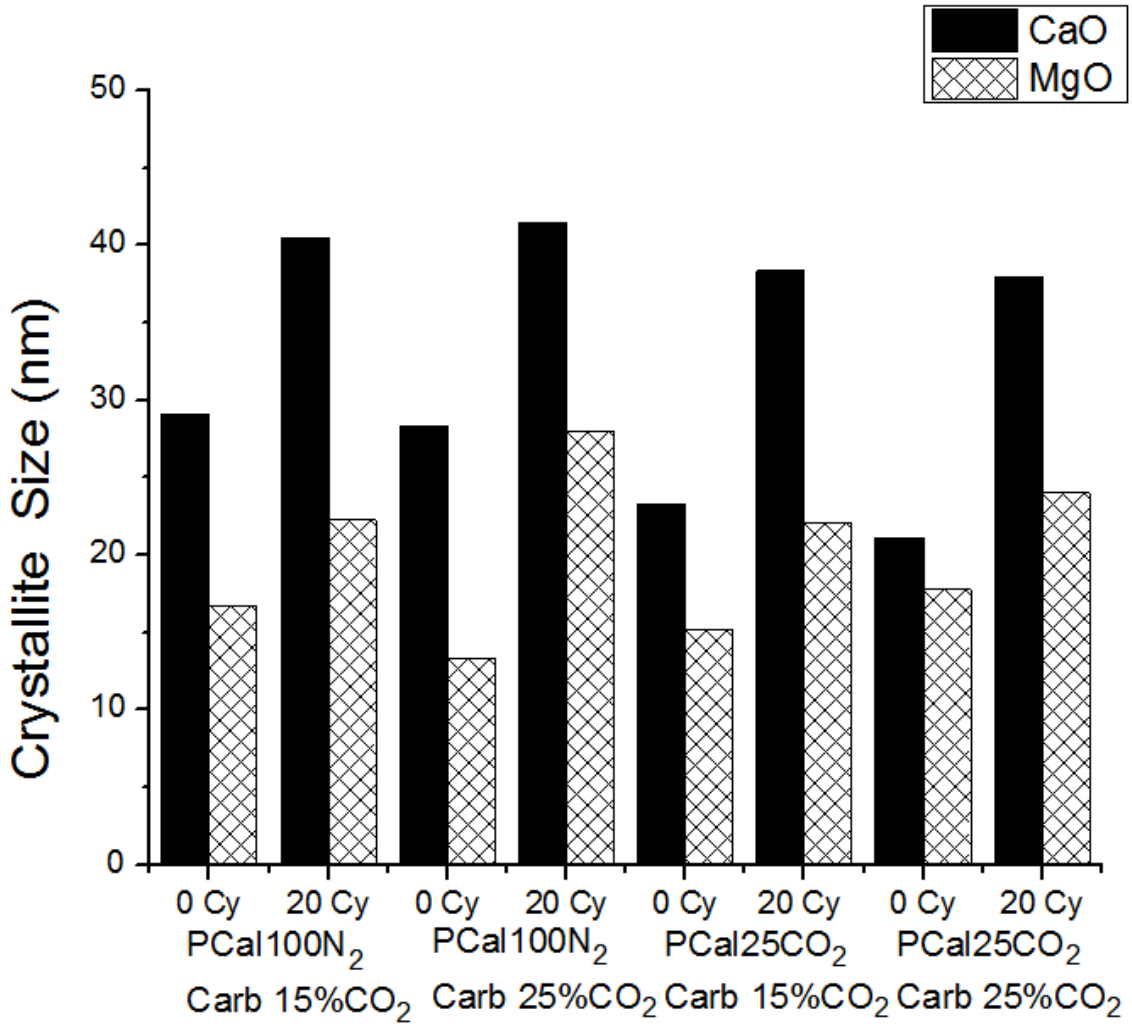

Figure 4.19 Crystallite Grain Size for different pre-calcination of dolomite β

The carbonation adsorption profile in the first cycle (15% of CO_2) for dolomite β under different pre-calcination atmospheres was compared with those obtained for $CaCO_3$ and MgO (Figure 4.20). As described in section 2, two carbonation stages can be observed. The first fast carbonation that is chemically controlled and a second slow carbonation stage that is controlled by the diffusion of the CO_2 in the sorbent.

In the case of MgO, no carbonation was observed at 700°C. Reactivity tests were performed with MgO samples using different carbonation/calcination temperatures: 700 °C/800 °C, 600 °C/700 °C, 500 °C/600 °C and 300 °C/400 °C. The results showed that MgO almost didn't capture CO_2 along the cycles. The main reason for the lack of CO_2 capture capacity by MgO, are the interactions between Mg^{2+} and O^{2-}, which are very strong and disenable to destroy the bonds. Moreover, similar studies confirmed that pure MgO has low CO_2 capture capacity which is the reason of slow kinetic reactivity [83]. Comparatively with the $CaCO_3$ sorbent, dolomites show a lower deactivation with the increasing number of cycles, which could be related to the lower CO_2 diffusion limitations in this sorbent. Due to the presence of MgO particles, the CaO are not so close to each other so, the blockage due to the formation of the $CaCO_3$ layer during the carbonation is less relevant and the CO_2 diffusion along the dolomite is

easier, which means that less time is needed in the carbonation step. In Figure 4.20, as expected it can be observed, that the diffusion stage of the first cycle carbonation is slower for the case of the $CaCO_3$ sorbent.

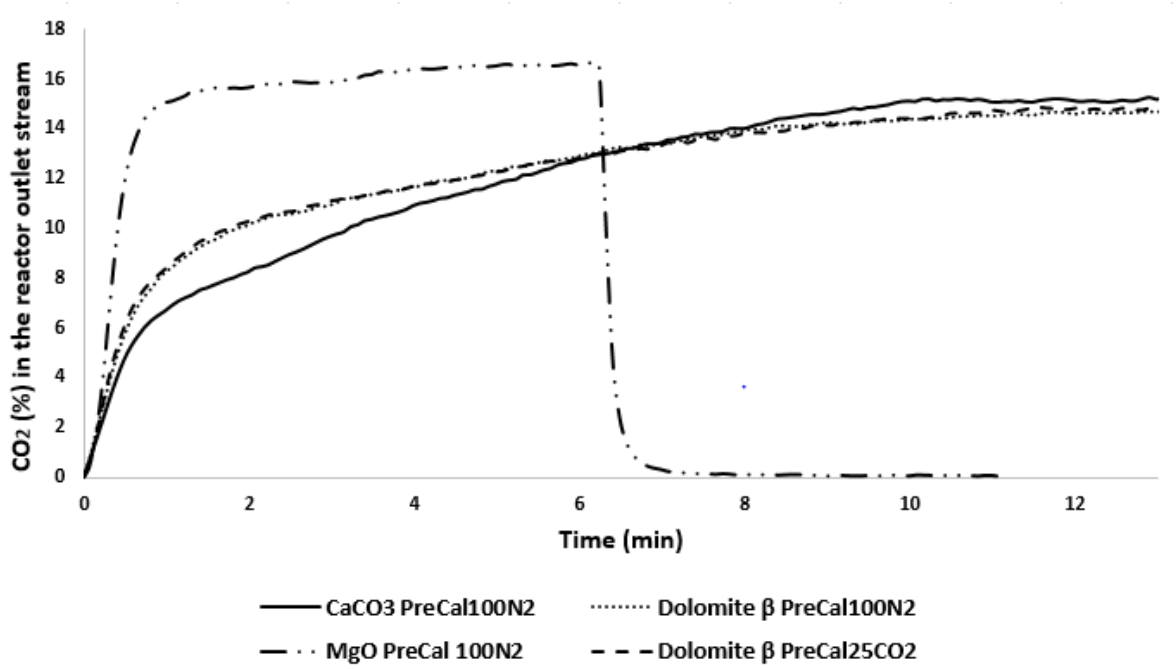

Figure 4.20 Comparison of 1st carbonation profile of different sorbents

All the used sorbents were analysed by SEM after 20 cycles and the images are presented in Figure 4.21. The aim was to find the relationship between the morphological aspect and the sorbents carrying capacity. The magnification (40000x) was the same for all the samples. It was possible to distinguish two types of morphologies: zones with small particles, especially for samples pre-calcined and carbonated with 25% of CO_2 (Figure 4.21(d)) and zones more compacted, apparently sintered. Martos *et al.* [84] found the same type of morphology for dolomite after 20 cycles and identified the smaller particles as MgO and the zones more compacted as sintered CaO. The appearance of sintered zones was more visible for sorbents pre-calcined with 100% of N_2, as indicated by the dark circles, especially when compared with image (d). As the presence of CaO sintered particles are related with the sorbents deactivation, this agrees with the lower carrying capacity of sorbents pre-calcined with 100% of N_2.

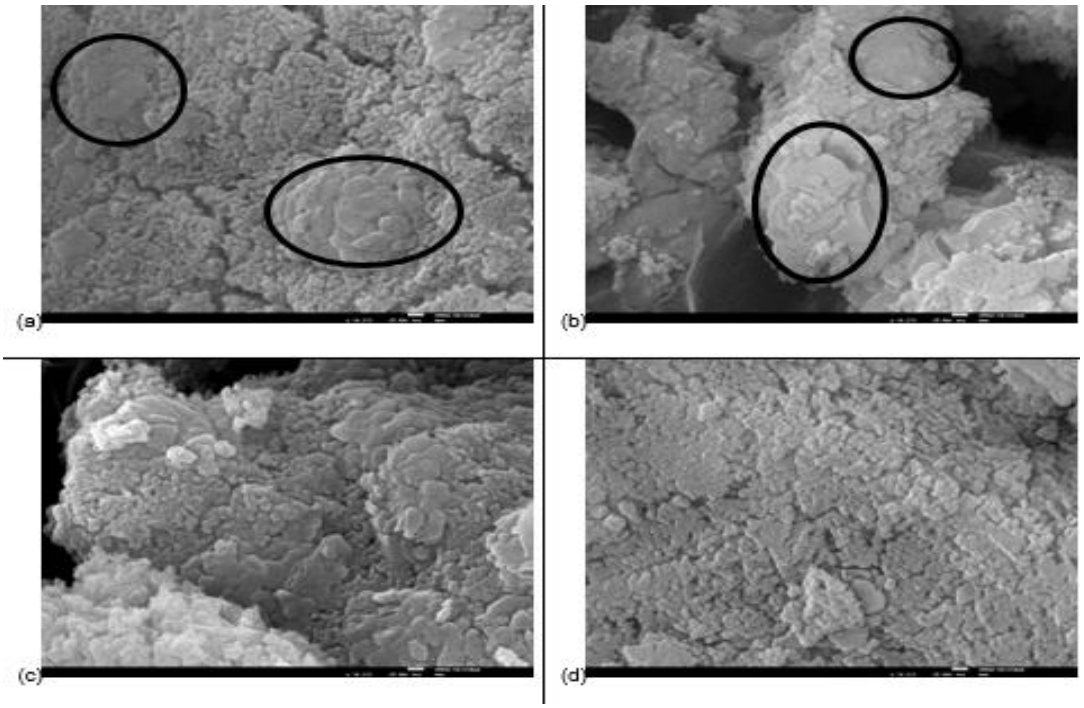

Figure 4.21 SEM images of dolomite β (a) Precal: 100% N_2, Carb: 15%; (b) Precal: 100% N_2, Carb: 25%CO_2; (c) Precal: 25%CO_2, Carb: 15%CO_2; (d) Precal: 25%CO_2 with Carb 25%CO_2 (magnification 40000x)

The results show that the best sorbent performance was obtained in the case of dolomite pre-calcined with 25% of CO_2 tested with 15% of CO_2 in the gas mixture in the carbonation steps, so these conditions were used in an experiment with 50 cycles of carbonation/calcinaton (Figure 4.22).

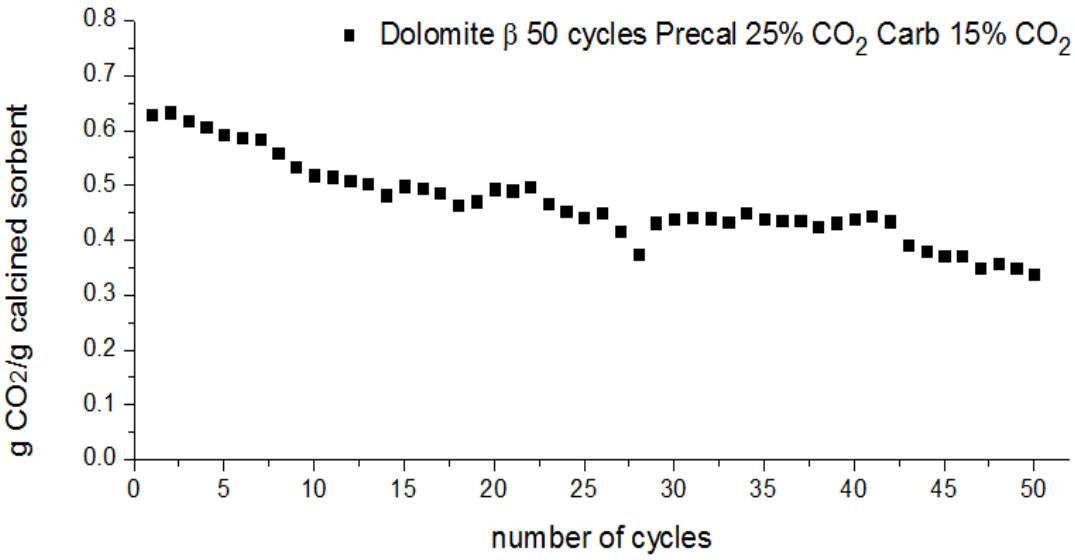

Figure 4.22 Carrying Capacity of the dolomite β through 50 cycles

The 50 carbonation/calcination cycles were performed in the fixed bed reactor for 5 days, where the oven was turned off and a lower constant flow of nitrogen was maintained during the night. All the parameters like temperature and time of calcination and carbonation were controlled manually. The first

20 cycles have a decreasing linear carrying capacity. A deviation in the uptake can be noticed before completion of the 30th cycle. It was caused by the problem with accidently lack of N_2 in the laboratory in the night and that is the reason why N_2 flow was not stabilised. After the 50 cycles, the dolomite β still has a carrying capacity of 0.34 g CO_2/g sorbent. The CO_2 carrying capacity data of Figure 4.22 was compared with data from Figure 4.15. The comparison shows that after 20 cycles the $CaCO_3$ and WMP carrying capacity is around 0.22 and 0.33 g CO_2/g sorbent, which means that the dolomite β pre-calcined with 25% of CO_2, even after 50 cycles still presents a better capture performance than $CaCO_3$ and is similar to WMP for 20 cycles.

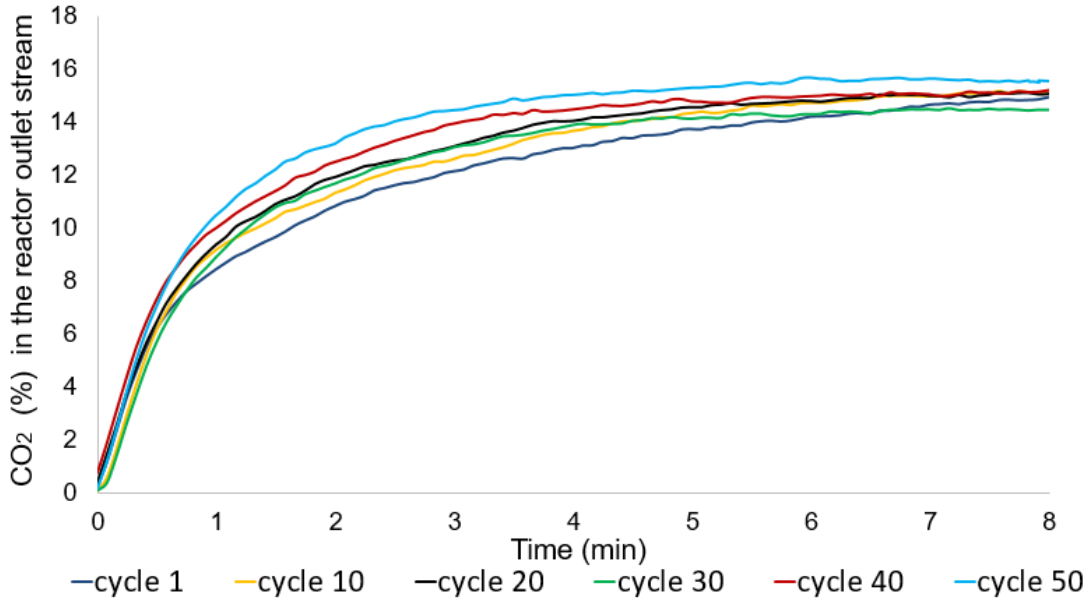

Figure 4.23 Graphical representation of carbonation conversion of dolomite β during 50 cycles presented for chosen cycle-number

Figure 4.23 presents the carbonation profiles for the different number of cycles of the 50 cycles experiment, namely: 1, 10, 20, 30, 40 and 50 cycles. The time for reaching complete carbonation decreases along the increasing number of cycles, and the slope of the first fast chemically controlled carbonation step increases with the number of cycles. This result is in agreement with the results presented in Figure 4.6, and can be explained by a decrease of the number of sorbent CaO molecules available at the beginning of each carbonation step for the reaction with CO_2 due to the increase of sorbent sintering and pore blockage with the number of cycles.

In the beginning of the cycle 1, the role of CO_2 diffusion between the CaO and MgO grains is more relevant, in spite of the $CaCO_3$ layer formed along the CaO and the lower pore size of sorbent there is some degree of diffusion. With the increase of number of cycles, the CaO and MgO crystallite size increases and can occur pores blockage (lower specific surface area), which hinders the CO_2 diffusion along the sorbent. The $CaCO_3$ layer formed during the carbonation step emphasizes this.
The diffusion is one of the main factors which influences the decreasing of the carrying capacity because of the formation of the carbonate layer [85].

5 Conclusions

The Carbon Capture and Storage Technologies are important solutions to prevent climate changes. Considering the aim to reduce GHG emissions with main focus on CO_2, the high-temperature Ca-looping for CO_2 capture is a promising technology to decrease the level of greenhouse gases emission in the atmosphere.

This MSc thesis focused on the post-combustion CO_2 capture process via Ca-looping cycles using natural dolomites as CaO based sorbents. The CO_2 uptake performance of two natural dolomite samples (α and β) as Ca-looping regenerable sorbents were investigated in this work under different conditions with the aim of improving the CO_2 capture capacity and overcoming the problem of sintering and pore blockage deactivation along the carbonation/calcination cycles which can limit the application of natural sorbents.

It was observed that the naturally occurring dolomite sorbents studied can be used as solid sorbents for CaL CO_2 capture with a high carrying capacity and stability along the cycles. As for other natural sorbents, the decrease in the carrying capacity along the cycles is also observed for both dolomites and can be directly related with the decrease of the specific surface area and increase of CaO and MgO crystallite size. But the results indicate that for the same S_{BET}, dolomite β has a lower CO_2 capture deactivation, meaning that the decrease of S_{BET} along the cycles is not the only reason for the sorbents deactivation. This is also in agreement with the results presented by Pinheiro *et al.* [44] for WMP sorbents.

After 20 cycles dolomite β has a better carrying capacity and higher S_{BET} than dolomite α. The calculated deactivation was 36% and 23% for dolomite α and dolomite β, respectively. It can be concluded that decrease in carrying capacity along the cycles is a common property of natural sorbents. The better results obtained with dolomite β were the reason to choose this sorbent for further investigation of different pre-calcination and carbonation conditions carried out in the fixed bed reactor. The best performance was achieved under the pre-calcination atmosphere with 25% of CO_2. In the carbonation steps, the two CO_2 gas feed compositions used were 15% and 25 %. The results obtained after the 20 cycles of carbonation/calcination with dolomite β, treated under different conditions, allowed to conclude that the % of CO_2/N_2 used in the pre-calcination influences the carrying capacity and the % of CO_2 during the carbonation step is less important.

The best carrying capacity was obtained for dolomite β, pre-calcined with 25 % of CO_2. It was concluded that pre-calcination of dolomites with CO_2, not only under pure N_2, resulted in a higher and more stable carrying capacity. It is worth mentioning that, the pre-calcination atmosphere (0 cycles) influenced the textural properties of the sorbent sample. For pre-calcination conditions of 100% of N_2 and 25% of CO_2, the S_{BET} were respectively, around the following values: 47-51 m^2/g and 37-38 m^2/g. Comparing these values, is might be observed that pre-calcination under CO_2 reduce the initial specific surface area of the sorbent, however during the carbonation-calcination cycles the sorbent CO_2 carrying capacity is higher and a lower deactivation is observed. This means that the CO_2 carrying capacity does not only depend on the S_{BET}, and also other factors that contribute to the reduction of CO_2 carrying capacity. Probably, the de-mixing of CaO and MgO during the CO_2 pre-calcination, contributes to a more stable sorbent structure/skeleton, and a strong stabilisation of the sorbent is observed from the first cycles.

For the case of CO_2 pre-calcination, the average pore width (BJH sorption branch) for 0, 10 and 20 cycles was stabilised around 300 $\dot{A}$ but in the case of pre-calcination with N_2 it is possible to observe that for 0 cycles, the average pore width value was around 200 $\dot{A}$, but for 10 and 20 cycles was around 300$\dot{A}$.The pre-calcination with CO_2 contributes to a faster stabilisation of the dolomite β textural properties and the different pre-calcination conditions influenced on the modifications of the pore sizes. The observation of CaO and MgO crystallite sizes of the sorbents samples for 20 cycles, showed that the highest CaO crystallite size was obtained in the case of pre-calcination with N_2 and the lowest in case of 25% of CO_2. It is in agreement with the literature [43] and it confirms that implementation of the CO_2 pre-calcination condition will delay the process of CaO sintering, especially in the first carbonation/calcination cycles.

All the used sorbents were analysed by SEM after 20 cycles. It was possible to distinguish two types of morphologies: zones with small particles, especially for samples pre-calcined and carbonated with 25% of CO_2 and zones more compacted, apparently sintered. The appearance of sintered zones was more visible for sorbents pre-calcined with 100% of N_2. As the presence of CaO sintered particles is related with the sorbents deactivation, this could explain the lower carrying capacity of sorbents pre-calcined with 100% of N_2.

Another test carried out with the 50 cycles of the dolomite pre-calcined with 25% of CO_2 and with 15% of CO_2 during the carbonation showed that after 50 cycles the dolomite sorbent presents a better CO_2 capture performance than $CaCO_3$ and is similar to the carrying capture capacity of the waste marble powder for 20 cycles.

The analysis of the different carbonation profiles obtained for the 50 cycles experiment revealed that the time for reaching complete carbonation decreases along the increasing number of cycles, and the slope of the first fast chemically controlled carbonation step increases with the number of cycles. Therefore, it can be concluded that there is a decrease of the number of sorbent CaO molecules available at the beginning of each carbonation step for the reaction with CO_2 due to the increase of sorbent sintering and pore blockage with the number of cycles.

In the first cycles, the role of CO_2 diffusion between the CaO and MgO grains is more relevant, in spite of the $CaCO_3$ layer formed along the CaO and the lower pore size of sorbent there is some degree of diffusion. With the increase of number of cycles, the CaO and MgO crystallite size increases and can occur pores blockage (lower specific surface area), which hinders the CO_2 diffusion along the sorbent. The $CaCO_3$ layer formed during the carbonation step emphasizes this.

The results obtained in this work are promising and confirmed that dolomites have high CO_2 carrying capacity and stability, that can be improved so that dolomites can be used in power plants or other industries where flue gases CO_2 concentration is around 10-15% and in cement industry, where the CO_2 concentration is around 25-30%.

Future work

Future work in a near future should be directed to:

- - the effect of different pre-calcinations conditions in the dolomites CO_2 carrying capacity and stability (e.g higher CO_2 amount);
- - test different types of dolomites with different amount of Mg and Ca;
- - evaluate the steam effect on the CO_2 carrying capacity of the dolomites;
- - focus on in situ XRD (e.g to observe the mineralogical composition changes during the cycles)

6 References

[1] Greenhouse Gas Emission: Overview of Greenhouse Gases, EPA website, https://www.epa.gov/ghgemissions/overview-greenhouse-gases, accessed 30 July **2017.**

[2] United Nations Framework Convention on Climate Change (UNFCC). (2008). Kyoto Protocol, http://unfccc.int/kyoto_protocol/items/3145.php, accessed 30 July **2017**

[3] Introduction to the Framework Convention on Climate Change Convention, http://unfccc.int/essential_background/convention/items/6036.php, accessed 30 July **2017**.

[4] Climate Action: Paris Agreement, https://ec.europa.eu/clima/policies/international/negotiations/paris_en, accessed 30 July **2017**

[5] Energy Technology Perspectives 2015, Mobilising Innovation to Accelerate Climate Action, International Energy Agency. https://www.iea.org/publications/freepublications/publication/, assessed 10 March **2017**.

[6] Climate Change 2014, Synthesis Report Summary for Policymakers. https://www.ipcc.ch/pdf/assessment-report/ar5/syr/AR5_SYR_FINAL_SPM.pdf, assessed 20 March **2017**

[7] C. Hung, CS. Tan, A Review CO_2 Utilization. Aerosol and Air Quality Research, Handbook of Industrial Chemistry and Biotechnology, **2017**, pp.1781-1802, USA,

[8] DIRECTIVE 2009/31/EC OF THE EUROPEAN PARLIAMENT AND OF THE COUNCIL of 23 April 2009 on the geological storage of carbon dioxide and amending Council Directive 85/337/EEC, European Parliament and Council Directives 2000/60/EC, 2001/80/EC, 2004/35/EC, 2006/12/EC, 2008/1/EC and Regulation (EC) No 1013/200

[9] European Environment Agency Eurostat Statistics, Explained Greenhouse gas emission statistics.http://ec.europa.eu/eurostat/statisticsexplained/index.php/Greenhouse_gas_emission statistics, accessed 1 August **2017**

[10] CaO-Based Sorbents for Post Combustion CO_2 Capture via Carbonate Looping, Z. Skoufa, A. Antazara, I. Millios, E. Heracleous, A.A. Lemonidou, P. Grammelis Editor, Energy, Transportation and Global Warming, Springer, **2016**, pp.571-589.

[11] Global CCS Institute CO_2 Capture Technologies, Technology Options for CO_2 Cature, https://hub.globalccsinstitute.com/sites/default/files/publications/29701/co2-capture-technologies.pdf, accessed 1 August **2017**

[12] Climate Action 2050 low-carbon economy, Climate Action-European Commission. https://ec.europa.eu/clima/policies/strategies/2050_en, accessed 1 August **2017**

[13] D.Y.C. Leung, G. Caramanna, M.M. Valer, An overview of current status of carbon dioxide capture and storage technologies. Renewable and Sustainable Energy Reviews, **2014**, 39 (6), pp.426-443.

[14] Carbon Capture and Sequestration: Biological Technologies. K. Nouha, P. Rojan, S. Yang, R.D. Tyagi, R. Y. Surampalli, T.C. Zhang. Edited by R. Surampalli, T.C. Zhang, R.D Tyagi, R. Naidu, B.R., Gurjar, C.S.P. Ojha, S.Yan, S. Brar, A. Ramakrishnan, C.M. Kao, Carbon Capture and Storage: Physical, Chemical, and Biological Methods. American Society of Civil Engineers **2015**, pp.37-51.

[15] M. Kotyczka-Morańska, G. Tomaszewicz, G. Łabojko, Comparison of different methods for enhancing CO_2 capture by CaO-based sorbents. Review, Physicochemical Problems of Mineral Processing, **2012**, 48, pp.77–84.

[16] V.G. Gomes, KWK. Yee, Pressure swing adsorption for carbon dioxide sequestration from exhaust gases, Separation and Purification Technology, **2002**, 28, (2), pp.161–171.

[17] M. Yang, N. Chen, C. Huang, Y. Shen, H. Yang, C. Chou, Temperature swing adsorption process for CO_2 capture using polyaniline solid sorbent, Energy Procedia, **2014**, 63, pp.2351–2358.

[18] L. Zhao, M. Weber, D. Stolten, Comparative investigation of polymer membranes for post-combustion capture, Energy Procedia. **2013**, 37 pp.1125-1134.

[19] Y.Y. B. Xue, X.L. J. Chen, M. Wang, A comparative study of MEA and DEA for post-combustion CO_2 capture with different process configurations, International Journal of Coal Science and Technology, **2017**, 4 (1), pp.15–24.

[20] A. Samanta, A. Zhao, G. Shimizu, P. Sarkar, R. Gupta, Post-Combustion CO_2 Capture Using Solid Sorbents: A Review, Industrial and Engineering Chemistry Research, **2012**, 51 (4), pp.1438–1463.

[21] C. Xu, N. Hedin, Microporous adsorbents for CO_2 capture – a case for microporous polymers?, Materials Today, **2014**, 17 (8), pp.397–403.

[22] R. Gupta, H., Fan L-s., Carbonation-calcination cycle using high reactivity calcium oxide for carbon dioxide separation from flue gas. Industrial and Engineering Chemistry Research, **2002**, 41 (16), pp.4035-4042, 20.

[23] Y. Xu, C. Luo, Y. Zheng, H. Ding, D. Zhou, L. Zhang, Natural Calcium-Based Sorbents Doped with Sea Salt for Cyclic CO_2 Capture. Chemical and Engineering Technology, **2017**, 40, (3) pp.522–528.

[24] A. Lyngfelt, C. Linderholm Chemical Looping Combustion of Solid fuels – Technology Overview and Recent Operational Results in 100 kW unit, Energy Procedia, **2014**, 63 pp.98-112.

[25] Y. Li, X. Ma, W. Wang, C. Chi, J. Shi, L. Duan, Enhanced CO_2 capture capacity of limestone by discontinuous addition of hydrogen chloride in carbonation at calcium looping conditions, Chemical Engineering Journal, **2017**, 316, pp.438–448.

[26] A. MacKenzie, D.L. Granatstein, E.J. Anthony, J.C. Abandes. Economics of CO_2 capture using the calcium cycle with a pressurized fluidized bed combustor, Energy and Fuels, **2007**, 21 (2), pp.920–926.

[27] A. Bosoaga, O. Masek, J. Oakey, CO_2 Capture Technologies for Cement Industry, Energy Procedia. **2009**,1 (1), pp.133–140.

[28] McBride, B.J.; Zehe, M.J.; Gordon, S., NASA Glenn Coefficients for Calculating Thermodynamic Properties of Individual Species. National Aeronautics and Space Administration, Clevelan, OH, USA. **2002**. http://gltrs.grc.nasa.gov/reports/2002/TP-2002-211556.pdf

[29] M. Diego, B. Arias, G. Grasa, J. Abanades, L. Díaz, M. Lorenzo, A. Sánchez-Biezma, Calcium Looping with Enhanced Sorbent Performance: Experimental Testing in A Large Pilot Plant, Energy Procedia. **2014**, 63, pp.2060–2069.

[30] T. Hills, D. Leeson, N. Florin, P. Fennell, Carbon Capture in the Cement Industry: Technologies, Progress, and Retrofitting Environment Science Technology, **2015**, 50 (1), pp.368-377.

[31] R&D Achievements on Carbon Capture and Storage in ITRI, Taiwan, http://ccs.tw/sites/default/files/datashare/pdf/201410060923gong_yan_yuan_ccsyan_fa_cheng_guo_ying_wen_.pdf, accessed 30 July **2017**.

[32] ECRA, 2007. Carbon capture technology—options and potentials for the cement industry. http://www.nrmca.org/taskforce/item_2_talkingpoints/sustainability/sustainability/sn3022%5B1%5D.pdf, assessed 30 June **2017.**

[33] Experimental Facilities: La Pereda 1.7 MWth pilot plant, https://www.flexical.eu/experimental-facilities/, accessed 30 July **2017**

[34] World Business Council for Sustainable Development, CSI Guidance for reducing and controlling emissions of mercury compounds in the cement industry, Switzerland, Report (2015), http://www.wbcsdcement.org/pdf/CSI%20Guidance%20for%20reducing%20and%20controlling%20emissions%20of%20mercury%20compounds%20in%20the%20cement%20industry.pdf, assessed 10 May **2017**.

[35] 13th International Conference on Greenhouse Gas Control Technologies-Report, http://www.ghgt.info/images/GHGT13/Sponsor_Prospectus_GHGT-13_final.pdf,accessed, 30 July **2017**.

[36] M. Chang, C. Huang, W. Liu, W. Chen, Y. Cheng, Design and experimental investigation of calcium looping process for 3-kW_{th} and 1.9-MW_{th} Facilities. Chemical and Engineering Technology, **2013**, 36 (9), pp.1525–1532.

[37] C. Dean, J. Blamey, N. Florin, M. Al-Jebori, P. Fennell, The calcium looping cycle for CO_2 capture from power generation, cement manufacture and hydrogen production. Chemical Engineering Research and Design, **2011**, 89 pp.836-855.

[38] J.C. Abanades, ES. Rubin, EJ. Anthony Sorbent cost and performance in CO_2 capture systems. Industrial and Engineering Chemistry Research, **2004**, 43, pp.3462-3466.

[39] N. Deshpande, B. Yuh, Screening of multiple waste animal shells as a source of calcium sorbent for high temperature CO_2 capture. Sustainable Environment Research, **2013,** 23 (3), pp.227–232.

[40] G. Grasa, J. Abanades, CO_2 Capture of CaO in Long Series of Carbonation/Calcination Cycles. Industrial and Engineering Chemistry Research, **2006**,45, pp.8846-8851.

[41] K. Chrissafis, C. Dagounaki, K. Paraskevopoulos, The effects of procedural variables on the maximum capture efficiency of CO_2 using a carbonation/calcination cycle of carbonate rocks. Thermochimica Acta, **2005**, 428, pp.193–198.

[42] J. Valverde, P. Sanchez-Jimenez, L. Perez-Maqueda, Ca-looping for post-combustion CO_2 capture: A comparative analysis on the performances of dolomite and limestone. Applied Energy, **2015**, 138, pp.202–215.

[43] K. Wang, D. Han, P. Zhao, X. Hu, Z. Yin, D. Wu, Role of $Mg_xCa_{1-x}CO_3$ on the physical–chemical properties and cyclic CO_2 capture performance of dolomite by two-step calcination. Thermochima Acta, **2015**, 614, pp.199-206.

[44] C. Pinheiro, A. Fernandes, C.Freitas, E. Santos, M. Ribeiro, Waste Marble Powders as Promising Inexpensive Natural CaO-Based Sorbents for Post-Combustion CO_2 Capture. Industrial and Engineering Chemistry Research, **2016**, 55, (29), pp.7860-7872.

[45] S. Castilho, A. Kiennemann, M. Costa Pereira, A. Soares Dias, Sorbents for CO_2 capture from biogenesis calcium wastes. Industrial and Engineering Chemistry Research, **2013**, 226, pp.146-153.

[46] P. Xu, M. Xie, Z. Cheng, Z. Zhou, CO_2 capture performance of CaO-based sorbents prepared by a sol–gel method. Industrial and Engineering Chemistry Research, **2013**, 52, pp.12161-12169.

[47] X. Yang, L. Zhao, S. Yang, Y. Xiao, Investigation of natural CaO-MgO sorbent for CO_2 capture, Asia-Pacific Journal of Chemical Engineering, **2013**, 8, pp.906–915.

[48] M. Mai, T. Edgar, Surface area evolution of calcium hydroxide during calcination and sintering. American Institute of Chemical Engineers, **1989,** 35, (1) pp.30–36.

[49] A. Coppola, F. Montagnaro, P. Salatino, F. Scala, Fluidized bed calcium looping: The effect of SO_2 on sorbent attrition and CO_2 capture capacity. Chemical Engineering Journal, **2012**, 207-208, pp.445–449.

[50] AI. Lysikov, AN. Salanov, AG. Okunev, Change of carrying capacity of CaO in isothermal recarbonation–decomposition cycles. Industrial and Engineering Chemistry Research, **2007**, 46, pp.4633–4638.

[51] L. Bhatta, S. Subramanyam, M. Chengala, S. Olivera, K. Venkatesh, Progress in hydrotalcite like compounds and metal-based oxides for CO_2 capture: a review. Journal of Cleaner Production, **2015**, 103, pp.171-196.

[52] P. Sun, J.R. Grace, CJ. Lim, EJ. Anthony. The effect of CaO sintering on cyclic CO_2 capture in energy systems American Institute of Chemical Engineers Journal, **2007**, 53, (9), pp.2432–2442.

[53] R. Barker, The reversibility of the reaction $CaCO_3 \leftrightarrow CaO+CO_2$. Journal of Chemical Technology and Biotechnology, **1973**, 23, (10), pp.733-741.

[54] Z. Chen, H. Song, M. Portillo, C. Lim, J. Grace, E. Anthony, Long-term calcination/carbonation cycling and thermal pretreatment for CO_2 capture by limestone and dolomite. Energy Fuels, **2009**, 23, (3), pp.1437–1444.

[55] S. F. Wu, Q.H. Li, J.N. Kim, B. Y, Kwang, Properties of a Nano CaO/Al_2O_3 CO_2 Sorbent. Industrial and Engineering Chemistry Research. **2008**, 47 (1), pp.180–184.

[56] B. Feng, W. Liu, X. Li, H. An Overcoming the problem of loss-in-capacity of calcium oxide in CO_2 capture. Energy Fuels, **2006**, 20, pp.2417-2420.

[57] M. Aihara, T. Nagai, J. Matsushita, Y. Negishi, H. Ohya, Development of porous solid reactant for thermal - energy storage and temperature upgrade using carbonation/ decarbonation reaction. Applied Energy, **2001**, 69, pp.225-238.

[58] S. Wu, Q. Li, J. Kim, K. Yi, Properties of a Nano CaO/Al_2O_3 CO_2 Sorbent. Industrial and Engineering Chemistry Research. **2008**, 47 (1), pp.180–184.

[59] E. Santos, C. Alfonsin, A. Chambel, A. Fernandes, A. Soares Dias, C. Pinheiro, M. Ribeiro, Investigation of a stable synthetic sol−gel CaO sorbent for CO_2 capture, Fuel, **2012**, 94, pp.624−628.

[60] F. Zeman, Effect of steam hydration on performance of lime sorbent for CO_2 capture. International Journal of Greenhouse Gas Control, **2008**, 2 (2), pp.203–209.

[61] M. Samtani, E. Skrzypczak-Janktun, D. Dollimore, K. Alexander, Thermal analysis of ground dolomite, confirmation of results using an X-ray powder diffraction methodology. Thermochimica Acta, **2001**, 367–368, pp.297–309.

[62] S. Wang, L. Fan, C. Zhao, X. Ma, Porous spherical CaO-based sorbents via PSS-assisted fast precipitation for CO_2 capture, ACS Applied Materials and Interfaces, **2014**, 6, (20), pp.18072–18077.

[63] J. Readman, R. Blom, The use of in situ powder X-ray diffraction in the investigation of dolomite as a potential reversible high-temperature CO_2 sorbent. Physical Chemistry Chemical Physics, **2005**, 7 (5), pp.1214–1219.

[64] RH. Borgwardt, Sintering of nascent calcium oxide. Chemical Engineering Science; 44(1), 53–60, **1989.**

[65] M. Alonso, M. Lorenco, B.Gonzales, JC. Abanades, Precalcination of $CaCO_3$ as a Method to Stabilize CaO Performance for CO_2 capture from Combustion Gases, Energy Fuels, 2011, 25 (11), pp.5521-5527.

[66] DC. Ozcan, BH. Shanks, TD. Wheelock, Improving the Stability of a CaO-Based Sorbent for CO_2 by thermal Pretreatment, Industrial and Engineering Chemistry Research, **2011**, 50 (11), pp.6933-6942.

[67] V. Manovic, E.J. Anthony, Thermal activation of CaO-based sorbent and self-reactivation during CO_2 Capture Looping Cycles, Environment Science Technology. **2008**, 42 (11), pp.4170–4174.

[68] C. Herce, S. Stendardo, C. Cortés, Increasing CO_2 carrying capacity of dolomite by means of thermal stabilization by triggered calcination. Chemical Engineering Journal, **2015**, 262, pp.18–28.

[69] J.L Figueiredo, M.M. Pereira, Catalysis from Theory to Application: an integrated course, Imprensa da Universidade de Coimbra, **2015**, pp.87-88.

[70] K. Sing, The use of nitrogen adsorption for the characterisation of porous materials. Colloids and Surfaces, A Physicochemical and Engineering Aspects, **2001**, 187-188. pp.3–9.

[71] J. Dunn, Thermogravimetric analysis, Characterization of Materials, John Wiley and Son Inc., **2012**

[72] B.L. Dutrow, C.M. Clark, Report. Geochemical Instrumentation and Analysis: X-ray Powder Diffraction (XRD), accessed 30 July **2017.**

[73] Nanoparticle size determination by X-ray diffraction technique and dynamic light scattering method for colloidal nanoparticles, https://serc.carleton.edu/, accessed 30 July 2017

[74] S. Stendardo, L. Felice, K. Gallucci, CO_2 capture with calcined dolomite: The effect of sorbent particle size. Biomass Conversion and Biorefinery, Springer, **2011**, pp.149–160.

[75] M. Thommes, Physical Adsorption Characterization of Nanoporous Materials, Chemie Ingenieur Technik, **2015**, 82, (7), pp.1059–1073.

[76] Q. Zhu, Ying, S. Zeng, A Model to Stabilize CO_2 Uptake Capacity during Carbonation-Calcination Cycles and its Case of CaO-MgO, Environment Science Technology, **2017**, 51 (1), pp.552–559.

[77] S. Choi, J. Drese, C. Jones, Adsorbent materials for carbon dioxide capture from large anthropogenic point sources. Chemistry and Sustainability, **2009**, 2 (9), pp.796–854.

[78] D. Alvarez, J.C. Abanades Pore-size and Shape effects on the recarbonation performance of Calcium Oxide submitted to repeated calcination/recarbonation cycles, Energy and Fuels, **2005**, 19 (1) pp.270-27.

[79] A. Biasin, C. Segre, G. Salviulo, F. Zorzi, M. Strumendo, Investigation of $CaO–CO_2$ reaction kinetics by in-situ XRD using synchrotron radiation, Chemical Engineering Science, **2015**, 127, pp.13–24.

[80] S. Gunasekaran, G. Anbalagan, Thermal decomposition of natural dolomite, Bulletin of Materials Science, **2007**, 30 (4), pp.339–344.

[81] J. Valverde, A. Perejon, S. Medina, L. Perez-Maqueda, Thermal decomposition of dolomite under CO_2: insights from TGA and in situ XRD analysis Physical Chemistry Chemical Physics, **2015**, 17 (44), pp.30162–30176.

[82] K. Wang, Z. Yin, P. Zhao, D. Han, X. Hu, G. Zhang, Effect of Chemical and Physical Treatments on the Properties of a Dolomite used in Ca Looping, Energy Fuels, **2015**, 29 (7), pp.4428–4435.

[83] S. Lee, S. Cha, Y. Kwon, M. Park, B. Hwang, Y. Park, H. Seo, J. Kim, Effects of alkali-metal carbonates and nitrates on the CO_2 sorption and regeneration of MgO-based sorbents at intermediate temperatures. Korean Journal of Chemical Engineering, **2016**, 33 (12), pp.1-8.

[84] A. Martos, J Valverde, P. Sanchez-Jimenez, A. Perejón, C. García-Garrido, L. Perez-Maqueda, Effect of dolomite decomposition under CO_2 on its multicycle CO_2 capture behavior under calcium looping conditions, Physical Chemistry Physics, **2016**, 18, pp.16325–16336.

[85] G. Grasa, I. Martinez, M. Diego, M. Abanades, Determination of CaO Carbonation Kinetics under Recarbonation Conditions, Energy and Fuels, **2014**, 28 (6), pp.4033–4042.